6

Enderby Island Excavations

JO MCDONALD, WENDY REYNEN, ZANE BLUNT,
KANE DITCHFIELD, JOE DORTCH, MATTHIAS LEOPOLD,
CARLY MONKS, ALISTAIR PATERSON, PETER VETH

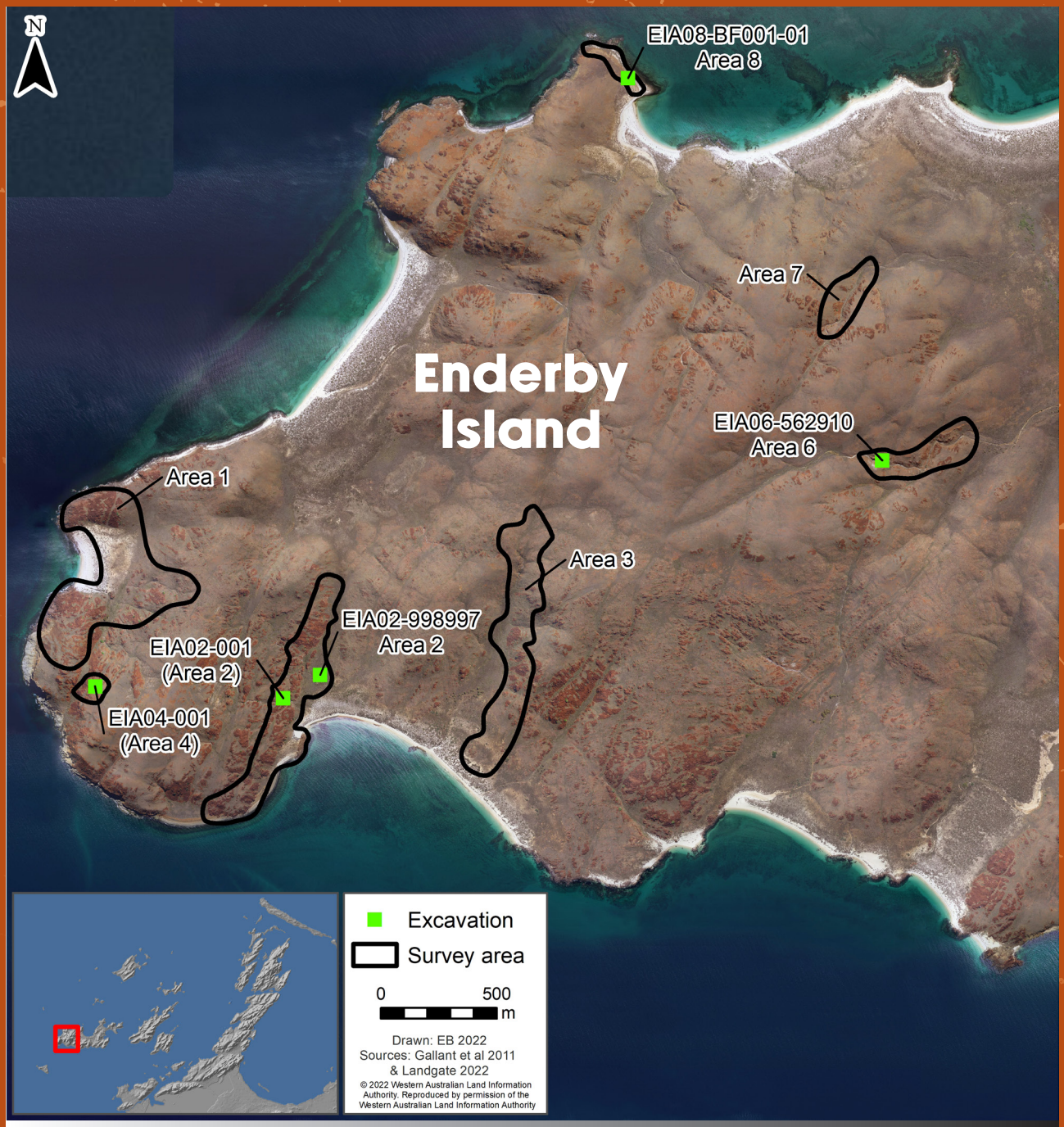
N
EIA08-BF001-01
Area 8
Area 7
Enderby
Island
EIA06-562910
Area 6
Area 1
Area 3
EIA02-998997
Area 2
EIA02-001
(Area 2)
EIA04-001
(Area 4)
Excavation
Survey area
0
500
m
Drawn: EB 2022
Sources: Gallant et al 2011
& Landgate 2022
© 2022 Western Australian Land Information Authority. Reproduced by permission of the Western Australian Land Information Authority

Excavations were undertaken in four of the sample transects/landscapes where rock art was recorded at the western end of Enderby Island (Figure 6.1).

In accordance with the goals of the project, these excavations aimed to contextualise the rock art production and stone feature construction at this western end of Enderby Island.

Enderby Island Sample Area 2

Two excavation squares were excavated in the Sample Area 2 (Area 2), located towards the western end of Enderby Island. Sample transect 2 was roughly 2 km long and captured a coastal set of landscape contexts at its southern end as well as extending into the interior along the western side of a valley. The geology here is granophyre/rhyodacite with a pocket of andesitic basalt at the southern end of the transect (Figure 5.2 in Chapter 5). Excavation square EIA02-001 investigated an elevated midden deposit adjacent to a semi-permanent pool with a large fig tree. This location is surrounded by panels with art and stone features amongst an extensive rock art site complex. The other square (EIA02-998997) was placed on a residual sand sheet (Qhms; Holocene coastal sand) in the middle of the valley, east of an ephemeral creek line meandering through this blocky valley system (Figure 6.2).

Square EIA02-001

This 0.5 m x 0.5 m square was located in a flat area with obvious *Terebralia* midden, relatively unimpeded by surface rocks (Figure 6.3). Surrounding panels contain rock art and grinding patches, and there are several recorded standing stones and other stone features nearby. The square was aligned north–south with all X-Y-Z measurements taken from the south-west corner. Excavation proceeded stratigraphically with 17 XUs dug in 2–4 cm depths (Figure 6.4). The scale was always photographed above the northern section.

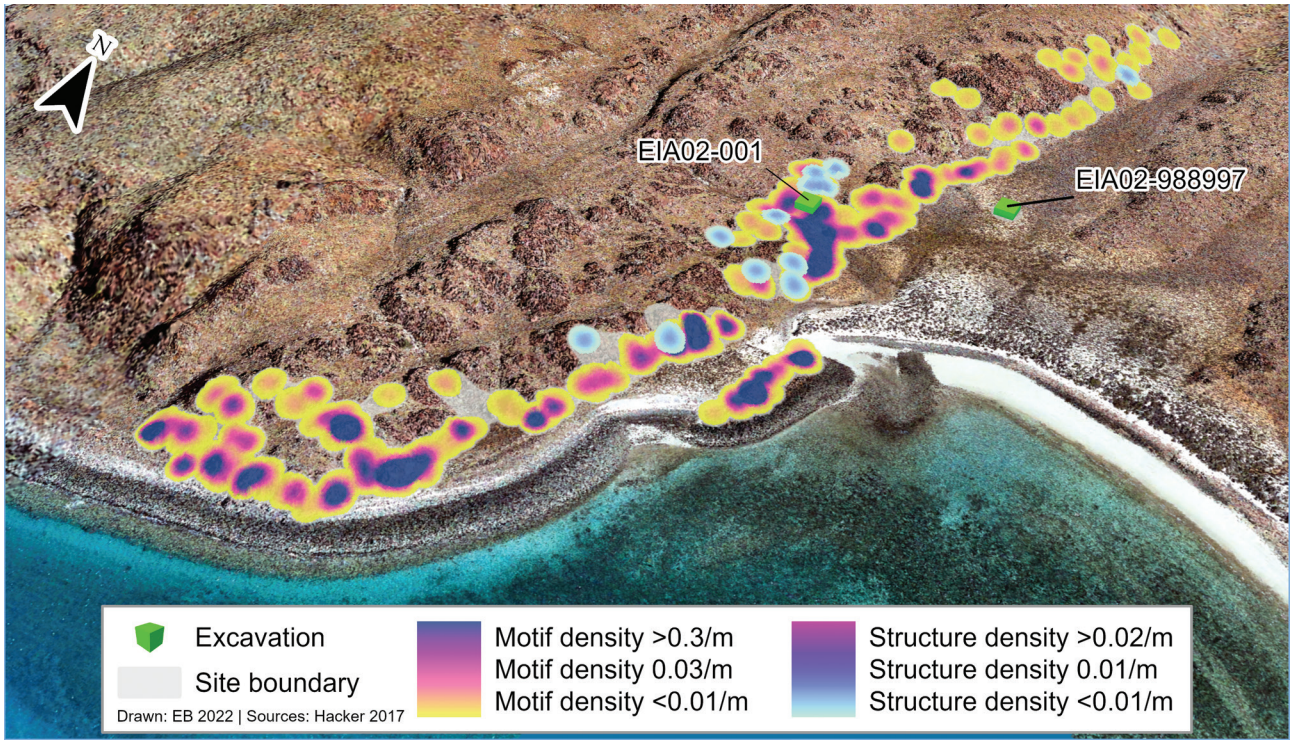

Figure 6.2. Enderby Island Area 2, showing location of the excavation squares and engraving and stone feature density.

Figure 6.3. Stringing up Square EIA02-001, June 2016. View to the south-east. Note top of fig tree at adjacent rock pool, and nature of the surface scatter.

Stratigraphy and dating

Three stratigraphic units are defined (Figure 6.5):

SU1 Dry loose sand, dull reddish brown sediment (5YR 4/4) with decomposing surface shell (*Terebralia*), one large surface cobble and bone (the Ao layer): pH 8;

SU2 Dark reddish brown (5YR 3/2) friable soil, with ant nest / bioturbation present across most of the square (not visible in all sections). Moderately compact, some burnt bone and charcoal observed (and collected). Bioturbation noted towards the base (XU12), e.g. termite burrow, eastern baulk, with introduced fresh grass fragments: pH 8–8.5;

SU3 Dark reddish brown sediment (5YR 3/2-4) becoming more clayey with increasing dampness just above interlocking basal rocks (unexcavated), which are assumed to be sitting on decomposing bedrock. Some larger rocky inclusions, mixed-sized rocky fragments and blocks. Sparse fragmentary shell: pH 7.

UNIT	DEPTH BELOW SURFACE (CM)	DEPOSIT EXCAVATED	WEIGHT ROCKS DISCARDED	PH	MUNSELL
XU01	2	8.5	0.5	8	5YR 4/4
XU02	4	8	0.1	8	5YR 3/3
XU03	6	7		8	5YR 3/2
XU04	8	7		8	5YR 3/3
XU05	10	9		8	5YR 3/2
XU06	12	6		8	5YR 3/2
XU07	14	9	0.05	8	5YR 3/2
XU08	16	9	0.1	8	5YR 3/2.5
XU09	18	9.5	0.155	8.5	5YR 2.5/2
XU10	20	8.5	0.2	8.5	5YR 2.5/2
XU11	22	8	0.1	8	5YR 3/3
XU12	24	7.5	0.08	8	5YR 3/3
XU13	27	7		8	5YR 3/3
XU14	28	8		8	5YR 3/2
XU15	31	9	1.5	8	5YR 3/4
XU16	34	9	0.25	8	5YR 3/2
XU17	39	26.25	12	8	5YR 3/4
Total		156.25	15.0		

Table 6.1. Square EIA02-001 excavation units, weights for deposit (kg) and sedimenat characteristics.

Within the profile, compaction increases and colour intensifies and becomes generally redder with depth (Table 6.1). Stratigraphic units 1 and 2 (SU1 and SU2) comprise the midden layer; SU3 contains some highly fragmented decomposing shell at its top but is much rockier and its only cultural remains are stone artefacts.

Four conventional radiocarbon dates and two OSL dates were returned from this excavation square. All AMS dates were from *Terebralia* shell. (Charcoal for paired shell samples were collected for analysis but unfortunately these had too little carbon for even AMS determinations; Fiona Petchey, pers. comm., 2017.) Two OSL tubes were inserted in SU3 (Figure 6.6). No complete shell or charcoal samples were observed in this stratigraphic layer (i.e. shell fragments were only recovered in the 2 mm sieves).

Figure 6.6. Square EIA02-001: eastern section before and after OSL sampling.

Terebralia samples from XU2, XU3 and XU4 were found to be statistically overlapping between 8.2 and 8.5 ka cal. BP. *Terebralia* from XU13 at the base of the interface between SU1 and SU2 was dated to 9,490 cal. BP, indicating that midden deposit accumulated over a roughly 1,000-year period between 9,500 and 8,500 BP (Table 6.2). The two OSL samples reveal older, but unfortunately inverted, dates at the Pleistocene/Holocene transition (Table 6.3).

LAB CODE	SAMPLE TYPE	XU	DEPTH BELOW SURFACE (CM)	% MODERN CARBON	CONVENTIONAL RADIOCARBON AGE (YRS BP, 1_σ ERROR)	CALIBRATED AGE RANGE
Wk-44890	Terebralia	2	4	38.3 ± 0.1	7,700 ± 20	7,860 ± 70
Wk-44892	Terebralia	3	6	38.3 ± 0.1	7,746 ± 20	7,900 ± 70
Wk-44894	Terebralia	4	8	38.3 ± 0.1	7,482 ± 20	7,680 ± 80
Wk-44896	Terebralia	13	27	38.3 ± 0.1	8,465 ± 24	8,720 ± 110

Table 6.2. Square EIA02-001. Radiocarbon dates returned on charcoal (calibrations using Marine20) and shellfish and OSL dates.

LAB CODE	FIELD REF.	DEPTH (M)	DE (GY)	OVERDISPERSION (%)	DOSE RATE (μGY/A–1)	AGE (KA)
Shfd18138	EIA02-001 OSL 1	0.35	52.51 ± 0.56	8	5467 ± 234	9.6 ± 0.4
Shfd18139	EIA02-001 OSL 2	0.25	50.79 ±1.38	15	4548 ± 195	11.2 ± 0.6

Table 6.3. Summary of single grain palaeodose data and ages for square EIA02-001 (see OSL Appendix).

Based on the stratigraphy, the excavated cultural assemblage (see below) and the dates, the cultural assemblage is divided into two analytical units:

Analytical Unit 1: Early Holocene *XU1–12*
Analytical Unit 2: Pleistocene/Holocene Transition *XU13–17*

Bayesian analysis

This chronostratigraphy was tested using a Bayesian sequence depositional model (Bronk Ramsey 2008, 2009a) following the criteria and parameters established in Chapter 2. The analysis was based on the two defined analytical units and the radiocarbon and OSL dates (Table 6.2 and Table 6.3). Since there is no clear evidence for depositional disconformity in Square EIA02-001, continuous boundaries (see Bronk Ramsey 2009a) are used to model this sequence, which has an Early Holocene phase and a Pleistocene/Holocene Transition phase.

Figure 6.4. Square EIA02-001: (top left) start level and (top right) end level for XU1 in square A; and (bottom left) end level of XU12 (base of SU2) and (bottom right) end of XU17 showing north-eastern corner and base of excavation.

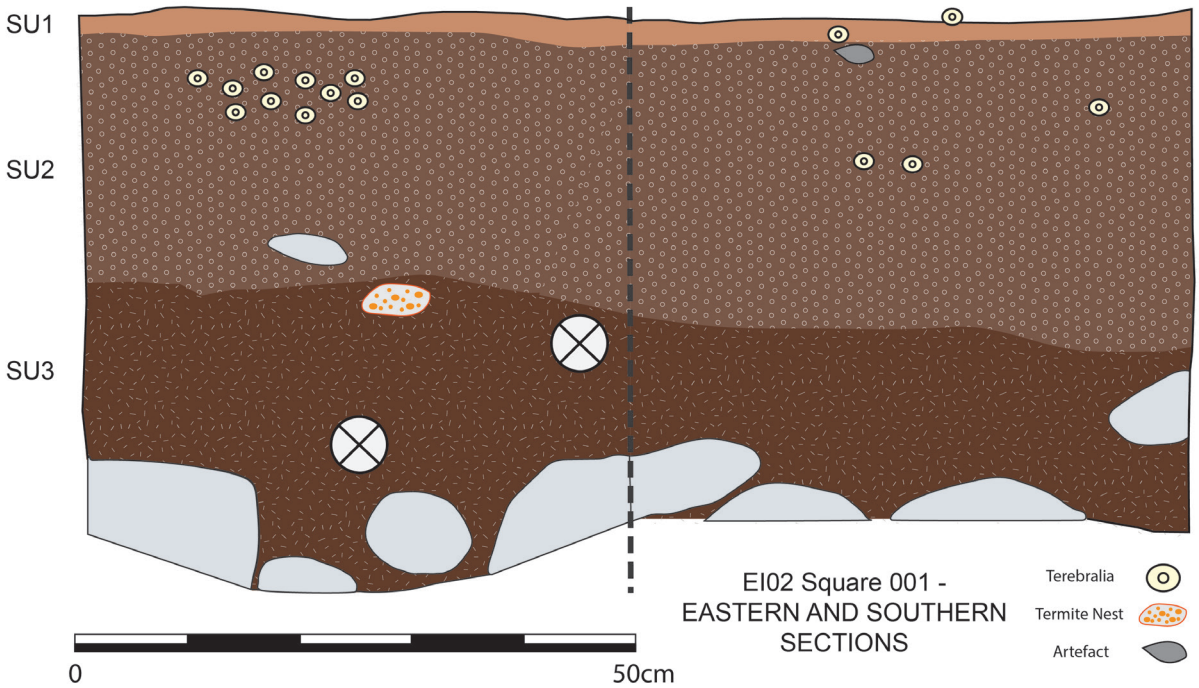

Figure 6.5. Square EIA02-001: stratigraphic section drawings (eastern and northern baulks).

The results for the Bayesian analysis are shown in Table 6.4 and Figure 6.7. The model returns good results where all dates have <10% chance of being an outlier with good agreement indices. At 68.2% probability, this model suggests that the deposit began accumulating between 12,580 and 10,000 cal. BP with the boundary between the two analytical units occurring at 8,270–7,860 cal. BP. This model estimates that occupation at square EIA02-001 ceased between 7,770 and 7,340 cal BP.

NAME	68.2%		95.4%		SUM. STATISTICS			INDICES	
	FROM	TO	FROM	TO	μ	σ	m	AI	OP
Boundary: Early Holocene – Top	7,770	7,340	7,890	6,510	7,410	380	7,530		
Phase: Early Holocene									
Wk-44890	7,930	7,790	8,000	7,720	7,860	70	7,860	102.6	96.6
Wk-44892	7,970	7,830	8,030	7,750	7,900	70	7,900	100.4	96.5
Wk-44894	7,755	7,598	7846	7,532	7,684	80	7,680	92.3	95.6
Boundary: Pleistocene/Holocene Transition	8,270	7,860	8,660	7,810	8,150	240	8,090		
Phase: Pleistocene/Holocene Transition									
Shfd18139	11,460	10,040	12,160	9,260	10,690	720	10,720	81.5	93
Wk-44896	8,810	8,600	8,940	8,540	8,730	110	8,720	100.6	96.1
Shfd18138	9,980	9,170	10,370	8,770	9,570	400	9,570	100.8	95.7
Boundary: Deposit Base	12,580	10,000	15,560	8,950	11,860	1,770	11,490		

Table 6.4. Bayesian analysis for Square EIA02-001 with restricted analytical units.
Note: 'AI' stands for 'Agreement Index' and 'OP' stands for 'Outlier Probability'.

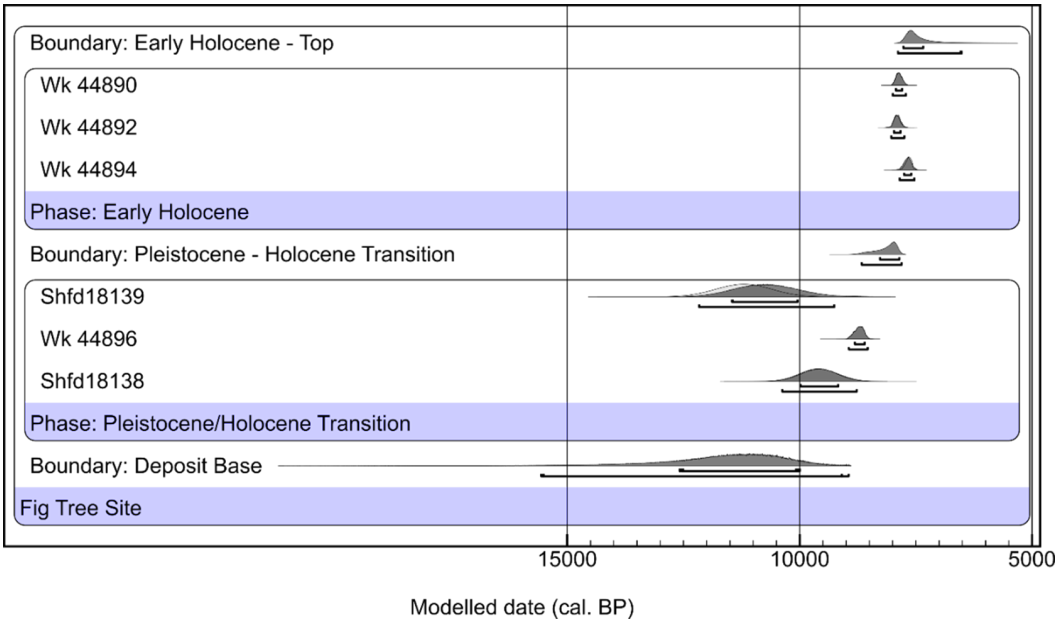

Figure 6.7. Bayesian analysis results for Square EIA02-001.

Excavated cultural assemblage

The excavated assemblage weighed over 30.7 kg and was composed predominantly of shellfish (30.4 kg), stone artefacts (234 g) and c. 100 g of bone (Table 6.5, Figure 6.8). Shell, bone and artefacts are found throughout AU1. While the weights of shell are consistently high throughout the midden layer, these are slightly higher in the later phase of midden use. Artefacts are found sporadically throughout the midden sequence and appear to be inversely correlated with shell deposition (i.e. the later peak in shell is matched by a concomitant decline in artefact numbers). Only stone artefacts are present in AU2: the Pleistocene/Holocene Transition layer (Table 6.5). Given the age range from the top of the midden (overlapping statistically) and the size of the test square, this may well be the result of small sample size.

UNIT	AU	FLAKED ARTEFACTS	SHELL	BONE	TOTAL CULTURAL DEPOSIT
XU01	1	0.24	2,480.5	5.55	2,486.29
XU02	1	2.84	3,730.89	1.39	3,735.12
XU03	1	2.92	1,869.7	7.98	1,880.6
XU04	1	0.09	2,867.09	9.902	2,877.08
XU05	1	6.31	4,582.49	22.98	4,611.78
XU06	1	16.23	2,571.11	6.98	2,594.32
XU07	1	16.6	622.38	8.74	647.72
XU08	1	27.8	2,484.66	12.4	2,524.86
XU09	1	38.55	2,520.09	16.01	2,574.65
XU10	1	40.75	2,209.85	6.791	2,257.39
XU11	1	27.1	2,121.78	2.87	2,151.75
XU12	1	20	1,851.95	2.9	1,874.85
XU13	2	16.79	430.82	1.6	449.21
XU14	2	1.22	65.73	1.18	68.13
XU15	2	4.51	7.17	0.15	11.83
XU16	2	12.42	6.86	0.05	19.33
XU17	2		1.9	0	1.9
Total		234.37	30,425	107.473	30,766.8

Table 6.5. Square EIA02-001: cultural material weights (in grams).

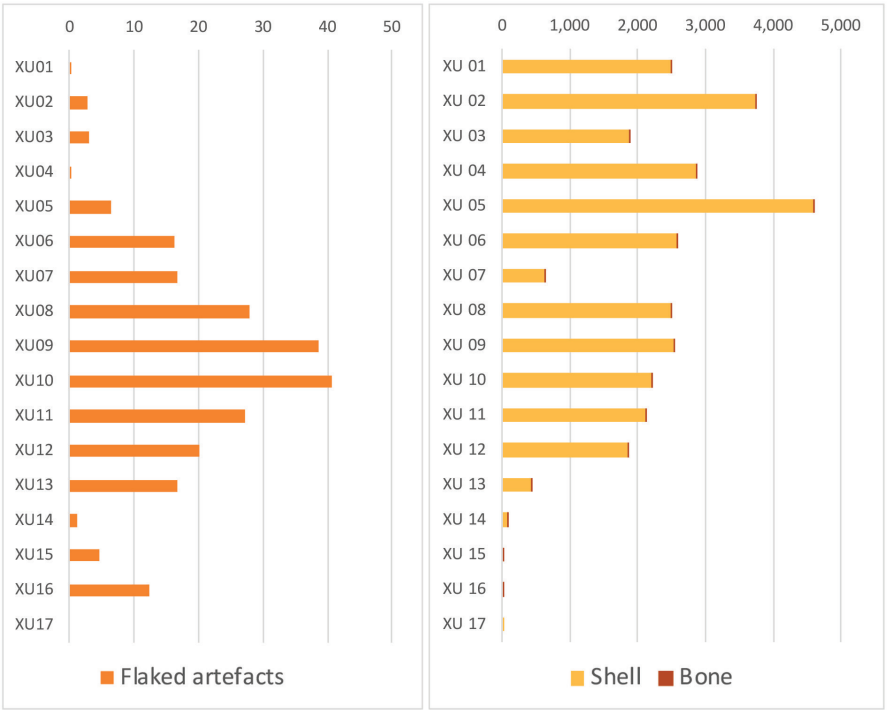

Figure 6.8. Enderby Island Square EIA02-001: proportions of shell and bone (left) and stone artefacts (right) found in this excavation. Weights in grams.

Economic shellfish

The vast majority of the economic species are found in AU1 and are predominantly (99.5%) mangrove species *Terebralia* (Table 6.6). Other minor species include Baler (*Melo*), Syrinx and Rock Oyster (*Saccostrea*), which are present in very low numbers and weights persistently through the midden layer. Baler (*Melo* spp.) fragments are found in XU1–XU11 and Rock Oyster (*Saccostrea*) in XU1–XU6. As fragments from these taxa were small and lacked unique features, MNI was not calculated. The Syrinx fragment was found in XU7. Only c. 460 g of shellfish was found in AU2. This material is all highly fragmented *Terebralia* and indicates mixing at the interface of these two occupation layers.

		AU1 (XU1–12)		AU2 (XU13–17)		TOTAL	
HABITAT	SPECIES	MNI	WEIGHT	MNI	WEIGHT	MNI	WEIGHT
Mangrove mudflats	Terebralia palustris	1,531	26,424.81	138	462.20	1,669	26,830.69
Rocky	Saccostrea	NA	22.14	0	0	NA	22.14
Sandy	Melo amphora	NA	94.99	0	0	NA	94.99
Sandy	Syrinx aruanus	1	6.39	0	0.0	1	6.39
Total			26,940.20		462.20		26,954.21

Table 6.6. Identifiable shellfish species found in the two analytical units. Weight in grams.

Minimum numbers of individuals (MNI) and dietary calculations

The MNI of *Terebralia* was provided by the number of complete anterior ends with part or all the aperture remaining. Of the 1,669 *Terebralia* ends so identified, 584 individuals were complete enough for the shell's maximum width to be measured, perpendicular to the shell axis on a plane aligned with the aperture. The mean width obtained was 21.1 mm, with a standard deviation (SD) of 2.91 mm. Measurements of 12 reference shells held by UWA Archaeology indicate length correlates to width (R = 0.94) and a 21 mm width translates to 61 mm length. This allows an estimate of live weight (shell plus meat) of 18.7 g for a shell with mean width of 21.2 mm (Meehan 1982). Following these estimates, the MNI of *Terebralia* in this one 50 cm x 50 cm square (1,669) represents c. 31 kg of fresh shellfish.

Using figures derived from ethnographic data in the Northern Territory, whereby women collected an average of 3 kg of shellfish per person per hour (Meehan 1982), this amount of shell represents just 10 person-hours of work to collect, not counting transport time or the fragmented remains also in this square. Following Meehan's (1982) calculations, the amount of meat represented per individual *Terebralia* (4.4 g), indicates square EIA02-001 represents c. 7.3 kg of shell meat. Extrapolating these values to the entire midden (covering an area of c. 50 m^2) implies c. 6,000 kg of shellfish – about 2,000 person-hours of work, over the 560 years that this Early Holocene midden accumulated. This equates to 10.7 kg of *Terebralia* meat per year being consumed at this midden.

Shellfish size distribution can indicate dietary and harvesting choices. *Terebralia* are a K-selected and long-lived species. They become adults at c. 8–10 years and live for >10 yrs. When they become adults, they change their habitat from the mud below the mangrove trees to graze instead on algae attached to the mangrove leaves (Wells and Lalli 2003). We understand that this change in diet may well affect the palatability of the *Terebralia* (although this requires further research). The archaeological data from the Fig Tree site indicates that people are harvesting a very narrow size/age range in the *Terebralia* population (Figure 6.9). The mean valve length (dots) and standard deviations (whiskers) vary very little through the 560 years that *Terebralia* was deposited at this site (t-tests indicate p H0 <0.0002, using two-tailed tests of paired XUs with unequal variance). This distribution suggests strong selectivity – and sustainability – in the harvesting of *Terebralia* throughout the occupation of the Fig Tree site.

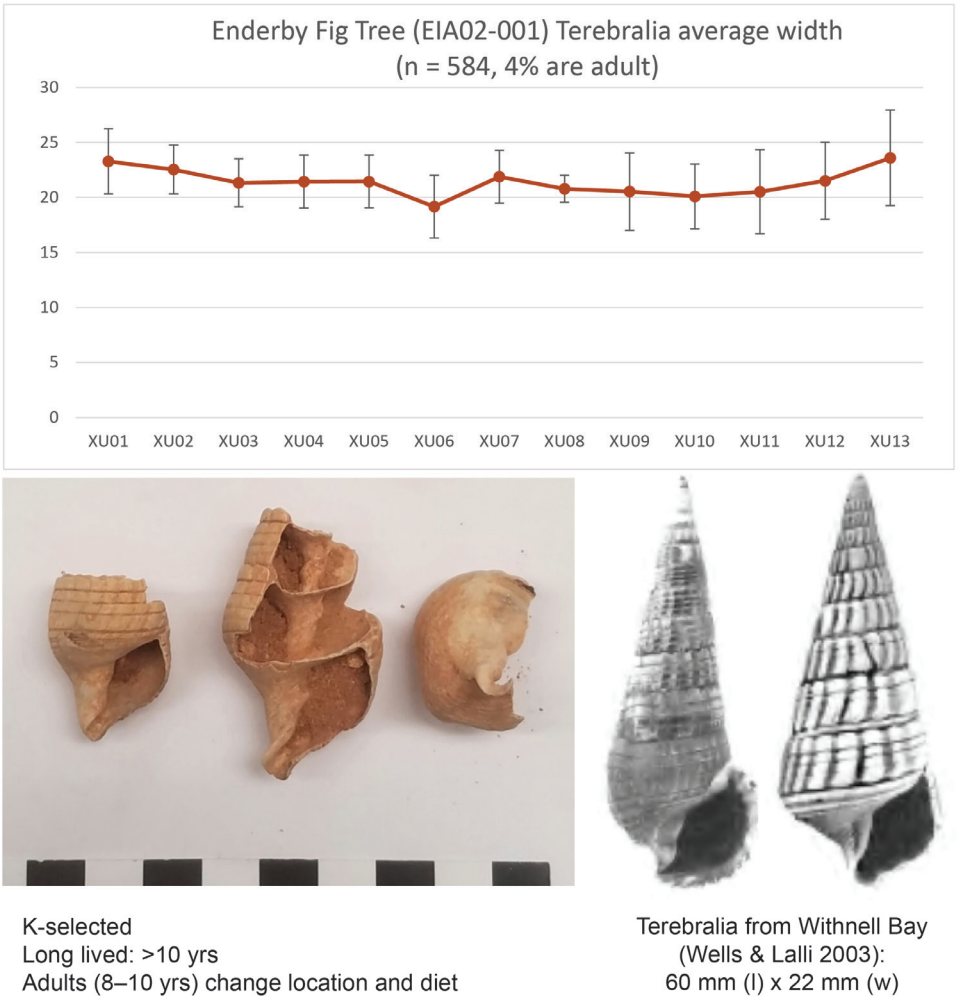

Figure 6.9. *Terebralia* shells juvenile (B) and adult (A) showing differences in aperture morphology and (inset) from the archaeological assemblage (left) and Square EIA02-001 *Terebralia* size averages through XU1–13 (right).

Stone artefacts

The stone artefacts, including residues, were analysed by Zane Blunt for his Honours thesis (Blunt 2019). To ensure project-wide comparability, this analysis has been audited by Wendy Reynen. The EIA02-001 assemblage consists of 200 artefacts, weighing 230.6 g. Of these artefacts, 38 are microdebitage (<1 cm maximum dimension). The stone artefact assemblage was analysed according to the two defined analytical units (Figure 6.10). Most of the assemblage (n = 170, 85%) was in the Early Holocene unit, with 30 artefacts (12.75%) deposited during the Pleistocene/Holocene Transition (Figure 6.11).

Assemblage composition

Lithic materials at EIA02-001 were characterised using a combination of visual inspection and comparison with known geological thin section samples from Rosemary Island (Fairweather 2019). The assemblage is predominantly composed of andesitic basalt (n = 173, 86.5%) throughout, with more local rhyodacite being used only (but not intensively) in the later period of site use (n = 25, 12.5%, Figure 6.10 and Table 6.7). Two quartz artefacts were found (one each in XU1 and XU14).

MATERIAL/AU	ANDESITIC BASALT	%F	QUARTZ	%F	RHYODACITE	%F	TOTAL
1	144	84.7	1	0.6	25	14.7	170
2	29	96.6	1	3.3	0	0	30
Total	173	86.5	2	1	25	12.5	200

Table 6.7. Square EIA02-001: raw materials per analytical unit.

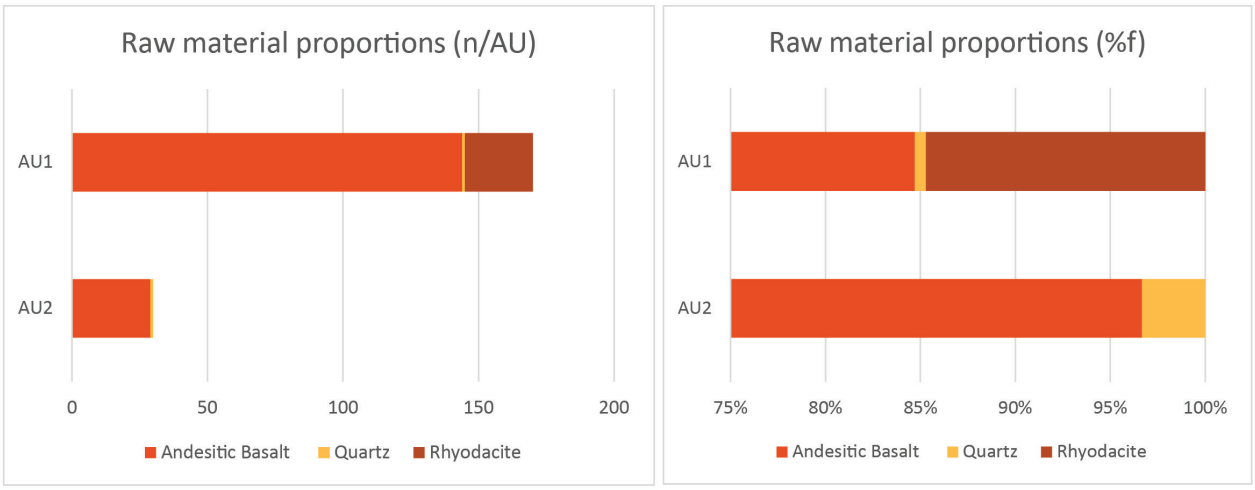

Figure 6.10. Square EIA02-001: proportions of materials through the analytical units.

Overall assemblage composition is dominated by complete and broken flakes, of which most (93%) are tools, i.e. with evidence for some use (Table 6.8). The small sample size of AU2 makes it difficult to meaningfully compare assemblage composition through time; however, the Early Holocene occupation represents a wider use of lithic materials than found in the Pleistocene Transition assemblage.

ARTEFACT TYPE/MATERIAL	BROKEN FLAKE		COMPLETE FLAKE		TOOL		TOTAL	
	N	%	N	%	N	%	N	%
Andesitic basalt	9	5.5	4	2.5	124	92.7	137	84.6
Rhyodacite	0	0	0	0	25	100	25	15.4
Total	9	5.5	4	2.5	149	92	162	100

Table 6.8. Square EIA02-001: stone assemblage (>10mm) composition by frequency and proportion.

Assemblage reduction

Complete flakes made from both materials have very low average SDI values (Table 6.9), suggesting low intensity nodule reduction. No marked change in reduction intensity is apparent between materials or through time on the andesitic basalt.

Despite the low SDI values on all flakes, most have no remnant cortex (n = 116, 71.6%). As with other sites on Enderby Island, andesitic blocks are predominantly non-cortical, and the low proportion of cortex most likely reflects the source material rather than reduction intensity.

MATERIAL	N	μ	SD
Andesitic basalt	44	0.43	0.39
Rhyodacite	8	0.41	0.39

Table 6.9. Square EIA02-001: Scar Density Index (SDI) for complete flakes (not including flakes <10 mm).

Rhyodacite flakes are, on average, slightly heavier with a greater surface area than andesitic basalt flakes (Table 6.10). High standard deviations for both materials indicate a wide variance in flake size. Elongated flakes are not common at the site (Table 6.11). No marked differences in flake shape or size occur through time on either material.

MATERIAL	WEIGHT (G)			SURFACE AREA (MM2)	
	N	μ	SD	μ	SD
Andesitic basalt	41	1.2	2.8	236.8	320.7
Rhyodacite	8	1.4	1.1	577.4	335.8

Table 6.10. Square EIA02-001: weight and surface area for complete flakes (not including flakes <10 mm).

MATERIAL	N	μ	SD
Andesitic basalt	41	1.6	0.6
Rhyodacite	8	1.34	0.8

Table 6.11. Square EIA02-001: elongation ratio for complete flakes (not including flakes <10 mm).

Tool selection and use

The 149 artefacts identified as tools at EIA02-001 have macroscopic and/or microscopic evidence for use along their edges and surfaces. Broken flakes make up most of the tool assemblage (n = 101, 67.8%).

Usewear and residue analysis

All artefacts from the >10mm EIA02-001 assemblage were inspected for usewear and 46 (28%) were tested for residues based on microscopic inspection (Figure 6.11).

	USEWEAR		NO USEWEAR	
	N	%	N	%
AU1 – andesitic basalt	115	92.7	9	7.3
AU1 – rhyodacite	25	100	0	0
AU2 – andesitic basalt	9	69.3	4	30.7
Total	149	92	13	8

Table 6.12. Square EIA02-001: stone artefacts with evidence for use.

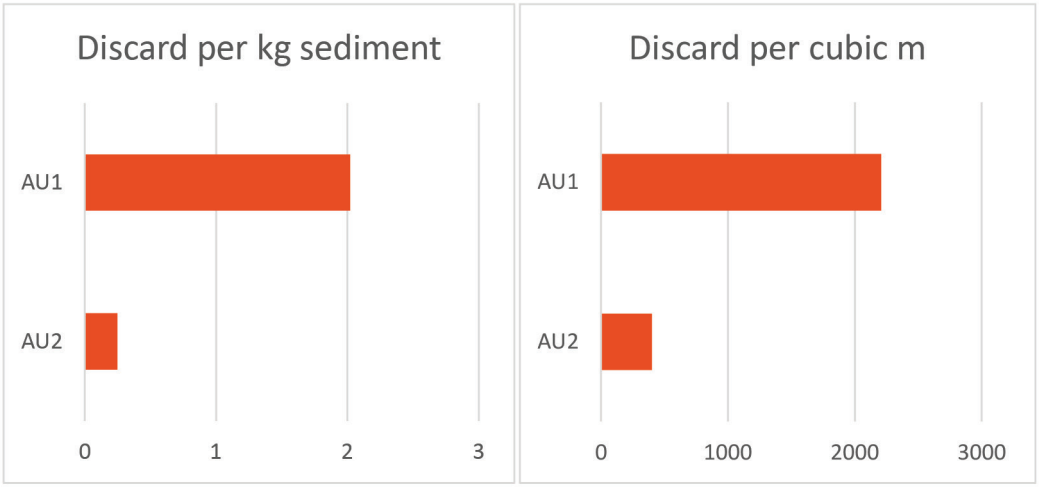

Figure 6.11. Square EIA02-001: artefact density per kilogram sediment and per cubic metre for each analytical unit.

Usewear was identified on a large proportion of the >10mm assemblage (n=149, 92%; Table 6.13 and Figure 6.12). Shallow edge scarring is the dominant usewear type in AU2, but this changes to polish for both materials in AU1. Rhyodacite artefacts have a higher instance of striations and polish than andesitic basalt artefacts in AU1 and AU2, indicating that these two raw materials were used for different activities. The decrease in shallow edge scarring and increase in polish (which, in the absence of positive blood tests, suggests the artefacts were used to process siliceous plant material) indicate that andesitic basalt artefacts in the Early Holocene were used to process softer plant resources than artefacts of the same material in the Terminal Pleistocene.

		MACROSCOPIC EDGE WEAR		POLISH		SHALLOW EDGE SCARRING		STRIATIONS		EDGE ROUNDING	
		N	%	N	%	N	%	N	%	N	%
AU1 – ANDESITIC BASALT	Y	23	18.5	81	65.3	56	45.2	47	37.9	22	17.7
	N	101	81.5	43	34.7	68	54.8	77	62.1	102	82.3
AU1 – RHYODACITE	Y	2	8.0	20	80.0	11	44.0	13	52.0	3	12.0
	N	23	92.0	5	20.0	14	56.0	12	48.0	22	88.0
AU2 – ANDESITIC BASALT	Y	0	0	5	38.4	7	53.8	2	15.3	0	0
	N	13	100	8	61.6	6	46.2	11	84.7	13	100
TOTAL		162		162		162		162		162	

Table 6.13. Square EIA02-001: presence and absence of usewear types identified on artefacts.

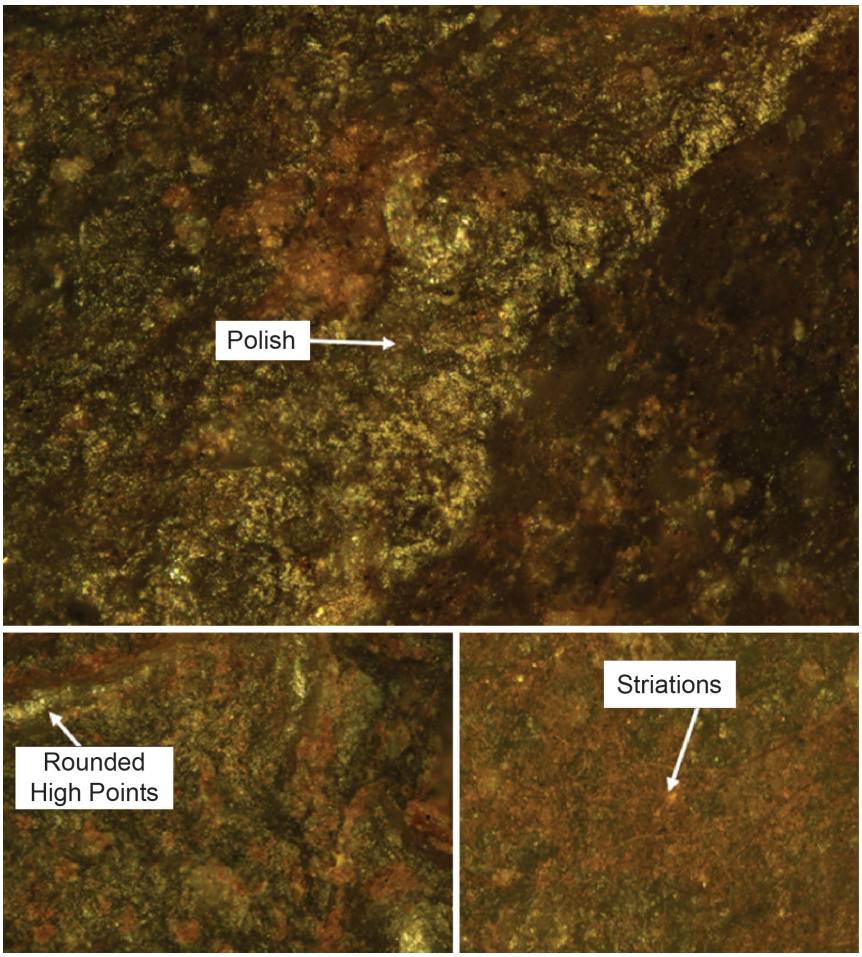

Figure 6.12. Square EIA02-001: examples of usewear present on tools.

Forty-six (30.1%) of the 142 identified tools from EIA02-001 were tested for blood and plant fibres. All 46 were positive for plant fibres but none tested positive for blood (Table 6.14). There is high variability in morphology and species of recovered plant fibre (Figure 6.13). A decrease in the fibre to artefact ratio through time occurs on andesitic basalt artefacts, and rhyodacite has a comparatively lower occurrence of fibres per artefact. There is also marked difference in the types of fibre recovered through time and between material types. Smaller, more fragmented plant fibres with low species diversity were recovered from the terminal Pleistocene assemblage, while larger, more intact fibres with a much wider species diversity were present on artefacts from the early Holocene. While there is potential for preservation to be a factor, this result suggests that ways in which andesitic basalt flakes were used changed through time. Rhyodacite flakes had a lower ratio of fibres present and the recovered fibres are smaller and more fragmented than andesitic basalt flakes in the Early Holocene (Figure 6.14 and Figure 6.15). This suggests that rhyodacite flakes were used for different types of activity than andesitic basalt flakes during the same time period. No statistically significant relationship could be established between the presence of plant fibres and the types of usewear present on the artefact (p = >0.05 in all cases), indicating a preference for multi-functional lithic toolkits at this site.

	TESTED	NOT TESTED	PLANT FIBRES IDENTIFIED	POSITIVE BLOOD TESTS
AU1 – ANDESITIC BASALT	34 (27%)	90 (73%)	204	0
AU1 – RHYODACITE	10 (40%)	15 (60%)	35	0
AU2 – ANDESITIC BASALT	2 (15%)	11 (85%)	16	0
TOTAL	46 (28%)	116 (72%)	297	0

Table 6.14. Summary of artefacts tested for residues from Square EIA02-001.

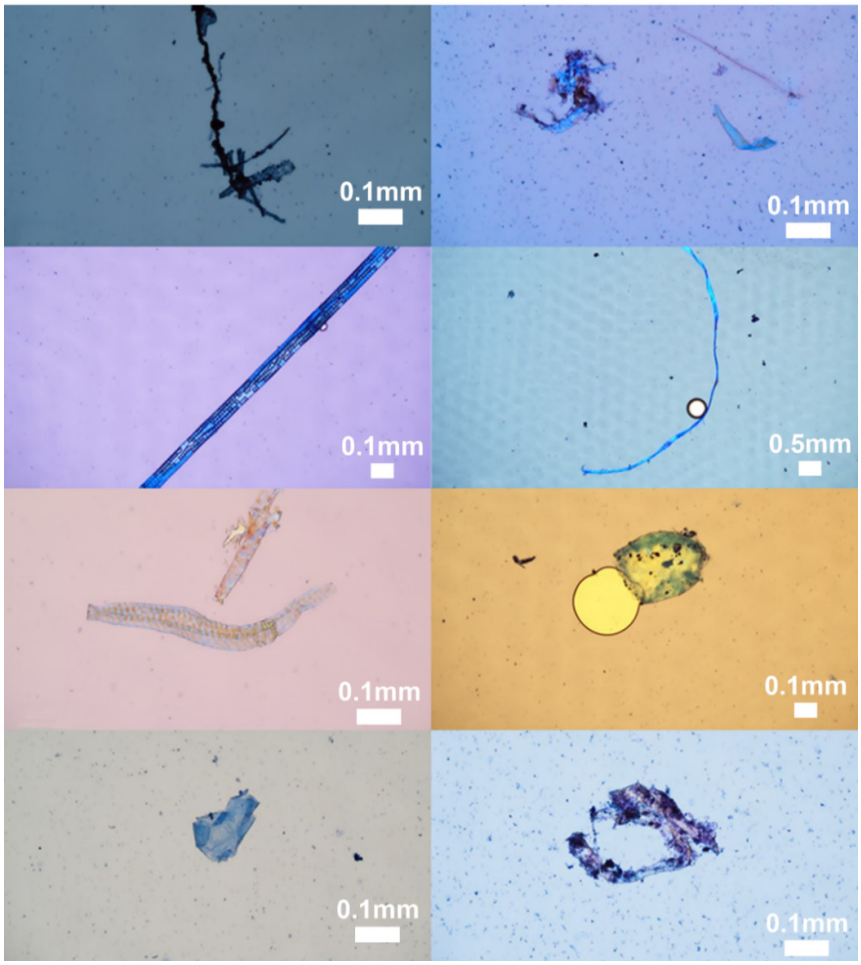

Figure 6.13. Wide variety of plant fibres recovered from andesitic basalt artefacts in AU1.

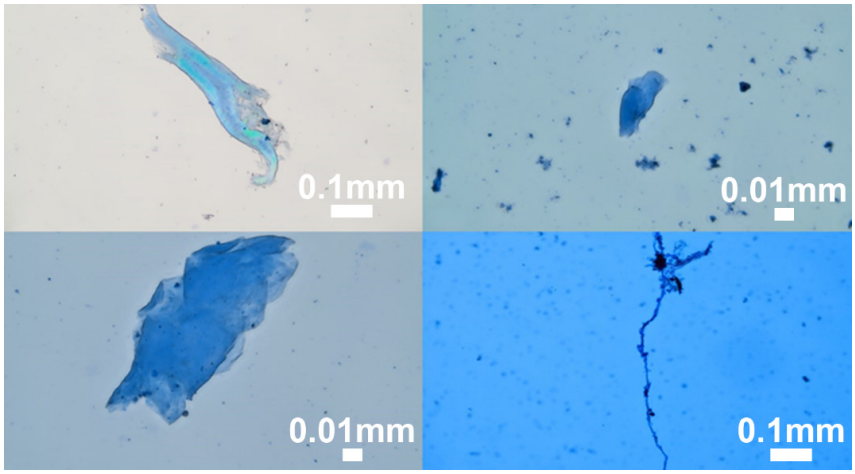

Figure 6.14. Plant fibres recovered from andesitic basalt artefacts in AU2 showing a reduction in fibre size and variation compared to andesitic basalt artefacts in AU1.

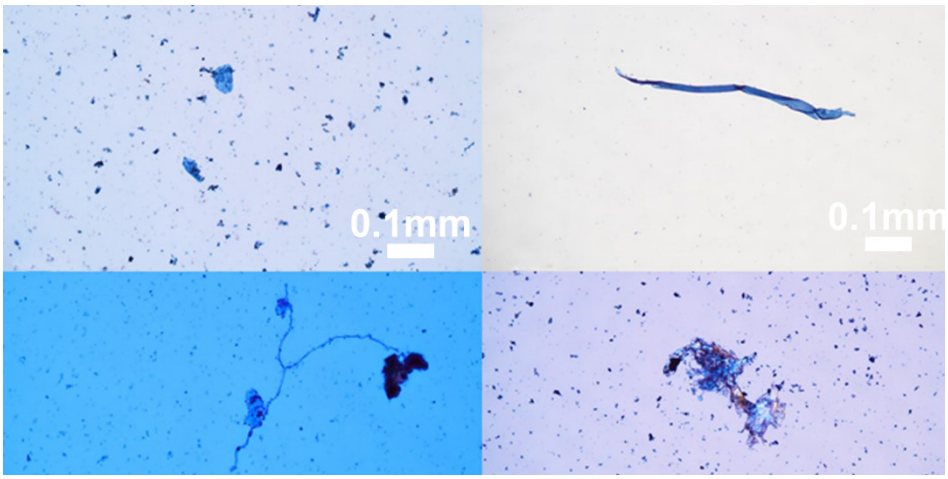

Figure 6.15. Plant fibres recovered from rhyodacite artefacts in AU1 showing smaller fibre sizes and a reduction in variation compared to andesitic basalt artefacts in AU1.

The combined usewear and residue analysis indicates that artefacts in the Terminal Pleistocene were used to process harder materials that resulted in less plant fibres adhering to the artefact and the creation of much more shallow scarring along the artefacts' margins. This changed in the Early Holocene to an assemblage dominated by activities which resulted in plant fibres and polished artefacts, indicating that the artefacts were used to process softer, and likely more siliceous, plant materials. The markedly high proportion of tools at this site is rare. Further work, including controlled sampling and analysis of non-artefactual rocks within the site, and usewear experiments to verify the use traces identified is planned.

Discussion

Aboriginal people appear to have used the Fig Tree site repeatedly for short stays, probably because of its reliable potable water source. Through time they brought stone artefacts from nearby lithic sources to process a very specific set of plants. The combined faunal and lithic results indicate that in their initial Pleistocene/Holocene Transition occupation of this location, people did not use this site intensively. At this time there was more shallow edge scarring and less polish, and the high number of hinge terminations suggests that harder materials were being processed. Plant fibres are also far smaller and more fragmented than found during the later use of the site.

During the Early Holocene occupation, as marine resources became more locally available and the site was used more intensively, small groups of people began occupying this locale to exploit the nearby mangroves for *Terebralia palustris* and probably other mangal resources. The artefact assemblage from the midden occupation layer reveals increased use of the lithic sources immediately adjacent to the site, more polish and edge rounding, more shallow edge scarring with feather terminations, and a wider variety of plant fibres being processed.

Changes in usewear between materials and through time indicates that during the Early Holocene people processed more diverse plant materials intensively using basalt flakes, before abandoning the site c. 7,530 years ago. It is possible that the preservation environment for residues here relates to the alkaline pH of the midden layer. Fibres in the Pleistocene/Holocene Transition layer are far more fragmented and smaller, which is interpreted to reflect different types of plant processing activity occurring at this time. There is a switch in raw material preference for this type of processing, as rhyodacite artefacts in AU1 have similar plant fibres to those found on basalt artefacts in the earlier layer.

The dominance of tools with recognisable and intensive usewear in this stone assemblage is unique in the current Murujuga excavation program and is discussed further in the next section in relation to Square EIA02-998997.

Square EIA02-998997

This 1.0 m x 1.0 m square was positioned on top of a notable rise in the sand body located in the valley adjacent to the rock art transect (Figure 6.1 and Figure 6.16). The square designation is based on its grid reference coordinates. There is no rock art in its immediate vicinity, and this square's placement was defined by the sedimentary opportunities of the sand body behind the modern dune system fronting the Holocene beach (Figure 6.16). The 1.0 m x 1.0 m square was aligned north–south with all X-Y-Z measurements taken from the south-west corner. An extension square (EIA02-998996) was excavated immediately to the south once the depth of the main square exceeded occupational health and safety limits, and to avoid the need for shoring. All levels and find locations were taken with an EDM. Excavation in this square proceeded in 2–4 cm units or stratigraphically with a total of 49 XUs dug in 2–4 cm depths. The scale was always photographed above the northern section. The additional square was not excavated to its base, and the analysis of recovered assemblages here concentrates only on the original square dug to its base.

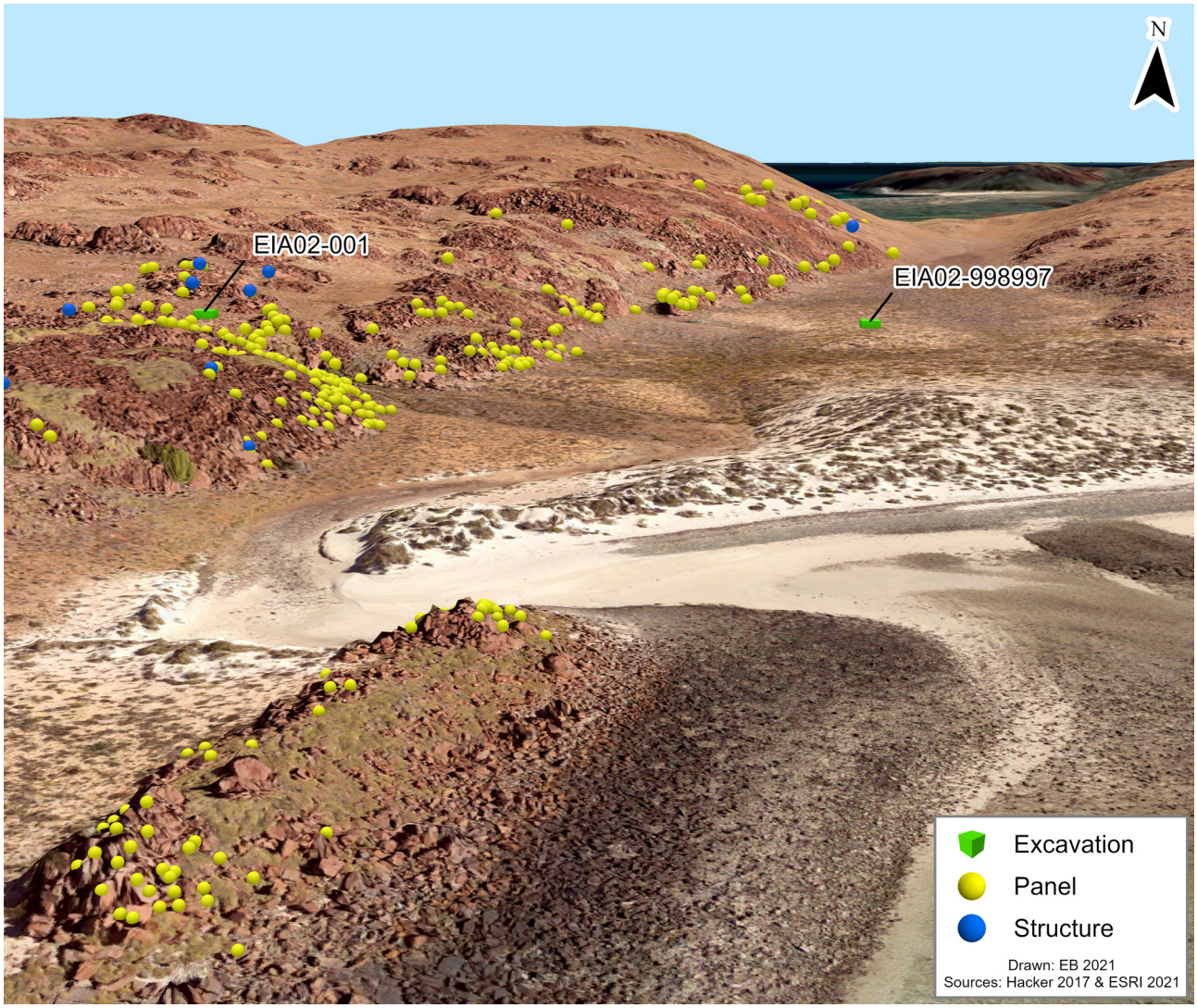

Figure 6.16. Context view: visualisation of the valley with squares EIA02-001 and 998997 showing topographic relief of square's locations relative to the recorded art and stone features. Source: Imagery and elevation surface courtesy of the DHSC project (Hacker 2017).

Stratigraphy and dating

Over 3,000 kg of sand was removed from square 998997. Six stratigraphic units were encountered in this deep sand body (Figure 6.17). Within the profile, colour intensifies and becomes generally redder with depth (Table 6.15). Compaction also increases with depth. Stratigraphic units 1 and 2 (SU1 and SU2) comprise the midden layer; SU3 contains some decomposing shell at its top but is much rockier and contains only stone artefacts.

SU1 – Dry loose bioturbated sand, bright brown (7.5YR 5/6) with fine tree roots, insect tunnels (the Ao layer). Boundary to next unit approximate: (pH 6);

SU2 – Firm bright reddish brown sand becoming even more consolidated and redder towards the base. Fine shell grit throughout; some small tree roots at top. Small fragments of economic shell, no major rock inclusion. Some artefacts (5YR 5/6 > 5YR4/6: pH 8);

SU3 – Similar sediment texture to above but more consolidated and with bigger shell fragments. Fragmentary midden layer: Trochus dominant, with Terebralia increasing at base. Orange reddish brown (5YR 6/6): pH 8; (OSL4);

SU4 – Terebralia layer in similar sediment texture to above (5YR6/6; pH 8). Consolidated fine sand with shell grit (OSL3);

SU5 – Very consolidated layer with some small rocky inclusions (5YR6/6; pH 8). Decomposing (smaller quantity) of Terebralia fragments (OSL2);

SU6 – Very hard white carbonaceous sediment mixed with bright reddish sand. Only partially excavated. A single quartz artefact (no shell) was retrieved from this layer (5YR 5/6; pH 8). OSL1 was taken from this layer.

OSL dates were taken down the sequence to understand the age of the stratigraphy and cultural layers (see Figure 6.17). These were analysed by the Nordic Laboratory for Luminescence Dating at Aarhus University (Table 6.16). The lab performed feldspar pIRIR dating to confirm that the quartz is well bleached (feldspar IRSL and post-IR IRSL signals bleach much slower than quartz so if feldspar agrees with quartz, the quartz is definitely well bleached; Murray et al. 2012). The slight inversion at 91 cm depth (sample 176906) is likely a dose rate problem (Jan-Pieter Buylaert, pers. comm., 1 June 2017) and could indicate a period of increased bioturbation / dune mobilisation (Figure 6.18).

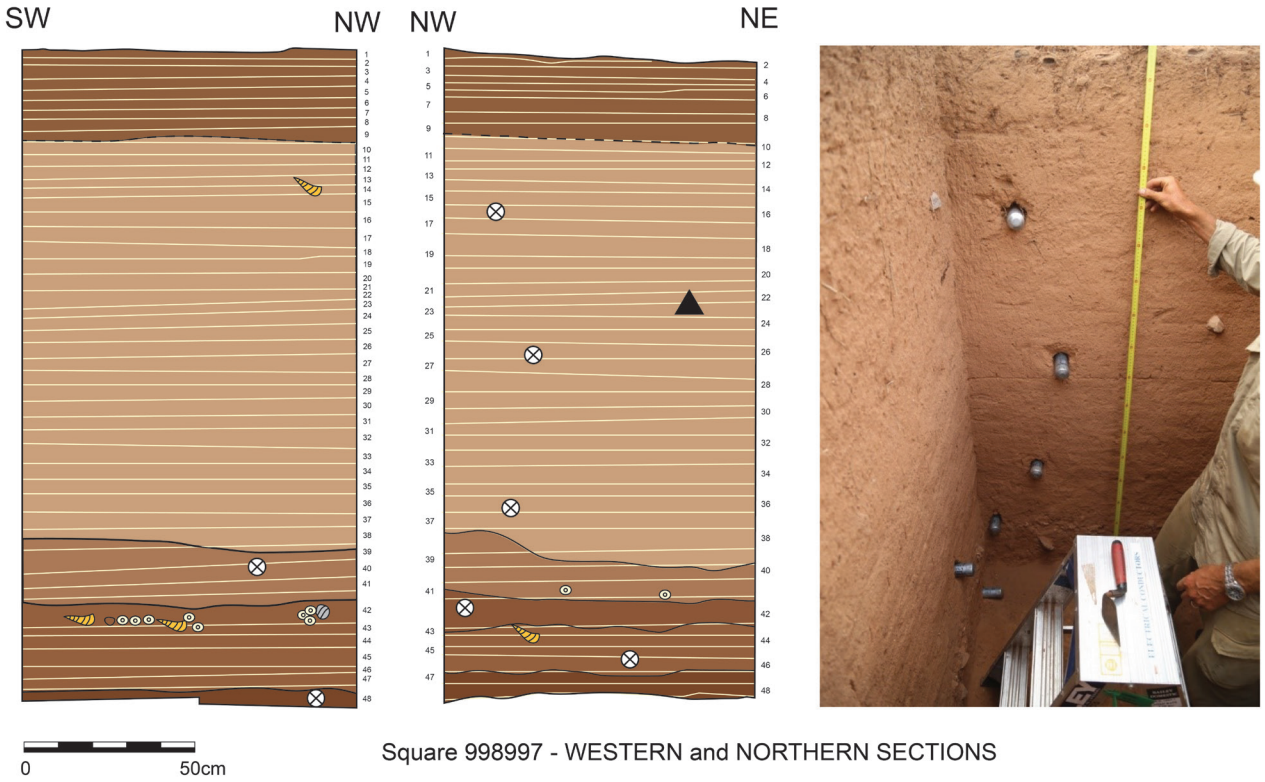

Figure 6.17. Stratigraphic sections for western and northern baulks Square EIA02-998997 showing correlation with excavation units.

UNIT	DEPTH BELOW SURFACE (CM)	DEPOSIT EXCAVATED (KG)	WEIGHT ROCKS DISCARDED (KG)	PH	MUNSELL
XU01	1.00	37.8	–	7	7.5YR 5/6
XU02	3.0	34.8	–	7	7.5YR 5/6
XU03	5.9	49.8	–	7	7.5YR 5/6
XU04	9.5	44.2	–	7	7.5YR 5/6
XU05	12.2	41.4	–	7	7.5YR 5/6
XU06	15.6	49.6	–	6	7.5YR 5/6
XU07	19.2	45.2	–	6	7.5YR 5/6
XU08	22.2	43.1	–	6.5	7.5YR 4/6
XU09	27.6	75.8	–	6.5	7.5YR 4/6
XU10	31.0	49	–	6.5	7.5YR 4/6
XU11	34.4	53.4	–	6.5	7.5YR 5/6
XU12	37.6	55.4	–	6.5	7.5YR 5/6
XU13	41.0	49.8	–	6.5	7.5YR 5/6
XU14	44.9	55.8	–	7.5	7.5YR 5/6
XU15	48.6	60.6	–	7.5	7.5YR 5/6
XU16	53.1	73.5	–	7.5	7.5YR 5/6
XU17	58.6	75.6	–	7.5	7.5YR 5/6
XU18	62.9	59.6	–	8	7.5YR 5/6
XU19	67.5	80.5	–	7.5	7.5YR 5/6
XU20	72.6	62.6	–	7.5	5YR 5/6
XU21	75.7	40.1	–	8	5YR 5/6
XU22	79.6	66.3	–	8	5YR 5/6
XU23	83.1	58.2	–	8	5YR 5/6
XU24	87.1	82.6	–	8	5YR 5/6
XU25	91.4	56.7	–	8	5YR 5/6
XU26	95.8	72.2	–	8	5YR 5/6
XU27	100.8	104	–	8	5YR 5/6
XU28	105.4	74.5	–	8	5YR 5/6
XU29	109.9	70	–	8	5YR 5/6
XU30	114.2	76.2	–	8	5YR 4/6
XU31	118.9	77.8	–	8	5YR 4/6
XU32	124.3	82.4	–	8	5YR 4/6
XU33	128.2	87.3	–	8	5YR 5/6
XU34	133.5	73.1	–	8	5YR 5/6
XU35	137.9	96.2	–	8	5YR 5/6
XU36	142.0	80	–	8	5YR 5/6
XU37	147.5	77.4	–	8	5YR 5/6
XU38	153.4	11.8	–	8	5YR 5/6
XU39	159.3	80.9	–	8	5YR 6/6
XU40	163.3	80	–	8	5YR 6/6
XU41	167.3	76.3	–	8	5YR 6/6
XU42	172.3	58.2	–	8	5YR 6/6
XU43	175.3	15.6	3.2	8	5YR 6/6
XU44	179.0	65.2	2.8	8	5YR 6/6
XU45	182.8	52.8	6.4	8	5YR 6/6
XU46	186.8	66.9	3.6	8	5YR 5/6
XU47	189.9	70.3	1	8	5YR 5/6
XU48	193.1	72.8	0.8	8	5YR 5/6
XU49	195.2	21.56	–	8	5YR 5/6
Total	–	3,057.9	17.8	–	–

Table 6.15. Square 998997 excavation units, weights for deposit (kg) and sediment characteristics.

FIELD CODE	LAB CODE	XU CORRELATE	SU	AU	DBS (CM)	TOTAL DOSE RATE (GY/KA)	CALIBRATED AGE RANGE
EIA02 OSL 7	17 69 07	11–37	2	1	45	2.28 ± 0.09	2,850 ± 240
EIA02 OSL 6	17 69 06	11–37	2	1	91	2.10 ± 0.08	4,680 ± 370
EIA02 OSL 5	17 69 05	11–37	2	1	136	3.80 ± 0.19	2,980 ± 210
EIA02 OSL 4	17 69 04	38–41	3	2	152	2.83 ± 0.11	6,650 ± 480
EIA02 OSL 3	17 69 03	42–43	4	3	167	3.25 ± 0.12	9,500 ± 700
EIA02 OSL 2	17 69 02	44–46	5	3	182	3.37 ± 0.13	10,500 ± 700
EIA02 OSL 1	17 69 01	47,48	6	4	191	3.32 ± 0.13	13,500 ± 1000

Table 6.16. Summary of single grain palaeodose data and ages for Square 998997 (see OSL methods section in Chapter 2).

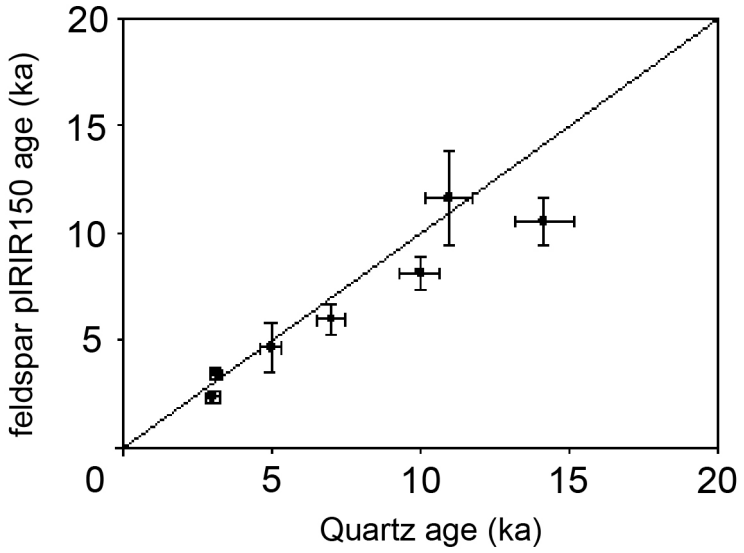

Figure 6.18. Square 998997 six OSL samples showing well-bleached quartz through feldspar IRSL and post-IR IRSL signals.

Bayesian analysis

The Bayesian analysis for Square 998997 followed the methodology applied on all Murujuga excavation sequences (Chapter 2). Four major analytical units with OSL determinations (based on the stratigraphy and the returned dates) were modelled as phases for Square 998997: AU1 = Late to Mid-Holocene, AU2 = Mid-Holocene, AU3 = Early Holocene and AU4 = Late Pleistocene. Since there is no evidence for discontinuities in deposition at Square 998997, continuous boundaries were used to separate the phases in the model. No calibration curve was used since no radiocarbon dates are available for Square 998997.

Results for the Bayesian analysis are shown in Table 6.17 and Figure 6.19. This model estimates that this part of the sand body was first occupied between 15,760 and 11,970 cal. BP and was occupied throughout the Holocene until 2,990–1,710 cal. BP. The sequence is well supported by the outlier analyses, and each date has <6% chance of being an outlier. The model, more generally, also returns high agreement indices (A_{model} = 99.7; $A_{overall}$ = 100.1).

The Square 998997 Bayesian ranges on boundary age estimates are large. This is partly because the OSL age determinations have much larger ranges than radiocarbon, but also because several analytical units are represented by a single OSL date, increasing the potential range of these analytical unit boundaries.

NAME	68.2%		95.4%		SUM. STATISTICS			INDICES	
	FROM	TO	FROM	TO	μ	σ	M	AI	OP
Boundary: Mid-Holocene / Late Holocene	2,990	1,710	3,210	–760	1,860	1,230	2,250		
Phase: Late Mid-Holocene									
17 69 07	3,140	2,670	3,370	2,420	2,900	240	2,900	101.5	95.8
17 69 06	4,950	4,170	5,350	3,720	4,530	420	4,550	96	94.5
17 69 05	3,210	2,780	3,420	2,580	3,000	210	3,000	102.2	95.9
Boundary: Mid-Holocene Transition	6,120	4,530	7,020	4,020	5,410	780	5,360		
Phase: Mid-Holocene									
17 69 04	7,140	6,190	7,620	5,710	6,660	480	6,660	101.6	95.6
Boundary: Early Holocene / Mid-Holocene	9,700	7,210	10,360	6,330	8,390	1,100	8,440		
Phase: Early Holocene									
17 69 03	10,350	9,070	10,960	8,380	9,690	650	9,700	102.6	95.6
17 69 02	10,910	9,620	11,580	9,010	10,280	640	10,280	102.4	95.5
Boundary: Late Pleistocene / Early Holocene	12,410	10,160	13,800	9,492	11,510	1,120	11,400		
Phase: Late Pleistocene									
17 69 01	14,040	11,990	15,060	11,040	13,040	1,010	13,030	94.3	95.2
Boundary: Deposit Base	15,760	11,970	21,830	10,740	14,960	3,070	14,160		

Table 6.17. Bayesian analysis results for Square 998997.

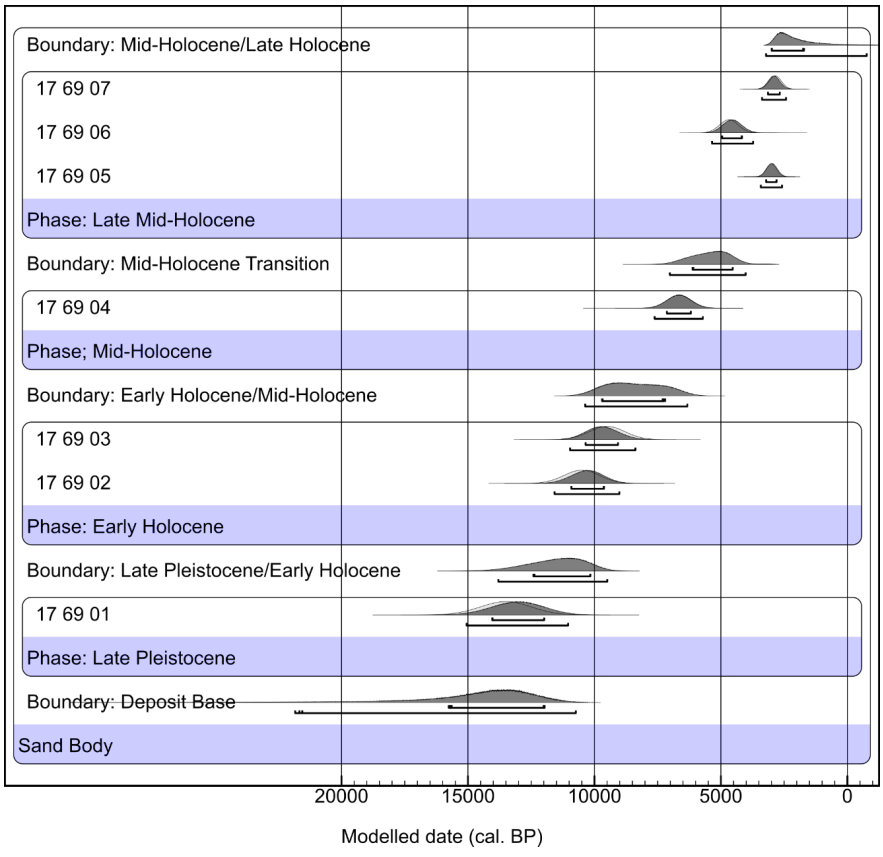

Figure 6.19. Bayesian analysis results for Square 998997.

ANALYTICAL UNIT	PHASE	TIME FRAME	XUS
AU1	Post islandisation	Mid-Late Holocene 6,120–1710 cal. BP)	XU1–36
AU2	Insulation	Mid-Holocene (7,210–6,190 cal. BP)	XU37–41
AU3	Coast proximal	Late Pleistocene / Early Holocene (12,410–9,700 cal. BP)	XU42–47
AU4	Coast >20km	Late Pleistocene (14,040–11,990 cal. BP)	XU48

Table 6.18. Square EIA02-998997: analytical phases correlated with Bayesian modelled dates (Table 6.17) and environmental phases.

Excavated assemblage

The Square 998997 cultural assemblage weighed over 10.6 kg. This predominantly comprised shellfish (8.3 kg), stone artefacts (2.2 kg) and c. 28 g of bone (Table 6.19).

The very low occurrence of cultural material in the upper section of AU1 suggests that this loose sandy surface layer may be a modern depositional feature, although it should be noted that the nearby foredunes have numerous surface camp sites, and it is clear from historic accounts (e.g. King 1818) that Aboriginal people were camping in this area into the historic period. Shell and bone are found sporadically throughout AU1, with shell increasing in the earliest levels of AU3. There is an artefactual feature in the centre of AU3 (dated to 2.8 ka from OSL7). Note that several items were mislabelled as from XU49: there were only 48 excavation units, and these mislabelled items have been analysed in their correct AUs (Table 6.19).

UNIT	AU	FLAKED ARTEFACTS (G)	SHELL (G)	BONE (G)	CULTURAL MATERIAL TOTAL WEIGHT (G)
XU01	1		0.52		0.66
XU02	1	5.23	0.44		9.5
XU03	1	0.02	0.61		0.71
XU04	1	0.07	0.11	0.52	0.87
XU05	1	0.03	1.57	0.01	3.05
XU06	1		1.97		1.97
XU07	1	3.4	3.15	3.46	7.54
XU08	1	2.15	2.95	2.16	19.09
XU09	1	12.76	7.11	5.6	39.05
XU10	1	0.15	4.52	1.32	7.22
XU11	1	21.06	5.93	4.6	52.89
XU12	1		2.8	3.63	6.69
XU13	1	0.15	4.48	0.61	310.61
XU14	1		4.46	0.33	4.89
XU15	1		4.16	0.45	4.85
XU16	1		8.93	0.27	9.68
XU17	1	41.45	14.68	0.2	103.94
XU18	1	4.37	12.32		17.62
XU19	1	0.76	17.7		18.98
XU20	1	0.09	24.8		26.34
XU21	1		18.491		18.491
XU22	1		41.951	0.001	41.952
XU23	1	0.01	41.5	0.61	42.69
XU24	1		37.441		37.501
XU25	1	0.21	34.69		35.33
XU26	1	1.04	54.59		56.85
XU27	1		52.011		52.771
XU28	1		49.07		49.35
XU29	1		33.86		33.98
XU30	1	0.1	81.03		81.29
XU31	1		17.83	0.01	17.84
XU32	1	0.85	32.07		33.99
XU33	1		50.803		52.003
XU34	1	0.51	59.3	0.1	60.36
XU35	1		105.9		105.9
XU36	1	0.38	143.68		144.48
XU37	2		529.95		529.95
XU38	2	1.44	1026.08		1028.98
XU39	2	0.17	189.401		189.801
XU40	2		135.98		154.84
XU41	2	54.5	312.19		421.77
XU42	3	339.14	2934.29	3.08	3644.7
XU43	3	56.04	1876.83	1.47	2000.19
XU44	3	40.76	254.75		336.83
XU45	3	261.82	58.3		581.83
XU46	3	88.77	54.07		211.85
XU47	4		6.57		6.57
XU48	4	0.09	7.12		7.23
Total		937.5	8,362.9	28.4	10,625.5

Table 6.19. Square EIA02-998997: excavation units and weights for deposit (in kg) and cultural materials (all in g).

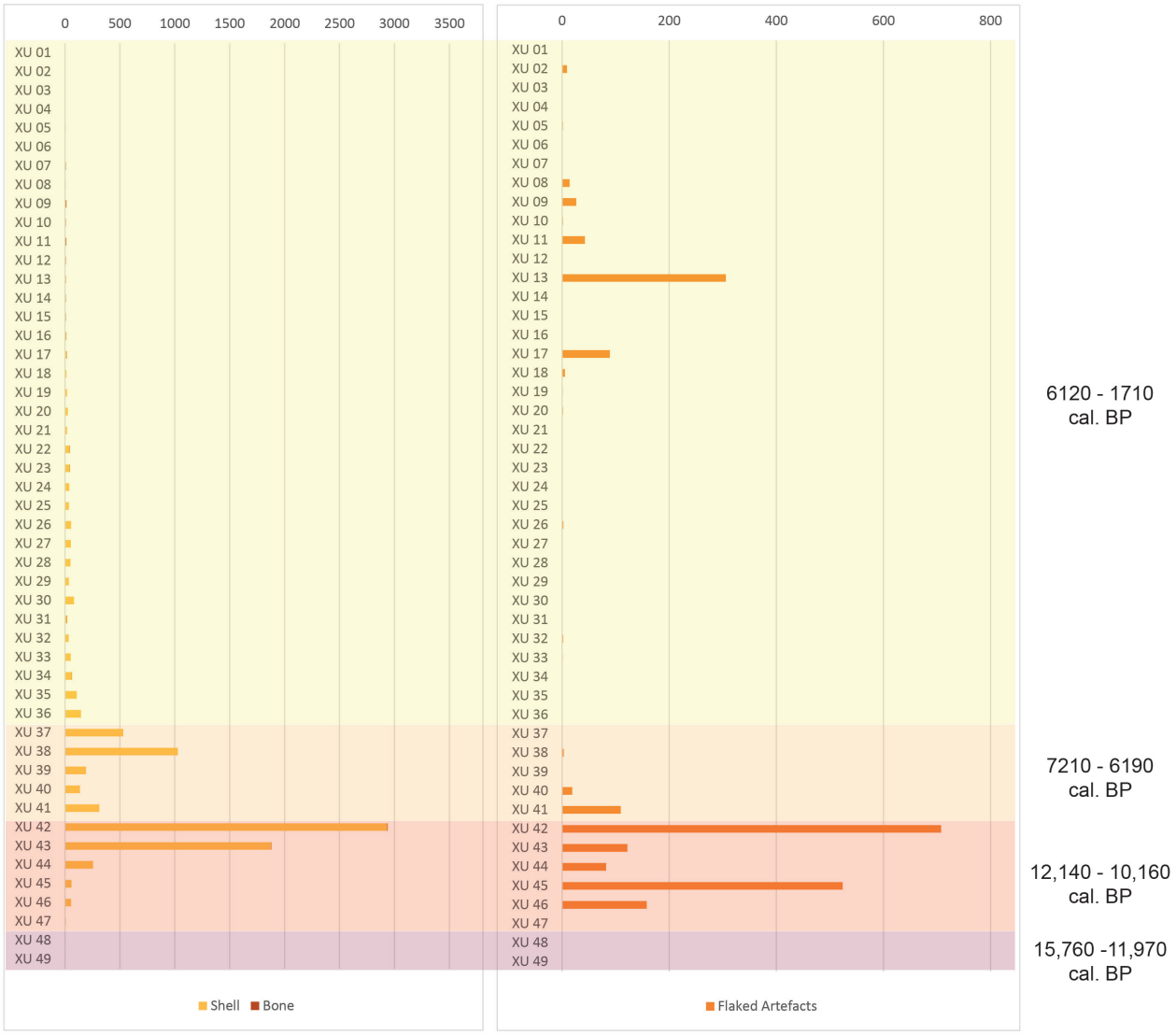

Figure 6.20. Square EIA02-998997: proportions of shell and bone (left) and stone artefacts found (right) (showing Bayesian modelled median ages, Table 6.18).

Economic shellfish

AU4 is dated to the Terminal Pleistocene (after 15.7 ka cal. BP) and contains only a single artefact as evidence for people occupying this broad featureless landscape. AU2 and AU3 represent two midden phases. AU3 relates to establishment of the mangrove forest coastal environment at the Pleistocene/Holocene (P/H) Transition. AU2 represents an islandisation phase event (after 7.2 ka BP). The weights of shell are highest in the P/H coastal establishment phase midden, and there is also a significant deposition of stone artefacts in this period. The post-islandisation phase midden represents a lower intensity occupation phase in terms of shell weights and a decrease in lithic tool use. It should be reiterated that this is a single metre square sample from a relatively featureless landscape which covers several hundred hectares, roughly 180 m from the Fig Tree waterhole.

The different phases of occupation (AU1–3) indicate changed predation zones in shellfish procurement (Table 6.20, Table 6.21 and Figure 6.21). The earliest occupation at the site focused on mangrove resources, mostly *Terebralia* but also *Telescopium*. Once Enderby Island formed, there was a major switch to rock platform species (particularly *Turbo* and *Trochid*), although *Terebralia* and *Telescopium* remained significant contributors to the diet.

HABITAT	SPECIES	AU1 (G)	AU2 (G)	AU3 (G)	AU4 (G)	TOTAL (G)
Mangrove mudflats	*Terebralia palustris*	66.59 (1)	332.59 (24)	4,171.28 (411)	4.72	4,575.18
Mangrove mudflats	*Telescopium*	0	0	463.62	0	463.62
Rocky	*Polyplacophora*	154.21	41.09	0	0	195.3
Rocky	*Saccostrea sp.*	23.813	0.8	28.66	0.68	53.953
Rocky	*Trochid*	129.45 (6)	318.05 (19)	0.55	0	448.05
Rocky	*Dentalium*	0.35	0	0	0	0.35
Rocky	*Echinoida*	2.36	0.311	0	0	2.671
Rocky	*Turbo*	479.48	769.44	66.3	0	1,315.22
Sandy	*Melo amphora*	1.5	0.53	17.44	0	19.47

Table 6.20. Shellfish species and their habitats in the different analytical units (MNI in brackets, where available).

During the Holocene, when this part of the island was some distance from the mainland, shell deposition was significantly less frequent, and rock platform species – particularly chiton and *Turbo* – dominated the shellfish diet. *Terebralia* contributed only a very minor component of the diet at this time. Scaphopods (potentially beads, not economic shellfish) were found at the site in this later Mid-Holocene period (XUs 20, 23, 28).

HABITAT	AU1	AU2	AU3	AU4	TOTAL (G)
Mangrove mudflats	66.59	332.59	4,634.9	4.72	5,038.8
Rocky	789.663	1,129.691	95.51	0.68	2,016.7
Sandy	1.5	0.53	17.44	0	19.5

Table 6.21. Summarised shellfish habitat information for the different analytical units

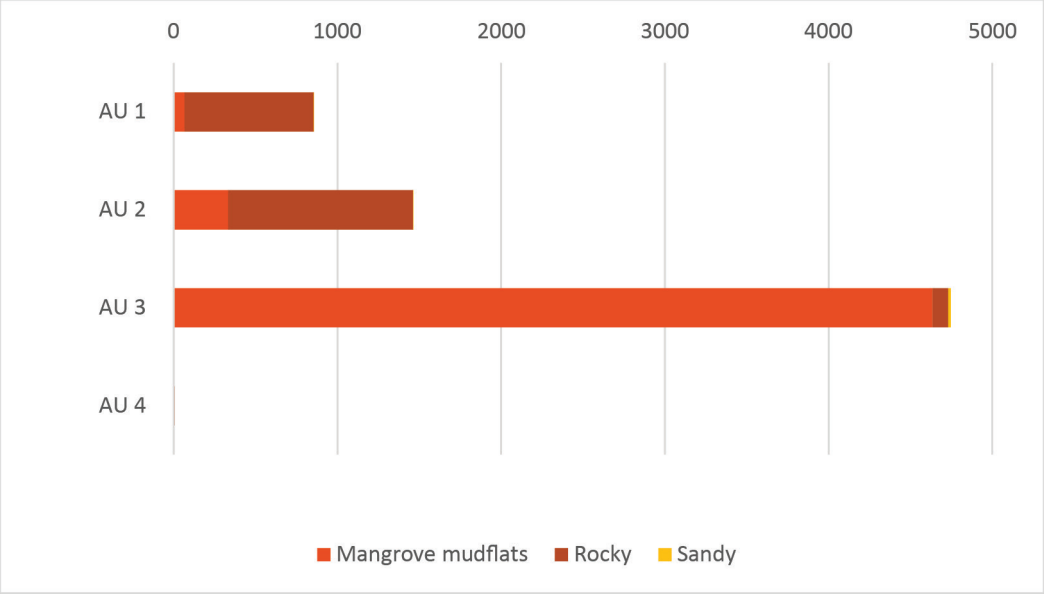

Figure 6.21. Square EIA02-998997: changed habitat preferences in the different analytical units shown as proportions of shellfish (weights in grams).

Minimum numbers of individuals (MNI)

As at Fig Tree, the MNI of *Terebralia* and *Trochid* species was provided by the number of complete anterior ends with a majority part (or all) of the aperture present (Table 6.20; for method, see Chapter 2). The other taxa provided small, non-diagnostic fragments and additional MNI could not be calculated. Calculation of *Polyplacophora* MNI has not been attempted here.

Of the 436 identified *Terebralia*, 208 individuals could be measured. Their mean width was 22.00 mm, with a standard deviation (SD) of 3.36 mm. The MNI and size of shellfish are important indicators of past collection strategies and diet. We cannot calculate total shellfish meat weights from this sand body (from Square 998997) as the midden layer is deeply buried and its area/volume cannot be estimated from its surface extent. However, using estimates for live weight (shell plus meat) given earlier, the 436 *Terebralia* in this one 1 x 1 m square represents c. 8 kg of shellfish. The amount of meat represented per individual *Terebralia* (4.4 g), indicates Square 998997 represents c. 1.9 kg of shell meat, which

could have been collected in a very short time. Using Meehan's (1982) Northern Territory observations, this food represents a collection time of c. 2.5 hours.

Shell size distribution can indicate dietary and harvesting choices (Figure 6.22). Mean valve length (dots) and standard deviations (whiskers) vary very little through the P/H analytical unit (t-tests indicate p H0 <0.02, using two-tailed tests of paired XUs with unequal variance). Again, this distribution suggests strong selectivity in the harvesting of *Terebralia* in the Early Holocene occupation of the sand body (cf. Figure 6.9). This size selectivity is very similar to that demonstrated at Fig Tree c. 8,000 cal. BP, indicating a long-term sustainable harvesting practice.

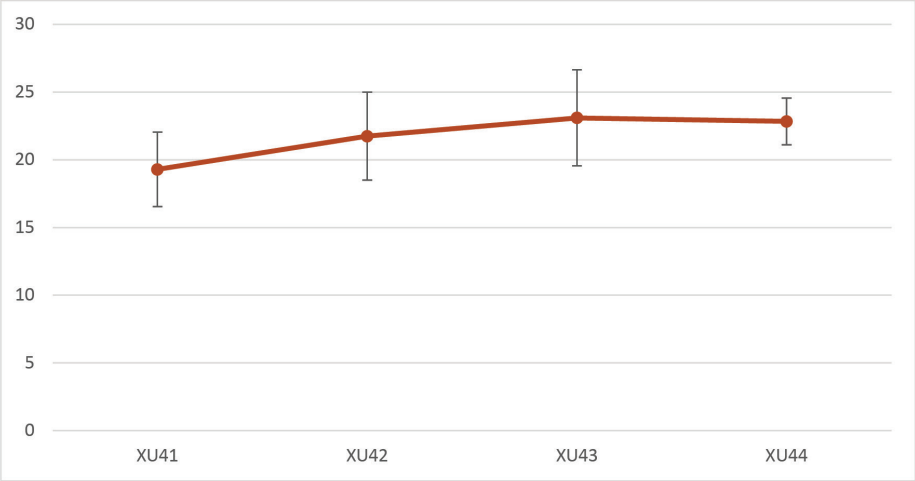

Figure 6.22. Square EIA02-998997: distribution of average widths (mm) of *Terebralia* through four XUs (n = 208, 1% are adult).

Stone artefacts

The lithic assemblage from this site was initially analysed by Tessa Woods for her Honours research (Woods 2018). Here, the assemblage (111 stone artefacts) was re-recorded and analysed in the defined analytical units. The relatively small lithic assemblage is disproportionately distributed between the four analytical units (Figure 6.23). Over half the stone assemblage sits within the P/H analytical unit, while most of the remaining assemblage derives from the Mid and Late Holocene unit (AU1, Table 6.22). The only artefact from the Late Pleistocene is a small distal flake made on high-quality quartz. The significant volume of artefacts (n = 66, 59.5%) corresponds with a sizeable shellfish accumulation in AU3, in contrast to the similar aged layer at Fig Tree which contains artefacts but no shell.

Assemblage composition

As indicated by pXRF analysis, the assemblage in square EIA02-998997 is predominantly composed of andesitic basalt (Table 6.22 and Figure 6.23). Rhyodacite, found in smaller frequencies here, is coarser grained and contains visible inclusions. The highest proportion of artefacts made on this material are found in AU3. Quartz artefacts occur throughout the sequence: the single earliest artefact is made of quartz.

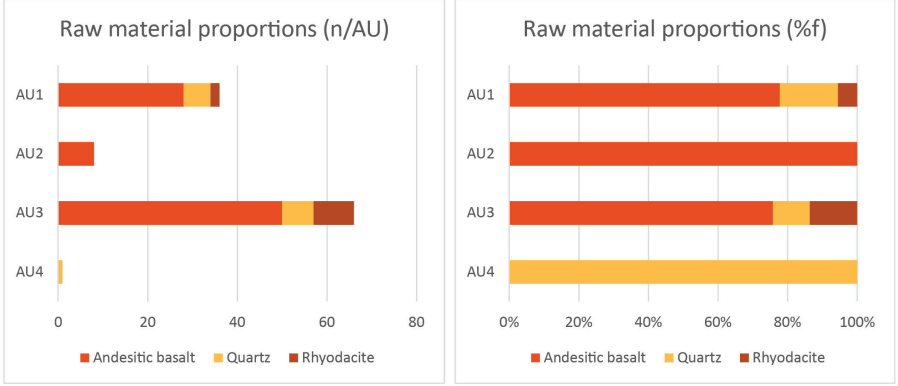

Figure 6.23. Square EIA02-998997: proportions of raw materials in the analytical units.

MATERIAL/AU	ANDESITIC BASALT	%F	QUARTZ	%F	RHYODACITE	%F	TOTAL
1	28	77.8	6	16.7	2	5.6	36
2	8	100	–	–	–	–	8
3	50	75.8	7	10.6	9	13.6	66
4	–	–	1	100	–	–	1
Total	86	77.5	14	12.6	11	9.9	111

Table 6.22. Square EIA02-998997: raw materials per analytical unit.

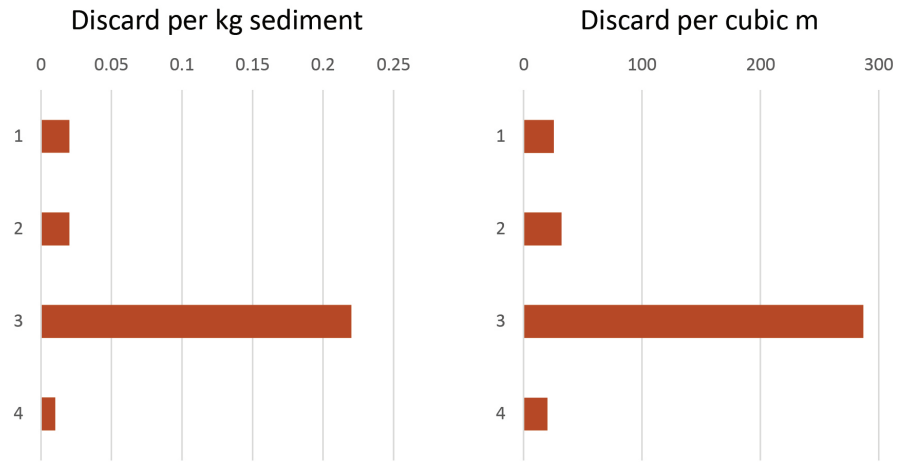

Figure 6.24. Square EIA02-998997: artefacts overlaid on the regional mapping of the different raw materials sampled from across the Dampier Archipelago.

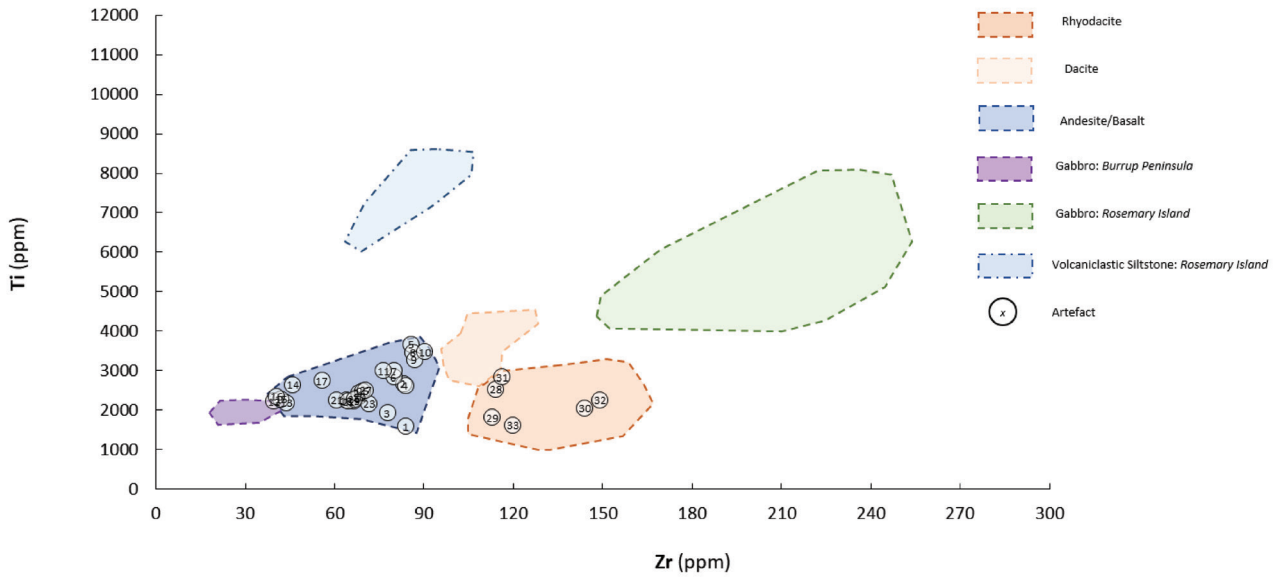

Figure 6.25. Square EIA02-998997: artefact density per kilogram sediment and per cubic metre for each AU.

The assemblage is dominated by complete flakes and broken flakes (Table 6.23), but also includes five tools, two complete cores and a core fragment. Except for one rhyodacite core, all cores and tools were made on andesitic basalt. As sample sizes are low throughout most occupation phases, it is difficult to meaningfully compare assemblage composition through time. It is worth noting, however, that all tools and cores were discarded during the Mid-Holocene or earlier (AU2–4).

ARTEFACT TYPE/ MATERIAL	BROKEN FLAKE		COMPLETE FLAKE		TOOL		CORE / CORE FRAGMENT		TOTAL	
	N	%	N	%	N	%	N	%	N	%
Andesitic basalt	19	29.2	40	61.5	4	6.2	2	3.1	65	77.4
Quartz	7	77.8	1	11.1	1	11.1	0	0.0	9	10.7
Rhyodacite	4	40.0	5	50.0	0	0.0	1	10.0	10	11.9
Total	30	35.7	46	54.8	5	6.0	3	3.6	84	100.0

Table 6.23. Square EIA02-998997: stone assemblage composition by frequency and proportion (artefacts >1 cm).

Assemblage reduction

Except for a single quartz flake with an SDI value of 2.18, flakes made on all materials have low average SDI values (Table 6.24), suggesting low intensity nodule reduction. The very low frequencies of flakes with platforms showing multiple previous flake removals also indicates this (flaked platforms = 3). The very low mean SDI value on rhyodacite flakes is not surprising given that this is a coarser-grained material compared with finer-grained andesitic basalt. No changes through time in andesitic basalt reduction intensity are apparent.

Most artefacts contain no remnant cortex (n = 74, 88.1%). Much like other Enderby Island stone assemblages, low proportions of cortex here seem to reflect proximity to source locations rather than high reduction intensity. Other reduction measures (SDI, flake attributes) support this interpretation about cortical presence.

Andesitic basalt flakes are, on average, markedly larger and heavier than the granophyre flakes (Table 6.25). Very high standard deviations on basalt flakes indicate a high variance in flake size, particularly during the Mid and Late Holocene (AU1). Flake shape for basalt and granophyre complete flakes is generally squat (Table 6.26). No marked differences in flake size or shape can be seen through time on either material.

MATERIAL	N	μ	SD
Andesitic basalt	40	1.07	0.49
Quartz	1	2.18	–
Rhyodacite	5	0.77	0.32

Table 6.24. Square EIA02-998997: Scar Density Index (SDI) for complete flakes (excluding flakes <10 mm).

MATERIAL	WEIGHT (G)			SURFACE AREA (MM2)	
	N	μ	SD	μ	SD
Andesitic basalt	40	7.5	10.4	715.3	697.8
Quartz	1	4.4	–	567.3	–
Rhyodacite	5	8.6	8.7	851.2	437.8

Table 6.25. Square EIA02-998997: weight and surface area for complete flakes (not including flakes <10 mm).

MATERIAL	N	μ	SD
Andesitic Basalt	40	1.1	0.6
Quartz	1	1.2	-
Rhyodacite	5	0.9	0.4

Table 6.26. Square EIA02-998997: elongation ratio for complete flakes (not including flakes <10 mm).

The two complete cores were discarded at EIA02-998997 during the Pleistocene/Holocene Transition (AU3). A rhyodacite core has a single platform with two flake removals and a low SDI value (0.5). In contrast, the basalt core was more intensively reduced (SDI: 1.9), having been rotated to remove eight flakes from two platforms. The basalt core fragment, also discarded in this period, has six partial flake removals. No cortex remains on the cores or core fragment.

Tool selection and use

The five tools recovered from this square all display minimal use before discard. The retouched complete flake discarded in the Mid-Holocene (AU2) exhibits approximately 20% scalar retouch along its usable edge margin. The complete used flake discarded during the Pleistocene/Holocene Transition (AU3) exhibits macroscopic usewear along approximately 35% of its perimeter, as do two other retouched artefacts with scalar retouch and some macroscopic evidence for usewear. Microscopic usewear and residue on the quartz tool discarded in the lowest unit (AU4) is detailed below.

The two complete basalt tools, which weigh 51.9 g and 4.6 g, indicate no preference for tool size. However, these basalt tools are more elongated (ratio 1.4 for both) than unused basalt flakes.

Usewear and residue analysis

One artefact was inspected microscopically for usewear and residue to assess macroscopic edge damage. The oldest artefact found in this square (artefact 998997-XU49-LA229) is a small broken quartz flake discarded during the Late Pleistocene (Figure 6.26). Conchoidal micro-fractured polish with multidirectional striations covers approximately 80% of the artefact, indicating that it was used intensively before being discarded. Residue analysis recovered plant fibres and silica, which is consistent with use (rather than latent soil contam-

ination). However, the plant fibres are small and non-diagnostic. Given the small and scattered nature of the plant fibres, highly polished artefact surface, and presence of silica, it is likely that artefact 998997-XU49-LA229 was used intensively to process highly siliceous plant material. The survival of these residues from this early period, on an artefact located in an open, exposed area, is remarkable.

Discussion

Artefact discard, stone reduction and shellfish consumption at Square 998997 all indicate that this place first records human presence during the Terminal Pleistocene, but that more regular occupation of this open landscape began during the Pleistocene/Holocene Transition. Some caution is required when making behavioural interpretations about increased artefact discard because artefact counts are low throughout the sequence.

This peak in stone artefacts coincides with a peak in shell discard, suggesting that this record does show focused human use of the open valley during this time – prior to the development of the deep sand body. This Terminal Pleistocene / Early Holocene use is earlier than the Early Holocene artefact and shellfish discard found at nearby Square EIA02-001. The results from these two very small excavations in different landscape contexts suggest that this part of Enderby Island was visited more frequently during the time that these sites were close to well-established mangrove forests and this landscape remained part of the mainland.

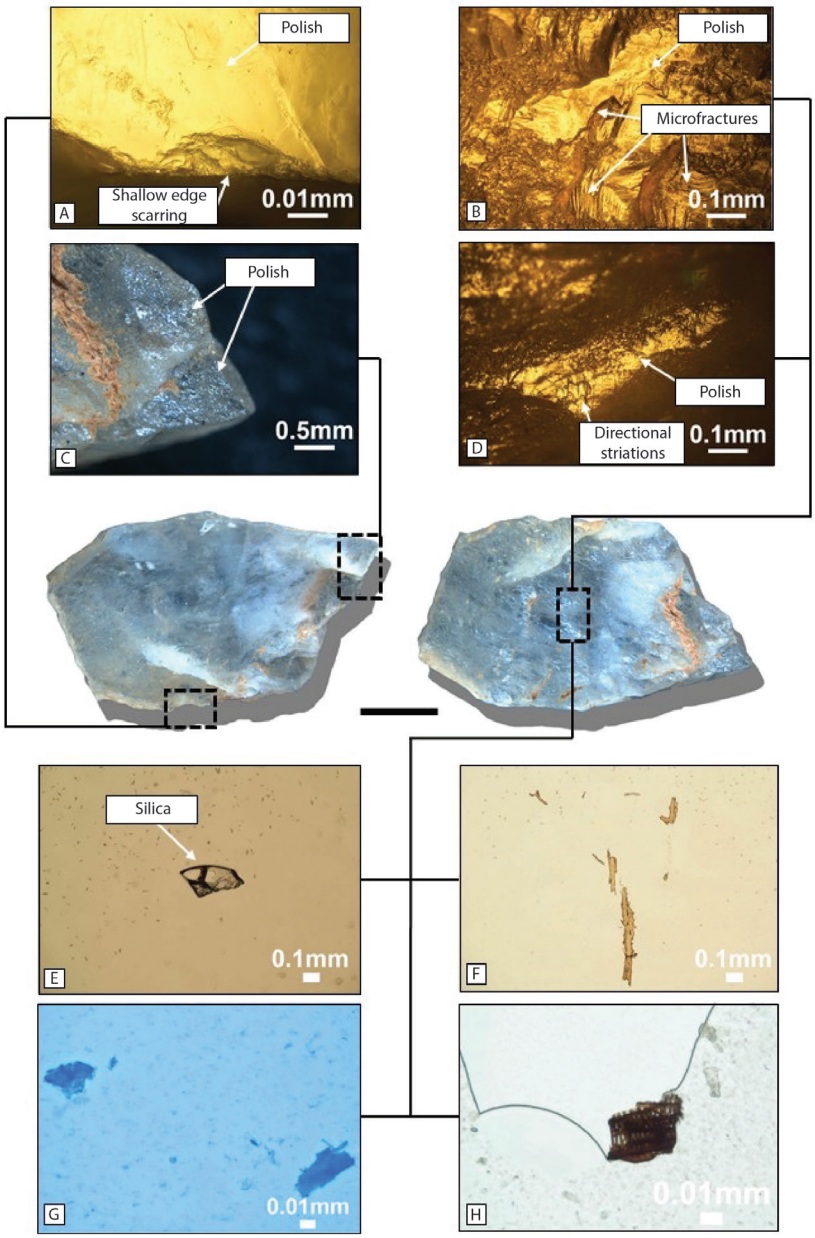

Figure 6.26. Square EIA02-998997: artefact 998997-XU49-LA229 (scale 5 mm). Usewear revealed shallow edge scarring (A), polish (B–D) and microfractures (B) and directional striations (D) on the artefact. Residue analysis revealed silica (E), small non-diagnostic plant fibres (F–G) and an unknown fibre (H).

Basalt was clearly the preferred material for (albeit non-intensive) stone artefact reduction and toolmaking throughout this open landscape's human history. Yet the use of basalt between the two excavation areas investigated varies substantially. These two assemblages represent very different task-scapes (Bird and Rhoads 2020). The stone assemblage in Square EIA02-001 mostly comprises discarded tools, while tools comprise less than 10% of the Square 998997 assemblage. It is possible that this results from sampling: all artefacts in Square 001 were inspected microscopically whereas only a single tool in Square 998997 was microscopically examined (based on the presence of macroscopic use). However, the markedly higher rate of artefact discard at Square 001 (2,207 artefacts discarded per cubic metre) compared to Square 998997 (287 per cubic metre) in the Early Holocene also reflects a preference for this elevated area immediately adjacent to a semi-permanent pool. The presence of extensive rock art and economic shellfish here demonstrates substantial and multi-component use of this location during the Early Holocene.

Dietary calculations

The MNI and size of shellfish are important indicators of past collection strategies and diet. The MNI analysis identified that 436 *Terebralia* were consumed during the Early Holocene on the sand sheet (in this 1 m x 1 m square). The 208 individuals that could be measured indicate that a very similar size range of this species was collected throughout this Early Holocene occupation. It is estimated that the live weight (shell plus meat) represented by this shellfish assemblage is c. 8 kg of shellfish, an amount which a woman could collect (not including transport time) in around 2.5 hours (Meehan 1982).

We cannot tell what this sample represents in terms of total shellfish weight consumed during this more intensive midden occupation as the midden layer is deeply buried in the sand body, thus its spatial extent and therefore volume cannot be estimated. We can, however, see that size distribution (cf. Figure 6.9 and Figure 6.22) varies very little throughout, suggesting strong selectivity in the harvesting of *Terebralia* from the Pleistocene/Holocene Transition through to the Early Holocene during this occupation of the sand body. This size selectivity is very similar to that demonstrated at the Fig Tree before 8,000 cal. BP, indicating several thousand years of focused, and arguably sustainable, harvesting practice.

In Square 001, 1,669 *Terebralia* were counted, of which 584 individuals could be measured. The *Terebralia* MNI from this 50 cm x 50 cm square represents c. 31 kg of shellfish, or 128 kg of *Terebralia* meat/m^2 collected between 7,680 and 7,340 cal. BP. This is 16 times as much meat per square metre as located in the sand body sample. We do not have the same fine-scale resolution for *Terebralia* accumulation in Square 998997 (i.e. 12,410–6,190 cal. BP, as we relied here only on OSL; Table 6.18). However, both the intensity of artefact tool use and scale of shellfish predation at the Fig Tree site compared to the sand sheet location confirms that these two assemblages represent different task-scapes, and likely different types of habitus throughout the Early Holocene. This variability across the cultural landscape documents some of the rich associated material which likely accompanied high rates of art and stone feature production occurring more widely across the landscape at this time.

Enderby Island Sample Area 4

One test square was excavated in the Enderby Island Sample Area 4 (Area 4), at the western end of Enderby Island (Figure 6.1, Figure 6.27 and Figure 6.28). This sample transect is located south of Area 1's large quarry and was added when we encountered a series of stone structures on our way back to camp from Area 1. The geology in this area is complex (Hickman and Strong 2003), with the basal geology being rhyodacite but with basalt outcropping nearby and several dolerite dykes in the vicinity (Figure 6.27). Excavation square EIA04-001 was placed within one of the stone structures – in an area where there is sporadic art production. This test square was excavated on 8 June 2016 by Wendy Reynen assisted by Sarah de Koning. The deposit was wet sieved by Jo McDonald and Andrew Dowding, in rock pools adjacent to the southern coastline below. This was necessitated by recent rain, which made the deposit extremely difficult to dry-sieve.

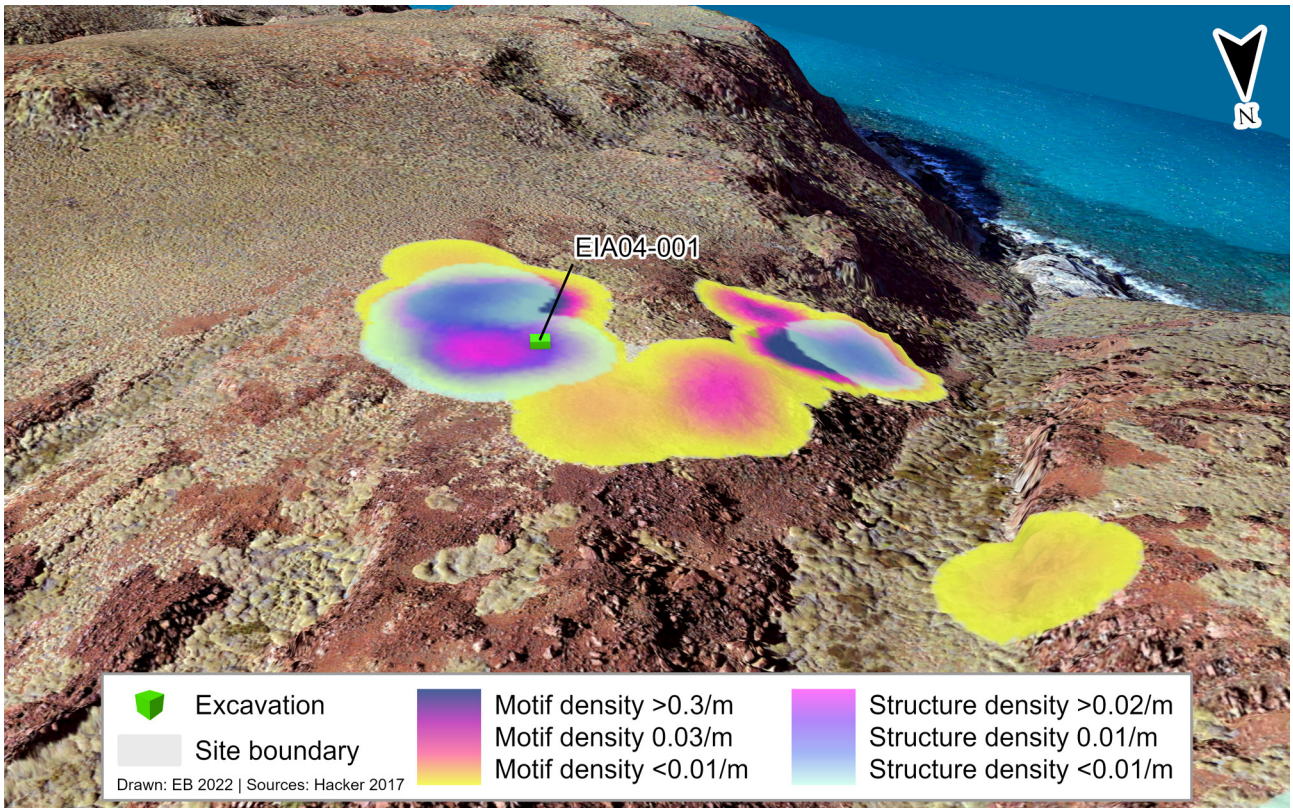

Figure 6.27. Square EIA04-001 showing location of the excavation square amongst the background of engraving and stone feature density.

Square EIA04-001

This 0.5 m x 0.5 m square was located within a circular stone feature which had a combination of sloping rock and flat floor area in its centre, the latter relatively unimpeded by surface rocks (Figure 6.28, Figure 6.29). The surrounding area has panels with rock art and grinding patches, and there are several recorded stone features nearby (see Chapter 5).

Figure 6.28. Square EIA04-001 visualised on the landscape showing other recorded features to demonstrate general context.

Figure 6.29. Square EIA04-001: (left) excavation in progress; (right) the stone features size with a seated occupant (Andrew Dowding).

Stratigraphy and dating

The square was aligned north–south with all X-Y-Z measurements taken from the south-west corner. Excavation proceeded stratigraphically with eight XUs dug in c. 2 cm depths (Figure 6.30). The excavation revealed a relatively shallow accumulation of fine sediment over a rocky matrix (Figure 6.30, Table 6.27). The deposit was moist (following rain) and contained a high density of artefacts. Within the profile, the colour intensified slightly, and compaction increased with depth. The rocky matrix become more dominant within the single stratigraphic unit until bedrock was reached (Figure 6.31):

SU1 – Very fine, dark reddish brown (2.5YR 2.5/4) moist silty loam. Artefacts were dense throughout. The sediment was more clayey at the base where it was found between bedrock blocks and large rocky inclusions. The deposit was persistently acidic, although slightly more so at the surface (pH 5.5; 6.5 at base).

Figure 6.30. Square EIA04-001 (top left) start levels and (top right) excavation end level for XU1; and (bottom left) end level of XU3 (base of SU2) and (bottom right) end of XU8 showing rocky interlocking surface at base of excavation.

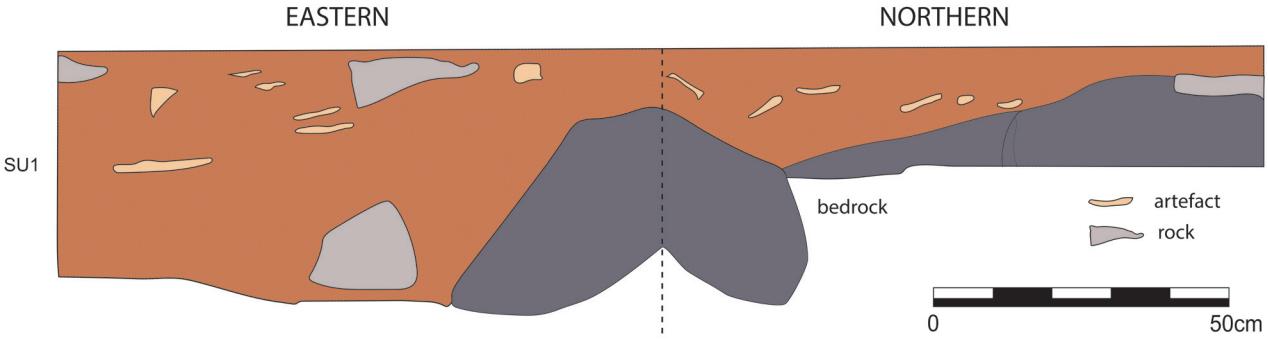

Figure 6.31. Square EIA04-001: eastern and southern sections, at completion of excavation.

UNIT	EXCAVATED DEPTH (CM)	TOTAL (KG) EXCAVATED	PH
XU01	2.1	9	5.5
XU02	2.9	3.8	6
XU03	5.0	6.4	6
XU04	6.9	10.2	6.5
XU05	8.8	9.1	6.5
XU06	11.8	8.9	6
XU07	15.7	9	6.5
XU08	17.2	7.4	6
Total		63.8	

Table 6.27. Square EIA04-001: excavation units and weights for deposit (in kg).

The cultural assemblages consisted predominantly of stone artefacts. We were unable to obtain an age estimation for this lithic assemblage and its associated stone structure (Table 6.28). No shell or bone was recovered (possibly due to the deposit's low pH). Some seeds were recovered during sieving (in XUs 4 and 5) and very small traces of charcoal (in XUs 6 and 7). Unfortunately, these provenanced charcoal samples did not survive pre-processing (Fiona Petchey, Waikato Radiocarbon Laboratory, pers. comm., 24 January 2017).

Two AMS radiocarbon dates were returned from the seeds found in the deposit during sieving (Table 6.28). These were indistinguishable from modern and were identified as *Trachymene oleracea* (native parsnip). This erect biennial herb grows to 0.3–1.5 m high and has white, blue or pink flowers (March to October). It grows on stony loam, ferrugineous outcrops throughout the Pilbara (Florabase 2021). Its tuberous root is fibrous and known to be edible. No plants were growing in the square at the time of excavation; it is possible that the seeds were introduced during transport of the buckets downhill for wet sieving or were introduced into the deposit by ants.

LAB CODE	SAMPLE TYPE	SAMPLE ID	XU	DEPTH BELOW SURFACE (CM)	F14C% MODERN CARBON	CONVENTIONAL RADIOCARBON AGE (YRS BP 1σ ERROR)
Wk-46411	Seed	END04-001-XU3-Seeds	3	sieve	107.3 ± 0.2	107.3
Wk-46412	Seed	END04-001-XU4-Seeds	4	sieve	107.6 ± 0.26	107.6
Wk-44897	Charcoal	END04-01-XU6-3	6	11	–	–
Wk-44898	Charcoal	END04-01-XU7-2	7	15	–	–

Table 6.28. Square EIA04-001: radiocarbon dates returned on charcoal and seeds.

Given the general absence of robust charcoal and other organics in the excavated assemblage, the magnetic susceptibility of the soils inside the stone rings was tested. Differences in magnetic susceptibility are often linked to heat caused by fires as part of human usage. Twenty samples were tested from a grid covering the interior of the small stone ring covering the surface and a 5–10 cm depth sample. The texture of the <2 mm fraction was uniform and can be classified as a silt-rich loam. Magnetic susceptibility values (10-5 SI) of the surface samples reached an average of 273.6 with an SD of 183 and the 0–5 cm samples yielded an average of 301.1 with an SD of 125 (Table 6.29). Nearby surface samples outside the stone rings showed a magnetic susceptibility between 204 and 315 (10-5 SI). No significant difference in magnetic susceptibility values were detected between samples from inside and outside the ring structure and hence magnetic susceptibility does

not assist in suggesting a specific function of the stone structure (e.g. either as a fireplace/hearth or intensive human occupation).

	MAGNETIC SUSCEPTIBILITY (10-5 SI)		
	Stone ring surface	Stone ring 0–5 cm	Surrounding 0–5 cm
Minimum	150	161	204
Maximum	428	561	315
Average	273.6	301.1	278.8
SD	183	125	36.5
Median	250	279.5	288

Table 6.29. Magnetic susceptibility values for samples inside (n = 20) and outside (n = 8) a stone ring structure at Enderby Island.

Cultural assemblage

The excavated stone artefact assemblage from EIA04 weighed just under 4 kg (Table 6.30). No shell or bone contributed to the weight of the cultural assemblage. Unfortunately, the XU6 deposit was mistakenly mixed with the deposit from XU5 during fieldwork, and therefore no artefacts are logged for XU6. The collected shells are all land snail (no midden was encountered here). Given the unchanging stratigraphy and shallow depth of deposit, the undated stone artefact assemblage is treated as a single analytical unit. This analysis provides a general characterisation of the total assemblage. Excavation units were analysed to show some patterning between the upper and lower assemblages.

UNIT	FLAKED STONE ARTEFACTS	LAND SNAIL	SEEDS
XU01	236.61	–	–
XU02	483.26	–	–
XU03	1,099.24	0.04	0.005
XU04	525.76	0.005	0.07
XU05	1,465.55	–	0.005
XU06	mixed > XU5	–	–
XU07	25.37	–	–
XU08	1.57	–	–
Total	3,837.82	0.045	0.08

Table 6.30. Square EIA04-001: excavation units and weights for cultural materials (all in grams).

Stone artefacts

The stone assemblage comprises 1,060 artefacts (Table 6.31), including 218 artefacts <1 cm in size. Artefact density projected from within the stone structure is 24,651 artefact/m^3: extremely high for the arid zone of Australia (see McDonald et al. 2018).

Assemblage composition

A sample of 19 artefacts from this square was analysed using portable XRF analysis (Figure 6.32). The pXRF results demonstrate that all artefacts sampled (regardless of grain size) were made on rhyodacite (dacite). Dacite artefacts are of varying grain sizes; however, the vast majority (99.7%) of these are medium grained. There are only three fine-grained artefacts in this sample. A small number of very fine-grained dark-coloured artefacts (with no visible quartz inclusions) were identified as basalt. The EIA04 stone assemblage is predominantly composed of local dacite (97.4%, Table 6.31) with small proportions of quartz and basalt also present.

MATERIAL/XU	BASALT	%F	DACITE	%F	QUARTZ	%F	TOTAL
Surface	–	0.0	2	100.0	–	0.0	2
1	1	0.3	296	98.7	3	1.0	300
2	3	1.0	300	98.0	3	1.0	306
3	2	1.1	184	98.9	–	0.0	186
4	1	0.9	110	98.2	1	0.9	112
5	4	3.4	108	92.3	5	4.3	117
7	–	0.0	23	85.2	4	14.8	27
8	–	0.0	9	90.0	1	10.0	10
Total	11	1.0	1032	97.4	17	1.6	1060

Table 6.31. Square EIA04-001: stone artefact assemblage showing frequency by XU.

Artefacts occur throughout the deposit but were discarded at much higher frequencies towards the top of the sequence – particularly in XU02 (Figure 6.33 and Figure 6.34). Although dacite is the dominant material through all excavation units, quartz artefacts are proportionally more common in the lowest (oldest) excavation units, while most of the basalt artefacts are found in the top half of the sequence. This suggests a shift in raw material preference through time during the use of this stone feature.

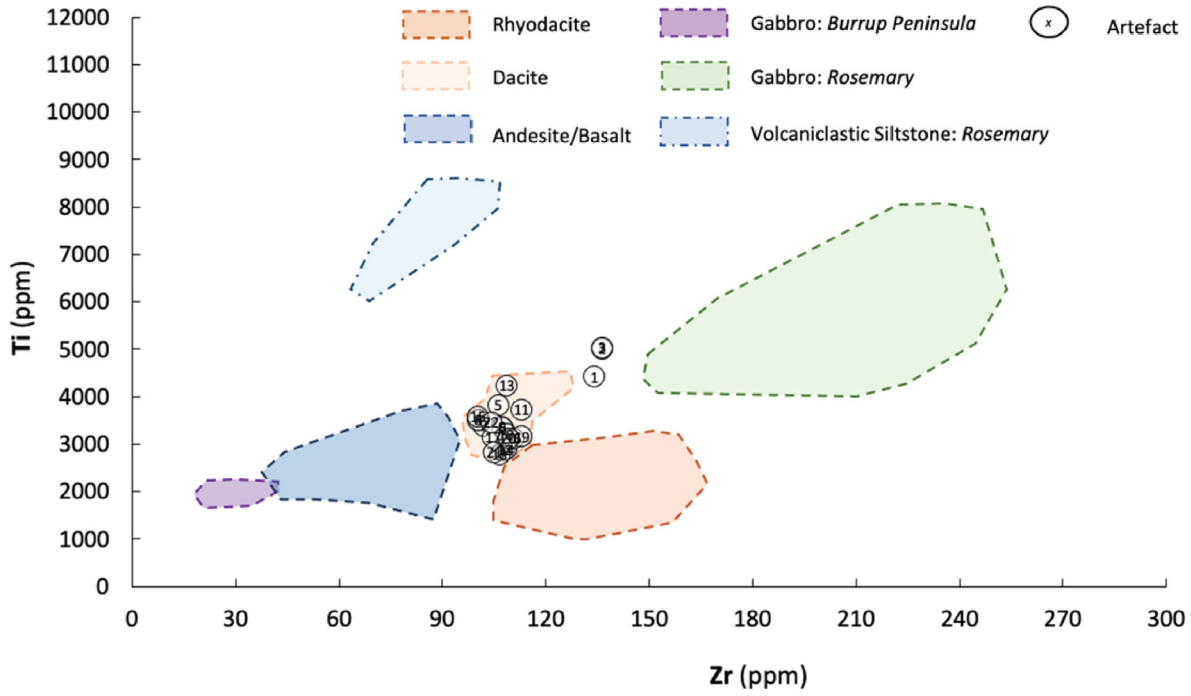

Figure 6.32. Square EIA04-001: artefacts overlaid on the regional distribution of raw materials sampled from across the Dampier Archipelago (see EIA02).

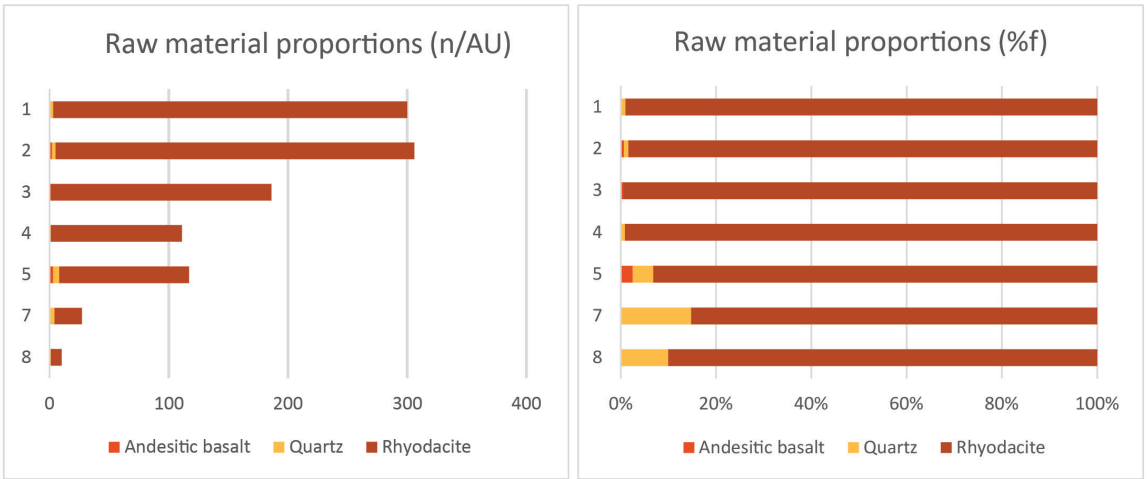

Figure 6.33. Square EIA04-001: proportions of raw materials throughout the excavation units. Data for XU5 is based on the combined assemblage from XUs 5 and 6.

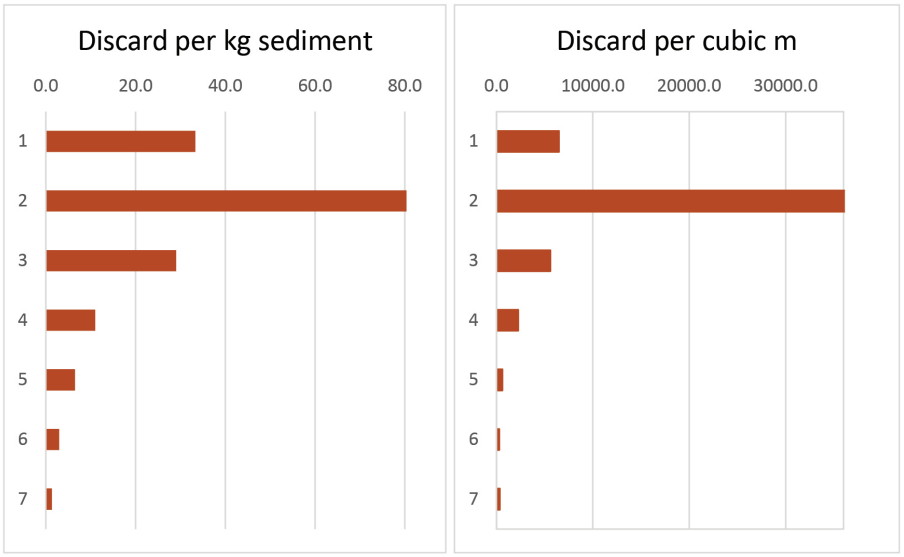

Figure 6.34. Square EIA04-001: artefact density. Artefact volume for XU5 is based on the combined excavation bucket weights and artefact counts for XUs 5 and 6.

The dacite-dominated assemblage is predominantly fragmented debitage (Table 6.32). This, along with a high frequency of longitudinally broken flakes (n = 230, 45.5% of the 'broken flake' category), indicates extensive on-site manufacture within the stone structure. The substantial microdebitage component also suggests that this location was used for *in situ* knapping.

Quartz has the highest proportion of broken flakes: demonstrated by NAS (total artefact count) to MNA (minimum number of artefact) ratios (Table 6.32). The presence of a quartz flake with clear crushing on its proximal and distal ends (1-XU05-LA984) indicates the use of a bipolar technique (hammerstone and anvil). Only a single rhyodacite core fragment was found here. This broken core, with three remaining flake scars, has clearly been produced by heat fracture from a larger nodule.

ARTEFACT TYPE/ MATERIAL	BROKEN FLAKE		COMPLETE FLAKE		CORE / CORE FRAGMENT		TOOL		TOTAL		NAS TO MNA RATIO
	N	%	N	%	N	%	N	%	N	%	
Basalt	1	16.7	5	83.3	0	0	0	0	6	0.7	1.2
Dacite	495	60.1	322	39.1	1	0.1	5	0.6	823	97.7	1.6
Quartz	9	69.2	4	30.8	0	0	0	0	13	1.5	2.9
Total	505	60.0	331	39.3	1	0.1	5	0.6	842	100	1.6

Table 6.32. Square EIA04-001: stone assemblage composition by frequency and proportion. The 2 mm assemblage (<10 mm) is not included here.

Assemblage reduction

The Scar Density Index for complete flakes is very low across all materials (Table 6.33), indicating an overall low intensity of reduction. Although interpretations are constrained by the fact this is an undated assemblage, the higher quartz SDI value suggests comparatively more intensive quartz reduction than dacite and basalt. There are no noticeable trends in the reduction intensity of dacite nodules between the top and base of the sequence (Table 6.34).

MATERIAL	N	μ	SD
Basalt	5	0.78	0.24
Dacite	322	0.76	0.34
Quartz	3	1.05	0.33
Total	330	0.76	0.33

Table 6.33. Square EIA04-001: Scar Density Index for complete flakes (>10 mm).

XU	N	μ	SD
1	106	0.80	0.34
2	88	0.74	0.32
3	50	0.76	0.29
4	37	0.69	0.32
5	37	0.76	0.42
7	1	0.45	–
8	1	0.46	–

Table 6.34. Square EIA04-001: Scar Density Index for complete flakes (>10 mm) across excavation units. Data for XU5 is based on the combined assemblage from XUs 5 and 6.

Further evidence for the non-intensive reduction of dacite are the very low proportions of flaked and faceted platforms on dacite flakes (i.e. those with complete platforms, n = 6, 1.4%). Additional evidence is the relatively low proportion of granophyre flakes with overhang removal (n = 81, 19.3%), which would indicate that care was taken to prepare core platforms for flake removals.

Most complete flakes do not have any cortex (n = 296, 89.7%). Cortex is often linked with reduction and, theoretically, the amount of cortex remaining on dorsal surfaces should reduce as reduction progresses. On its own, this cortex result suggests high intensity granophyre reduction. However, the cortex-reduction relationship assumes that nodules are fully cortical prior to initial reduction. This is not always the case, as many stone sources comprise small outcrops which become increasingly non-cortical as quarrying progresses over multiple extraction events. This result at Area 4 may therefore be less indicative of reduction intensity and more indicative of the original characteristics of the granophyre nodules selected for knapping. Other reduction measures (SDI, flake attributes) support this cortex interpretation.

Cores

The flake to core ratio cannot be reasonably calculated as only a single core fragment is present in the assemblage. This low proportion of cores within the assemblage may be due to the limited extent of the test square in what is an intensive reduction event.

Tool selection and use

Three dacite artefacts exhibit macroscopic and microscopic usewear along one or more edges. The high standard deviations for dacite flake weight and surface area (Table 6.35) indicate a high variance in the size of flakes discarded at Area 4. The two longitudinally broken tools (1-XU03-LA771 and 1-XU05-LA1019) have a markedly larger maximum dimension (35.6 mm and 38.3 mm respectively) than non-used dacite flakes (m 24.2 mm ± 15.8 mm). This suggests that larger flakes were preferentially selected for tool use.

MATERIAL	WEIGHT (G)			SURFACE AREA (MM2)	
	N	M	SD	μ	SD
Basalt	5	1.7	1.3	402.4	204.8
Rhyodacite	322	4.2	19.5	496.7	893.7
Quartz	3	0.9	0.7	189.3	79.2
Total	330	4.1	19.3	492.5	883.6

Table 6.35. Square EIA04-001: weight and surface area for complete flakes (not including flakes <10 mm).

The average shape of flakes across all three materials (Table 6.36) indicates that economising features – such as conserving mass by creating flakes with high amounts of working edges – were not important to the knappers using this stone circle.

MATERIAL	N	μ	SD
Basalt	5	1.1	0.5
Granophyre	322	1.1	0.6
Quartz	3	0.9	0.3
Grand Total	330	1.1	0.5

Table 6.36. Square EIA04-001: elongation ratio for complete flakes.

Usewear and residue analysis

Five artefacts were examined for microscopic usewear and residues based on the identification of macroscopic edge damage. Macroscopic edge damage on artefacts 1-XU03-LA773 and 1-XU05-LA965 was concluded to be the result of taphonomic depositional processes due to the absence of polish, scarring, striations or any other use traces or residues. Microscopic analysis of the three further artefacts (1-XU03-LA771, 1-XU04-LA1171 and 1-XU05-LA1019) showed evidence for use in the form of polish and striations. While one artefact returned a positive presumptive blood test, no other residues were recovered from the artefacts in concentrations consistent with their use.

Artefact 1-XU03-LA771 is a longitudinally broken flake made on coarse-grained dacite with desert varnish present on its ventral and dorsal surfaces. Parallel striations on the desert varnish run from the edge of the right ventral margin towards the centre of the artefact, and the margins of the desert varnish closest to the edge of the artefact also have well-developed polish (Figure 6.35). The traces of use on the ventral desert varnished surface therefore indicate two separate events: the initial flaking of the artefact, which was followed by a period during which desert varnish developed on the ventral surface; then subsequent use of the artefact that created the traces overlying the desert varnish on this ventral surface.

Artefact 1-XU05-LA1019 is a longitudinally broken dacite flake which has desert varnish located predominantly on the longitudinal break and the dorsal surface, indicating again that the varnish formed on the break after it was initially flaked. Traces of use in the form of polish and striations cover approximately 60% of the desert varnish and include the artefact edges (Figure 6.36). Polish and striations are also located on the unvarnished edges of the artefact. The polish on this artefact is far more developed, and the striations deeper and non-directional, when compared with the two other desert varnished artefacts examined at this site. The presence of usewear on the desert varnish over the break indicates that this artefact was initially flaked and then deposited long enough on the ground for the varnish to form, before being selected for additional use. Artefact 1-XU05-LA1019 returned a positive result for blood on the varnished surface of the break. However, the effect that desert varnish's geochemistry has on the efficacy of Siemens Multistix when testing for blood is unknown, since certain chemistries can return a false-positive (Matheson and Veall 2014).

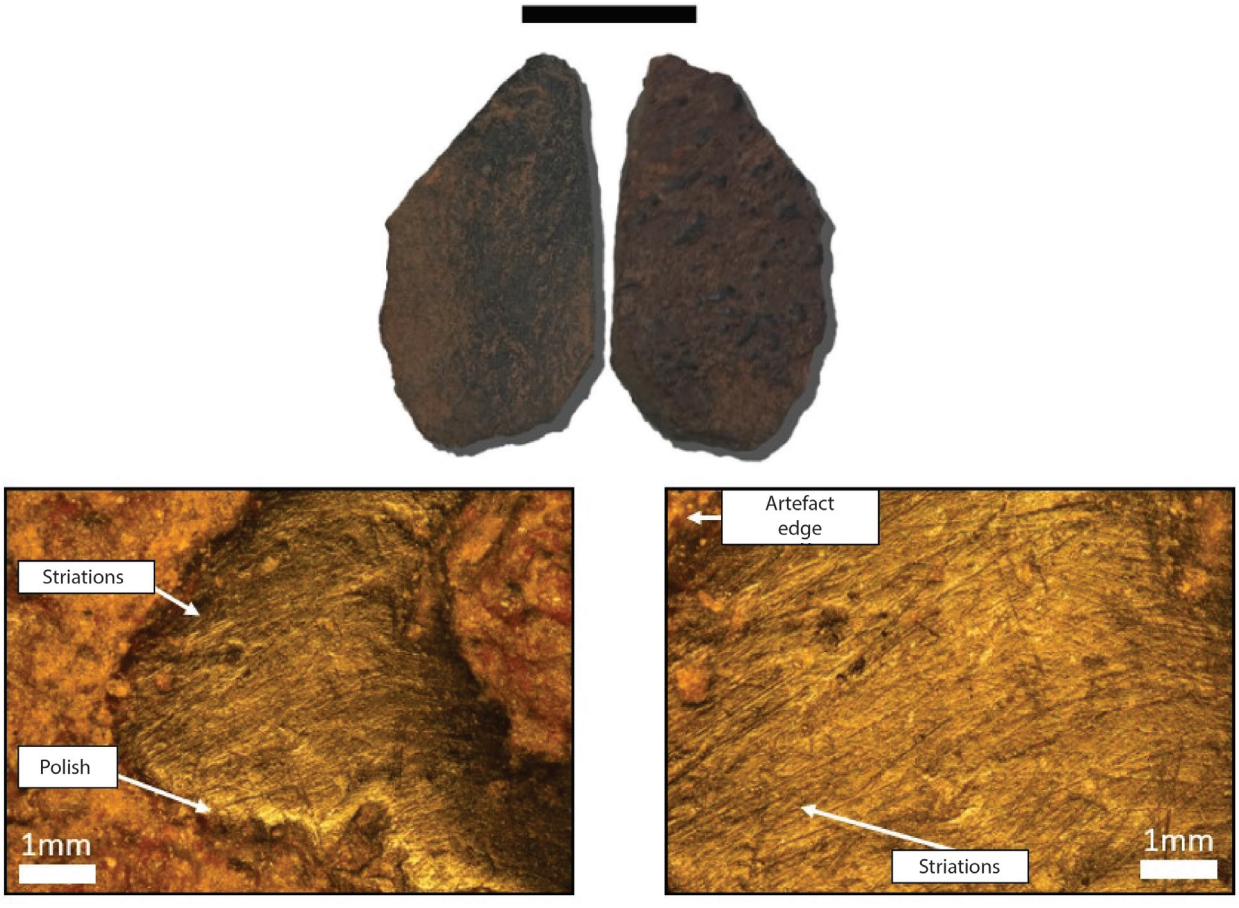

Figure 6.35. Artefact 1-XU03-LA771: image shows black desert varnish on both sides of the artefact (top), and an example of microscopic striations and polish (bottom) on the ventral desert varnish surface.

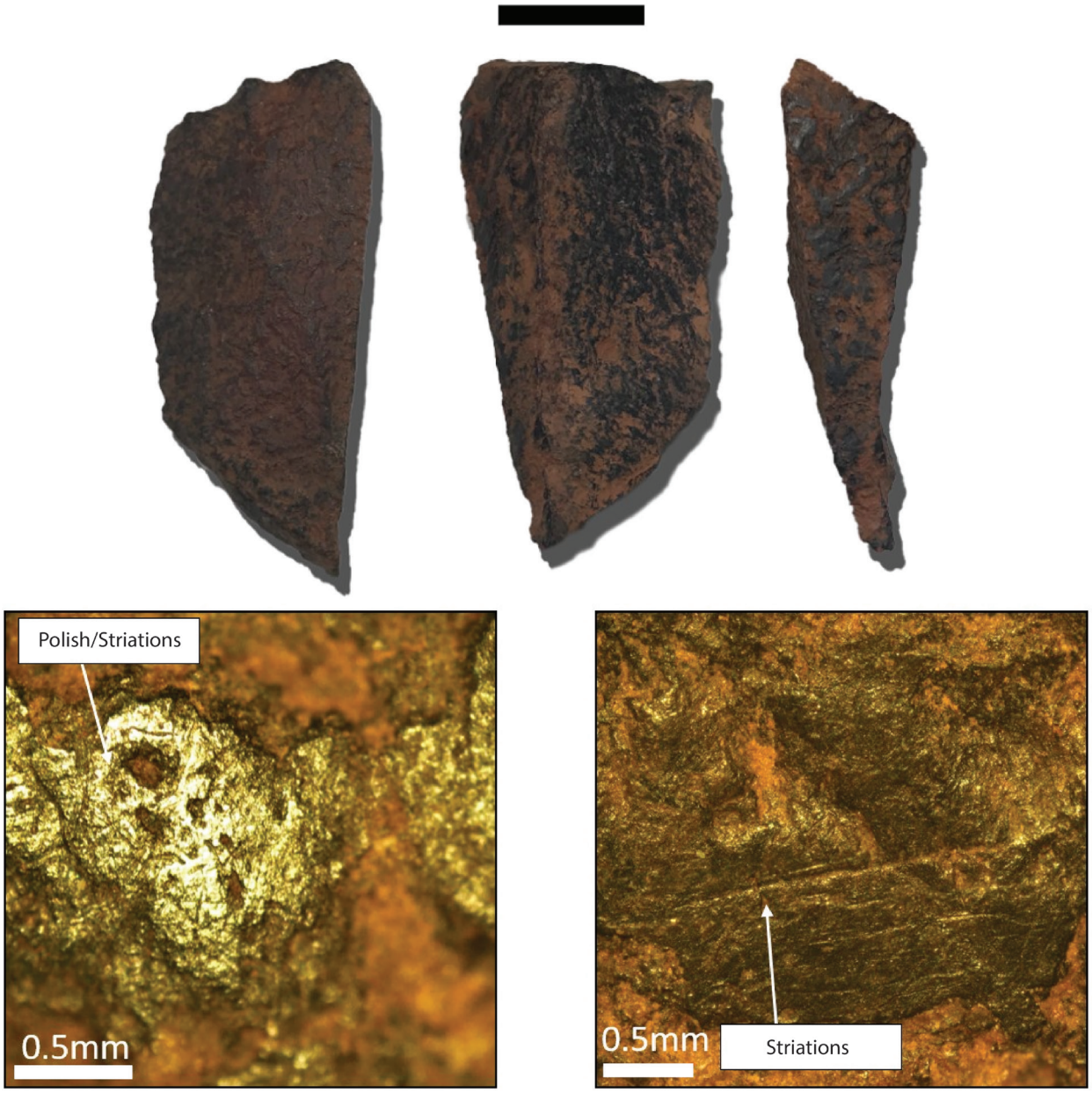

Figure 6.36. Artefact 1-XU05-LA1019: Image shows the heavily developed polish and deep striations identified on the desert varnish.

Artefact 1-XU04-LA1171 is a utilised piece of coarse-grained dacite with desert varnish located on both surfaces, with usewear traces limited to the dorsal surface. Polish is present on the high points of the artefact's dorsal surfaces, including across the desert varnish (Figure 6.37). Directional striations have formed in groups near to, but moving parallel to the artefact margins, with later striations superimposed at intersecting angles.

Clear differences in the traces of wear documented on these three artefacts suggest variability in tool use at the site. Artefacts 1-XU03-LA771 and 1-XU04-LA1171 have directional striations and polish formed on their surfaces and across areas of desert varnish. Artefact 1-XU05-LA1019 has well-developed polish with striations appearing more randomly, a type of usewear that has been linked to the recycling of tools in other contexts (cf. Schiffer 1987).

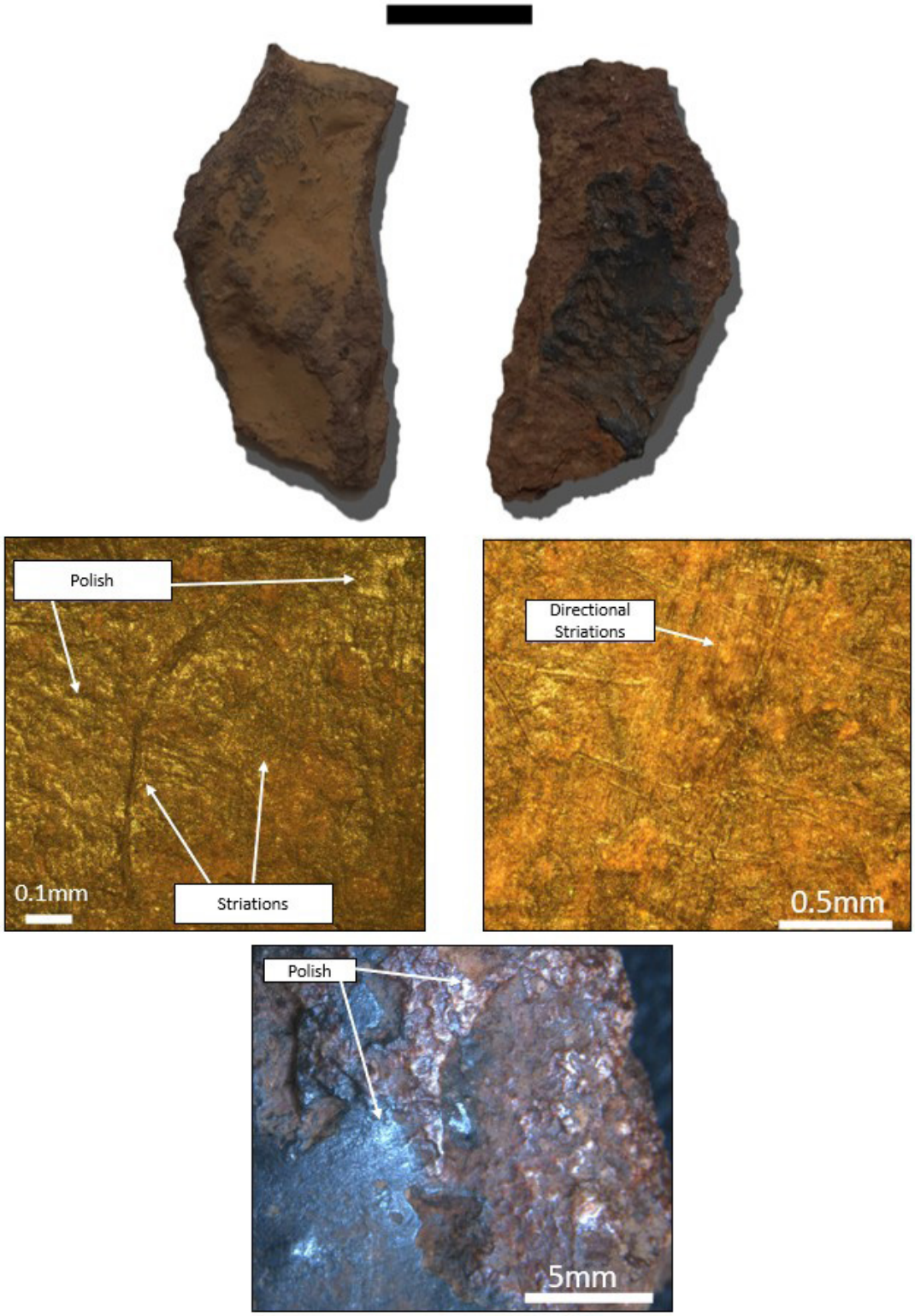

Figure 6.37. Artefact 1-XU04-LA1171, showing directional striations and polish.
Note the formation of polish on the high points of both non-varnished and varnished surfaces.

The presence of usewear overlying desert varnish on a ventral surface of artefact LA771 and longitudinal break of LA1019 also indicates temporally distinct use events. After these artefacts were initially flaked, they were deposited on the surface long enough for the varnish to form on these freshly exposed surfaces, which were then used subsequently in a way that created the usewear traces over the desert varnish of LA771's ventral surface and LA1019's break. It is difficult to establish whether there are traces of use along the other edges of artefacts 1-XU03-LA771 and 1-XU04-LA1171 because they are entirely overlaid with desert varnish. However, artefact 1-XU05-LA1019 shows clear signs of use along its unvarnished edges as well as on areas of desert varnish. The traces of use on these three artefacts are primarily located on desert varnished surfaces. At the time of publishing, no usewear studies on desert varnish exist and it is unclear how, or if, these traces definitively relate to use.

Discussion

Although the surface/living area within the stone circle at EIA04 is small, the excavated stone assemblage recovered from this 0.5 m x 0.5 m excavation is substantial. Artefact discard at EIA04 is extremely high (per kilogram sediment and per cubic metre) when compared to most other excavated stone assemblages in the Dampier Archipelago and more widely (see Chapter 18).

Characterisation of this small dense assemblage indicates that individual/s reduced locally sourced dacite nodules (most likely from the immediate vicinity) within the stone circle, where extensive but non-intensive core reduction was undertaken. The discard of only three minimally used tools suggests that subsequent activities that used stone tools (e.g. processing plant or animal remains) occurred only occasionally here. The presence of very small (<10 mm) complete dacite flakes suggests on-site tool manufacture or maintenance of tools (e.g. resharpening of tool edges), which were then transported away for use elsewhere (no retouched or formal tools were discarded on-site). The near absence of cores in the assemblage is noteworthy. Assuming that cores were not discarded in an unexcavated area inside the stone circle, where are the remaining cores from on-site nodule reduction? Given that the reduction of dacite nodules from the immediate vicinity was the primary activity undertaken here, cores may have been reduced at this location and then transported to other parts of the island and/or archipelago. Dacite occurs locally within this area, and EIA04 fits the characteristics of a tool-stone source location where nodules were procured and prepared for more intensive use elsewhere.

There is no clear indication that the smaller frequencies of basalt and quartz discarded at Area 4 were more intensively reduced than dacite: the higher basalt and quartz SDI values have large standard deviations that overlap with the dacite SDI values. Small basalt and quartz sample sizes – and the fact that we cannot constrain the ages of this knapping activity – means that making conclusions about these non-local materials is difficult. Nonetheless, the increased proportion of quartz in the lowest part of the deposit is of interest. Could this indicate differences in raw material preferences through time and/or by knappers, or perhaps changes in the movements of people across these landscapes (i.e. where different tool-stone sources were brought with people who came to EIA04-001 to construct this stone structure and knap the local material)? Larger sample sizes are clearly required to expand on these possible interpretations.

Artefact discard rates at EIA04-001 decrease with depth. This could indicate increased or changed site use through time (i.e. that the intensive knapping activity occurred well after the construction of the stone structure) although it is difficult to make a meaningful interpretation about these changes through the shallow sequence given the assemblage is undated. In the absence of shell material, it is tempting to suggest that this knapping activity in this stone feature may pre-date the arrival of the coastline and mangrove resources, which is demonstrated by focused *Terebralia* consumption in several Early Holocene sites across Enderby and Rosemary islands. Conversely the structures could relate to people coming and camping here soon after islandisation, when they were procuring tool-stone from the nearby major quarry complex on Area 1 (but consuming their shellfish elsewhere, closer to more permanent water sources). Yet, being located at the top of the hill and with no identifiable water source, this is not a simple conclusion to make (i.e. there is no obvious resource here which could create a focus of habitation beyond the knapping and toolmaking of locally available stone resources which are widespread across the landscape). The elevated position here gives the occupants of the site a significant viewpoint. The presence of desert varnish on several artefacts, on multiple surfaces, shows the repeated use of some material, and indicates that there is a high likelihood that at least some of this flaking event occurred earlier and perhaps in the Terminal Pleistocene. Further analysis of the desert varnish, being undertaken as part of the *Dating Murujuga's Dreaming* LP project, may result in further insights for this material.

The location of this assemblage within the built stone structure is remarkable. Several other stone structures are found around this excavated example at EIA04 where there is also evidence of rock art, grinding patches and other features. Were these structures made to provide shelter from wind and weather, or to define social space with increasing population pressure (McDonald and Berry 2016), and what does this high 'village' at the western end of Enderby Island represent in terms of the broader cultural landscape? Further detailed investigation of this landscape is required to answer these questions.

Enderby Island Sample Area 6
Site MLP-EI010

In the centre of Enderby Island is a site known as Enderby 10 (McDonald and Veth 2006), now named MLP-EI010 (Figure 6.38). Here we systematically recorded the rock art along a c. 500 m x 100 m transect of this interior valley centred on several semi-permanent rock pools (see Chapter 5), as well as excavating a small test pit. The rock art was recorded during two separate trips (Trip 3, 2016; and Trip 1, 2017) which documented a total of 2,067 motifs on 1,068 panels. The bedrock in this part of the island is andesitic basalt (see Figure 5.2 in Chapter 5). In the upper reaches of the site is a large semi-permanent pool with well-developed calcium carbonate drapes. The carbonate drape associated with one of these pools was cored in 2017. An extensive *Terebralia* midden on both sides of the pool covers many hectares. A single surface shell collected from this *Terebralia* midden was previously dated (by Ken Mulvaney), returning an age determination of c. 9,000 cal BP (ANU–18636). Our initial assumption, when we excavated this location, was that we were looking at a habitation site which pre-dated the islandisation of the Enderby Ranges. This landmass transformed initially into five separate smaller islands until Holocene sediments infilled the margins and joined the elevated land masses to form the current morphology of the single island (Semeniuk and Wurm 1987). The rock art is continuous along the creek line (Figure 6.38), though is found in higher densities around the larger pools. Smaller patches of *Terebralia* midden are found around the other pools downstream. All this shellfish material has been carried a minimum of 1.5 km (in a straight line) from the nearest northern beach; 1.7 km to the south; or c. 2 km to the west.

Surface shells were collected from several of these downstream middens during the current fieldwork and these, too, were submitted for dating (Table 6.37). One *Terebralia* shell was also collected from an eroding creek section downstream of the main site complex. All these surface/creek section *Terebralia* dates were Mid-Early Holocene. The surface *Melo* collected from the downstream surface scatter of the site was dated to the last millennium.

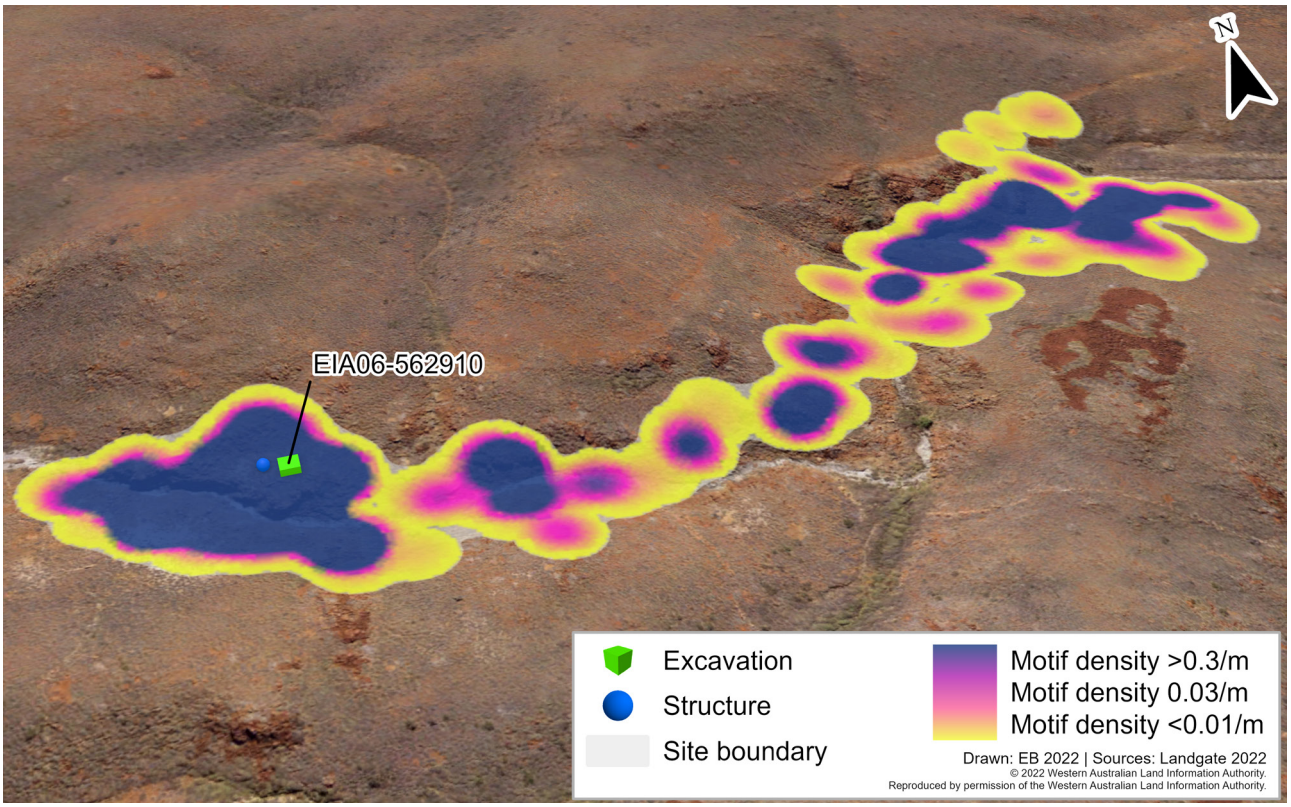

Figure 6.38. Enderby Island Sample Transect 6, showing location of the excavation squares amongst the background of engraving and stone feature density.

SHELL ID	LAB CODE	LAT	LONG	SHELL TYPE	RESULT	1SE	95% MIN	95% MAX	CAL. MEAN
EIA06-Creek profile	Wk-47202	–20.5992	116.5	Terebralia	7097	23	7970	7865	7917.5
EIA06-JM-357	Wk-47198	–20.6003	116.5	Melo	847	22	791	701	746
EIA06-JM-358	Wk-47203	–20.6003	116.5	Terebralia	6423	23	7422	7292	7357
EIA06-JM-359	Wk-47204	–20.6003	116.5	Melo	4891	21	5651	5594	5622.5

Table 6.37. MLP-EI010: surface and creek section shell dates.

Rock art assemblage

The rock art assemblage for Area 6 (see Chapter 5) describes the site complex recorded in the valley from the upper reaches above the main pool, extending to the art clusters observed below the downstream pool. While the engraved art is continuous along this stretch of the creek line (i.e. all features are within 25 m of each other), clear assemblage clusters can be defined.

The excavation was undertaken here to contextualise the art around the main pool. Hence, an analysis of the art around this upper pool is presented here (Figure 6.39, Figure 6.40). There are high-density clusters of art on both sides of the pool and these indicate distinct patterning. The density and nature of art found here is further indication of the intensive use of this place as a living site (Table 6.38). Many grinding patches were recorded (n = 190) around this upper pool, indicating that seed and other plant-material processing was a focused site activity (Table 6.39). 'Incised line sets' similarly are focused on this location and these are found in a sheltered area downstream of the main pool on the southern side of the gorge. There are also many 'random scratchings' in this area, possibly indicative of many rock-marking activities which are not specifically intended to be image-making.

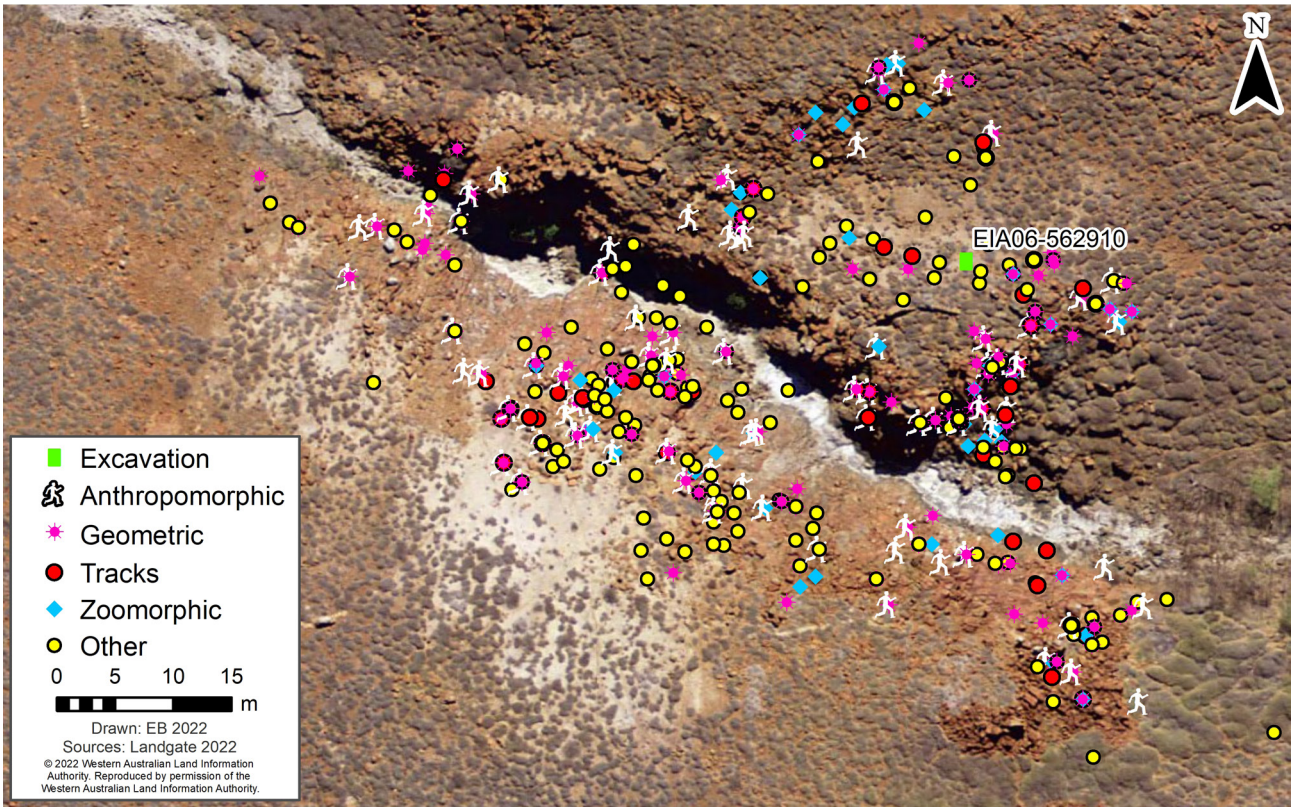

Figure 6.39. The location of Square 562910 amongst the numerous rock art panels from the upper rock pool assemblage, with motif types mentioned in the text highlighted.

ALL CLASSES	COUNT	%F	DEPICTIVE	COUNT	%F
Anthropomorphic	129	12.7	Anthropomorphic	129	20.2
Geometric	336	33.0	Geometric	336	52.6
Other	378	37.2			0.0
Tracks	90	8.8	Tracks	90	14.1
Zoomorphic	84	8.3	Zoomorphic	84	13.1
Total	1,017	100.0	Total	639	100.0

Table 6.38. MLP-EI010 upper pool – rock art subject classes.

SUBJECT	COUNT	%F
Amorphous area	2	0.5
Grinding patch	190	50.3
Incised line set	116	30.7
Linear	3	0.8
Random pecking	10	2.6
Random scratching	57	15.1
Total	378	100.0

Table 6.39. MLP-EI010 upper pool – other class counts.

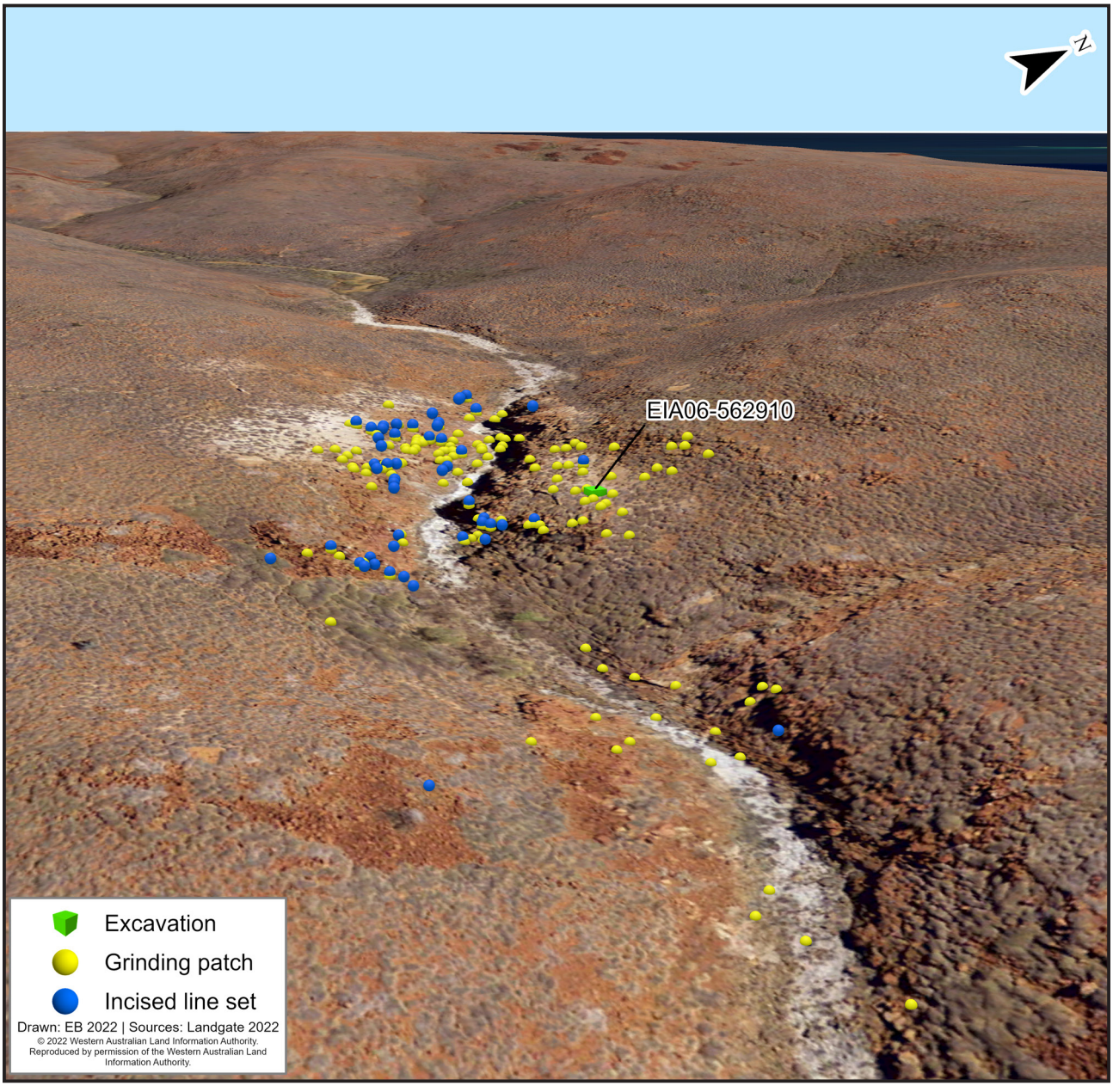

Figure 6.40. Upper pool showing location of panels with incised grooves and grinding patches.

More than half the motifs around the pool are geometric (Table 6.40): mostly linear, but with many ovals and arcs. There is a relatively large number of anthropomorphic motifs (mostly linear figures). There is one decorative infill figure, and a pair of disarticulated dot head figures (both older styles) but none of the more recent styles (with headdresses and/or exaggerated feet/arms/genitalia). The more recent zoomorphic subjects are all depicted around the pool.

Most of the identifiable motifs at the site are small, with 84% of the assemblage being smaller than 30 cm in maximum dimension (Table 6.41). The largest motif at the site is an elongated profile figure with an outlined body and both arms on the right-hand side; this has been positioned to fit on an elongated panel which faces into the site.

Significantly more of the art produced registers contrast state 1 (CS1) rather than CS5 (Figure 6.41), indicating that art has been produced here throughout the time frame of art being produced in the archipelago, but suggesting that there may have been less art produced in the most recent phases of art production. Given this site has been occupied into the last millennium and, indeed, up until just before European contact, this suggests that art production may not have been as intensive during the terminal occupation phases – when huge amounts of stone artefacts were being produced and large quantities of mixed-habitat shellfish were being transported into this location over at least 1.5 km. It is also possible that contrast state is not giving us an accurate picture of age sequencing here because a large proportion of this art is shallow and scratched and/or abraded (which has not necessarily penetrated through the patina on the smooth basalt surfaces).

SUBJECT	COUNT	%F	SUBJECT	COUNT	%F
Anthropomorphs			Tracks		
Combination figure	1	16.3	Bird track	70	11.0
DI figure	1	0.5	Human foot	15	2.3
Linear figure	104	0.2	Macropod track	3	0.5
Profile figure	3	0.2	Other track	2	0.3
Solid figure	20	3.1	Zoomorphs		
Geometric			Animal part	2	0.3
Angular	37	5.8	Bird	13	2.0
Arc	44	6.9	Dugong	1	0.2
Circular	3	0.5	Fish	23	3.6
Complex	2	0.3	Lizard	4	0.6
Linear	148	23.2	Macropod	7	1.1
Material culture	8	1.3	Marine other	1	0.2
Oval	74	11.6	Quadruped	2	0.3
Rayed	20	3.1	Snake	3	0.5
			Stingray	2	0.3
			Turtle	26	4.1
			Total	639	100.0

Table 6.40. MLP-EI010 upper pool rock art subjects.

SIZE	NO.	%	SIZE	NO.	%
1–10	168	26.3	51–60	11	1.7
11–20	269	42.1	61–70	3	0.5
21–30	107	16.7	81–90	2	0.3
31–40	47	7.4	NA	22	3.4
41–50	10	1.6	Total	639	100.0

Table 6.41. MLP-EI010 rock pool assemblage motif size (in cm).

Contrast state patterns give us an idea of changing subject choices through time – and by comparing subject choices and the recorded weathering state, we note that the artists at this site have always given preference to the production of geometric motifs, while human figures were depicted mostly during mid-late art production periods (Table 6.42, Table 6.43).

In terms of understanding the dietary preferences at the site, it is interesting to note that both macropods and fish are important subject choices throughout the entire art production phases, with macropods present in low numbers throughout. While marine themes are present throughout the entire assemblage, there is a clear increase in the main art production phases (CS3 and CS4) of turtles, fish and birds (Figure 6.41). This is a different pattern to that presented by the tracks at the site. Bird tracks are the most often depicted track – and these occur throughout the sequence of art production (Table 6.44). They are, however, most prevalent during the most intensive period of art production – represented by CS3 and CS4.

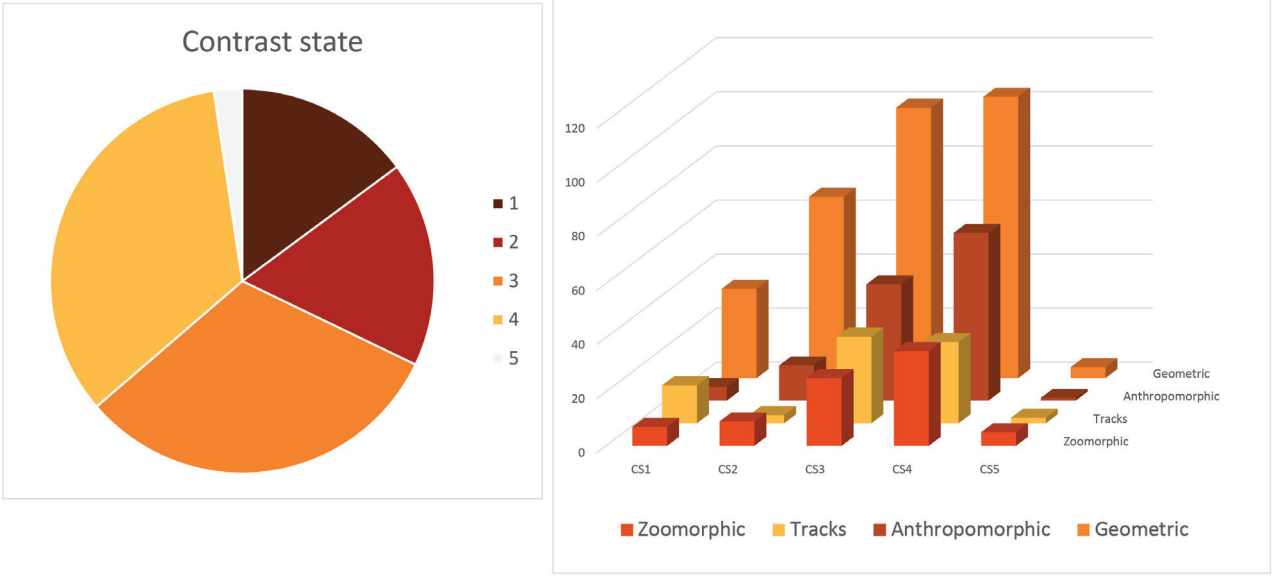

Figure 6.41. MLP-EI010 pool: contrast state.

CONTRAST STATE	COUNT	%F
1	59	9.2
2	92	14.4
3	200	31.3
4	231	36.2
5	12	1.9
NA	45	7.0
Total	639	100.0

Table 6.42. MLP-EI010 upper pool: depictive motifs contrast state.

ZOOMORPHS	CS1	CS2	CS3	CS4	CS5
Macropod	2	1	1	2	1
Bird		1	3	7	1
Quadruped				1	1
Lizard		1		3	
Snake		1	2		
Dugong			1		
Marine other		1			
Fish	4	2	6	8	1
Stingray			1	1	
Turtle	1	2	11	11	1
Marine tail				2	

Table 6.43. MLP-EI010 upper pool: changing zoomorphs through time (n = 84).

TRACKS	CS1	CS2	CS3	CS4	CS5
Human foot	2		7	5	
Macropod track			3		
Other track			1	1	
Bird track	12	3	21	24	2
Total	14	3	32	30	2

Table 6.44. MLP-EI010 upper pool: changing track depictions through time (n = 81).

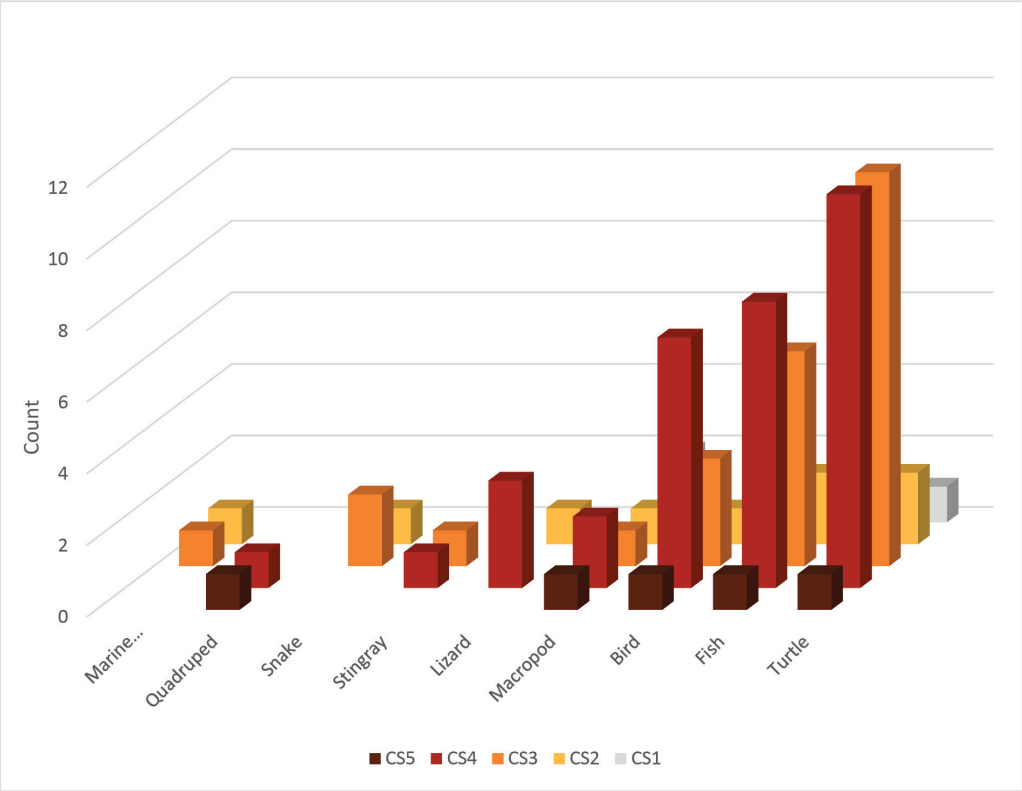

Figure 6.42. MLP-EI010 upper pool: zoomorphs and contrast state (n = 84).

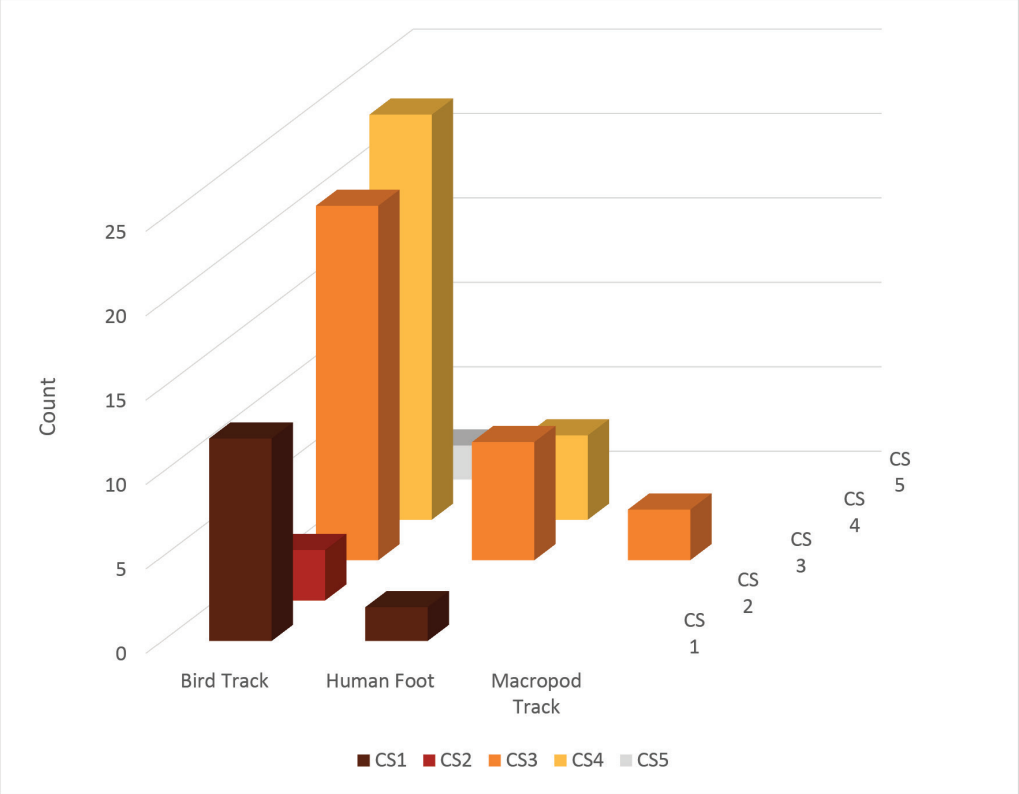

Figure 6.43. MLP-EI010 upper pool: tracks and contrast state (n = 81).

Square 562910 (including 562910B)

Square 562910 (1.0 m x 0.5 m) was placed in an elevated location on the northern side immediately above the main pool (Figure 6.38). Excavation was completed over three days in June 2016. Excavation was halted when human skeletal remains were encountered in Square 562910B (XU12). The project team contacted Sean McNeair (MAC Ranger Co-ordinator), Jeremy Elliot (DPLH) and the WA Police. The site was inspected by two Pilbara detectives, who confirmed that these were ancient Aboriginal human remains and not related to a recent homicide. The remains were left *in situ* and the square was backfilled in the presence of the police officers.

This 1.0 m x 0.5 m square was in a flat area with obvious surface *Terebralia* midden, relatively unimpeded by surface rocks (Figure 6.44). It started as a 50 cm x 50 cm square (Figure 6.45), which was expanded to an adjacent quadrant (562910B, Figure 6.46) when subsurface rocks impeded the extraction of sufficient sediment. The square was aligned north–south with all X-Y-Z measurements taken from the south-west corner. Excavation proceeded stratigraphically with 14 XUs dug in 2–4 cm depths (Table 6.45).

Figure 6.44. Setting up square 562910, June 2016. View to the north and south across the gorge (top). Note the nature of the surface *Terebralia* scatter, and the spinifex and boulder background.

Figure 6.45. Square 562910 (top left) at completions of XU1 and (top right) excavation features in XU2, including the hearth feature and (inset) a worked bone and the Dentalium fragment provenanced and dated. The end level of XU9 (bottom left) with a provenanced macropod bone and chopper tool (bag 9) and (bottom right) end of XU15 showing northern baulk and base of excavation both squares.

Figure 6.46. Square 562910B (top left) at completions of XU1 and (top right) excavation at end of XU8; (bottom left) human bone found *in situ* in XU11 with southern baulk and (inset) the bone in anatomically correct position; and (right) the photography of 562910B by police officer, prior to backfilling.

UNIT	DEPTH BELOW SURFACE (CM)	EXCAVATED WEIGHT (KG)	DISCARDED ROCK (KG)	PH	MUNSELL
XU01	4.6	33.2	2.9	8.5	5 YR 3/2
XU02	6.7	21.4	2.4	8	–
XU03	9.4	19.3	1.4	8.5	–
XU04	12.0	21.5	0	8.5	–
XU05	14.6	19.1	1.4	8.5	5 YR 2.5/2
XU06	17.1	18	1.4	9	5YR 3/3
XU07	19.8	19.5	1.3	8.5	5YR 3/2
XU08	22.5	18.5	1.9	8.5	5 YR 3/2
XU09	26.5	18.5	2.3	9.5	5 YR 3/2
XU10	30.2	29.3	4.6	9	5 YR 3/2
XU11	34.4	26.4	9.1	8.5-9	5YR 3/2
XU12	43.5	18.6	13.6	9	5 YR 2.5/2
XU13	50.6	7	5.8	9	5 YR 2.5/2
XU14	60.2	5	3	9	5 YR 2.5/2
Total		275.3	51.1		

Table 6.45. Square 562910: excavation weights for deposit (kg) and sediment characteristics.

Stratigraphy and dating

Excavation notes comment on the undisturbed nature of the archaeological deposit. Artefacts were found lying flat, and several intact hearth features were encountered (in XU1/2 and in XU4). Three stratigraphic units were encountered (Figure 6.47). Within the profile, colour intensifies and becomes generally redder with depth. Compaction also increases with depth. Stratigraphic units 1 and 2 (SU1 and SU2) are the midden layer proper; SU3 contains some decomposing shell at its top but is much rockier and contains only stone artefacts.

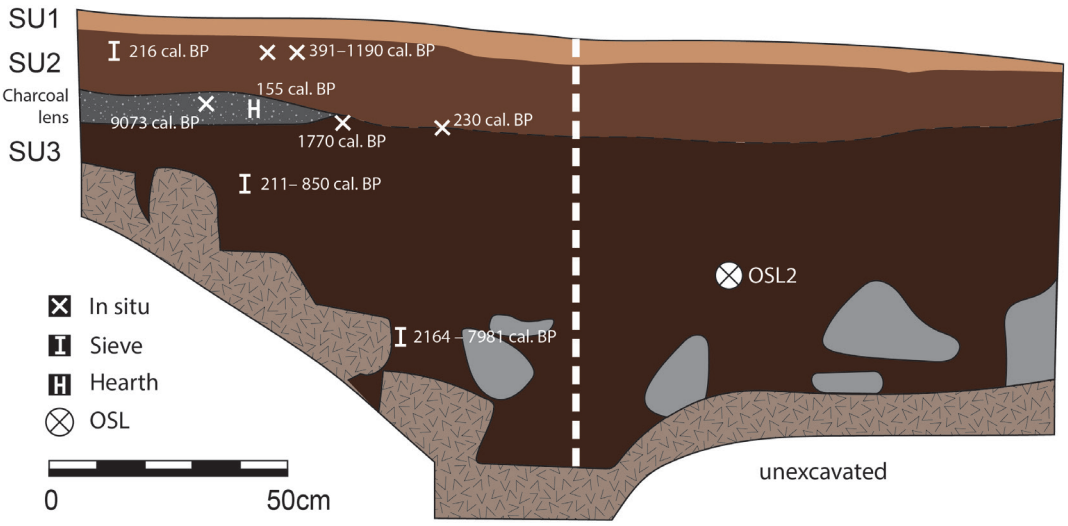

Figure 6.47. Square 562910 and Square 562910B: stratigraphic section drawings (eastern baulk).

The strata are described as:

SU1 – Light brown (5YR 3/2) unconsolidated silty sand with small gravels. Large, whole (*Terebralia*) shells and many lithics, no large surface cobbles; weathered surface midden: pH 8.5;

SU2 – Medium brown (5YR 2.5/2) moderately consolidated sandy deposit. Large shells and fragments continue, as do the lithics. Some burnt bone and charcoal observed (and collected): pH 8.5. While there is an indistinct boundary to SU3 in Square 562910B, there is a hearth at the interface of these two units in Square 562910.

SU3 – Dark reddish brown consolidated gritty sands, some silts with fragmented shell and lithics (5YR 3/2); becomes more moist and more clayey just above interlocking basal rocks (unexcavated) presumably sitting on bedrock: pH 9.

Twelve radiocarbon dates were returned from samples in this excavation square (Table 6.46, Figure 6.48). One OSL sample was collected, but, because of otherwise dateable materials throughout and the mixed radiocarbon results, this was not submitted for dating. Four of the radiocarbon determinations (*Dentalium* and charcoal) derive from provenanced samples collected during excavation; the others were submitted based on the sorted finds from XUs 2, 4, 7 and 11. One of the dated *Dentalium* fragments was a posterior end, the other was likely a bead (Figure 6.49). The charcoal from XU2 (Wk-44900) was collected from an intact hearth; the charcoal collected from XU4 (Wk-44902) was an isolated piece of provenanced charcoal.

LAB CODE	MATERIAL	XU	AU	DEPTH (CM)	D13C 0/00	RESULT	95% MAX	95% MIN	CAL MID
ANU-18636	Terebralia		S	0	36.67	8,060	9,120	9,113	9,000
Wk-46103	Terebralia	2	1	3–6	92.2	653	294	138	216
Wk-46104	Chiton	2	1	3–6	90.3	817	470	312	391
Wk-44899	Dentalium	2	1	4.5	3.2	1,716	1,350	1,030	1,190
Wk-44900	C14-hearth feature	2	1	4.5	NA	208	310	0	155
Wk-44901	Dentalium	4	1	11	3.5	1,839	1,830	1,710	1770
Wk-46105	Terebralia	4	1	8–11	34.7	8,504	9,174	8,971	9,073
Wk-46106	Chiton	4	1	8–11c	91.6	703	395	240	318
Wk-44902	Charcoal	4	1	13	NA	242	310	150	230
Wk-46107	Terebralia	7	1	22–26	84.3	1,371	925	775	850
Wk-46108	Chiton	7	1	22–26	92.3	644	288	134	211
Wk-46109	Terebralia	11	2	37–41	39	7,573	8,056	7,905	7,981
Wk-46110	Chiton	11	2	37–41	72.8	2,546	2,279	2,049	2,164

Table 6.46. Square 562910 and surface *Terebralia* radiocarbon (AMS) determinations.

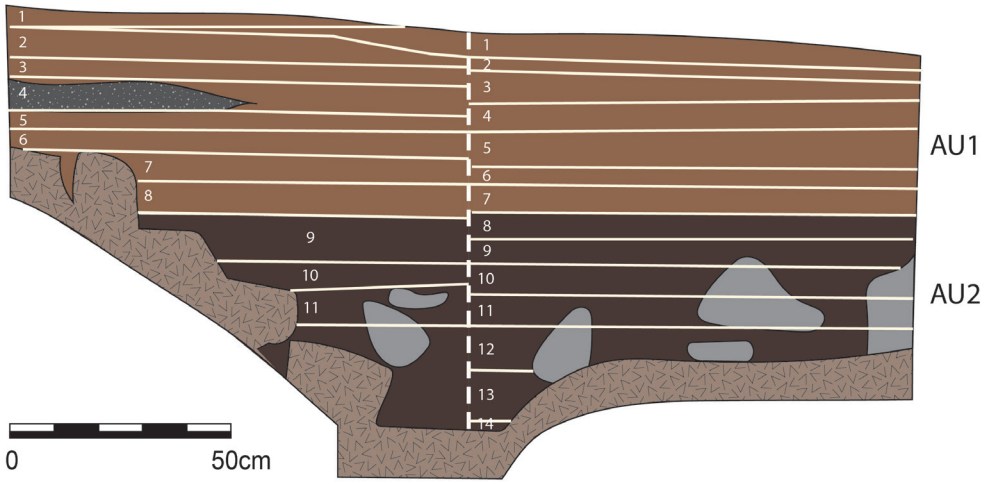

Figure 6.48. Square 562910 A+B showing dated samples against the stratigraphy (eastern baulk). X marks the provenanced date locations; I indicates sieved sample depths.

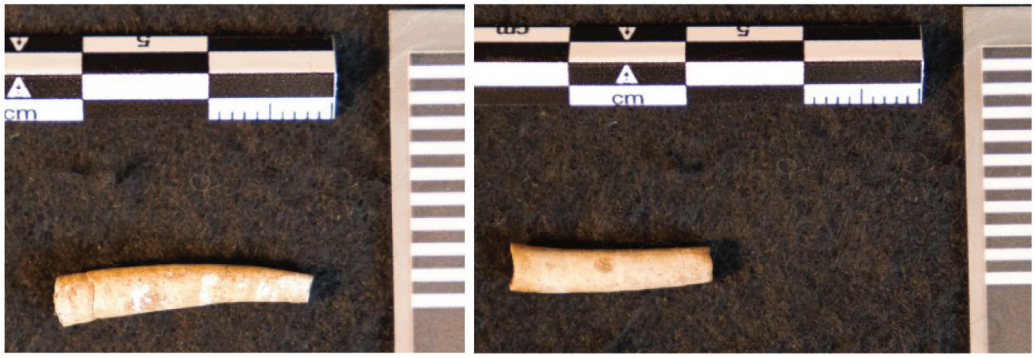

Figure 6.49. The two *Dentalium* fragments submitted for dating: (left) END06-562910-XU2-3 (Wk-44899) – a posterior end; and (right) END06-562910-XU4-4 (Wk-44901), which is a bead with a characteristic concave break.

The AMS dates were from different shell species in the different stratigraphic layers. In several cases, these were paired to test the reliability of the *Terebralia* dates (i.e. the reservoir effect: see Petchey and Ulm 2012). The radiocarbon determinations indicate that the deposit is very mixed, despite observations made during excavation and the intact profile in both squares (particularly 562910, which has an intact hearth near its top). We interpret this as partially due to the interment (human remains) in square 562910B – and to the fact that this mixed-matrix midden deposit is in the open and subject to seasonal cyclonic conditions.

Bayesian analysis

Given the numerous inversions present (Table 6.46), three sequence depositional models were used to analyse the Enderby 10 chronostratigraphy (Bronk Ramsey 2008, 2009a). The first two were based on the analytical and stratigraphic units identified (Table 6.47). The third model pooled all the dates regardless of stratigraphic or analytical unit. The models follow the parameters and methods outlined in Chapter 2. Dates for Enderby 10 individually and inter-stratigraphically overlap with other dates in the sequence. This indicates some level of continuous occupation and so continuous boundaries were used for the stratigraphic model. However, for the analytical unit model, a discontinuity is proposed between the Late Holocene (AU1) and the Early Holocene (AU2). To account for this, a sequential boundary is used to represent the discontinuity in the analytical model. It should be noted that ANU-18636 was not included in these models because it derives from the surface elsewhere on the site.

Neither the analytical or stratigraphic models resolve the mixed nature of Enderby 10 deposit. The results for an alternative basic model, one that combines all dates into a single phase with only a surface and base boundary, are displayed in Table 6.47 and Figure 6.52. In contrast to the analytical and stratigraphic models, this basic model returns good results with all dates above agreement index threshold values and all dates have a <5% chance of being outlier (Amodel = 96.3 and Aoverall = 89.9). The basic model estimates that occupation at Enderby 10 began at 9,800–8,680 cal BP and ends at 30–0 cal BP. Unfortunately, the model offers no chronological resolution for finer-grained analytical units.

NAME	68.2%		95.4%		SUM. STATISTICS			INDICES	
	FROM	TO	FROM	TO	μ	σ	M	AI	OP
Boundary: deposit surface	30	0	60	0	20	20	20	100	
Phase: Enderby 10									
Wk-46103	100	20	180	0	70	50	60	87.4	96.5
Wk-46104	240	90	290	20	160	70	160	102.2	96.4
Wk-44899	1,060	920	1,150	840	990	70	990	101	96.3
Wk-44900	280	140	290	70	200	50	200	100.2	96.5
Wk-44901	1,190	1,040	1,260	970	1,110	80	1,110	101.3	96.2
Wk-46105	8,840	8,630	8,950	8,570	8,740	100	8,740	101.7	96.1
Wk-46106	120	20	210	0	90	50	80	91.3	96.5
Wk-44902	290	150	300	150	210	50	190	99.7	96.8
Wk-46107	720	590	770	530	650	60	650	99.1	96.3
Wk-46108	100	20	160	0	70	40	60	87	96.5
Wk-46109	7,810	7,660	7,900	7,590	7,730	80	7,730	99.9	95.9
Wk-46110	1,980	1,820	2,060	1,730	1,900	80	1,900	99.9	96.2
Boundary: deposit base	9,800	8,680	11,600	8,570	9,620	950	9,320		

Table 6.47. Bayesian results for Enderby 10 using a basic model.

Ultimately, the analytical and stratigraphic unit models both demonstrate that Enderby 10 is a mixed deposit (see Appendix 3: tables A3:10, A3:11, A3:12). As a result, it is not possible to confidently establish meaningful chronological units using either model. The best model for Enderby 10 is the basic model (Table 6.47 and Figure 6.50).

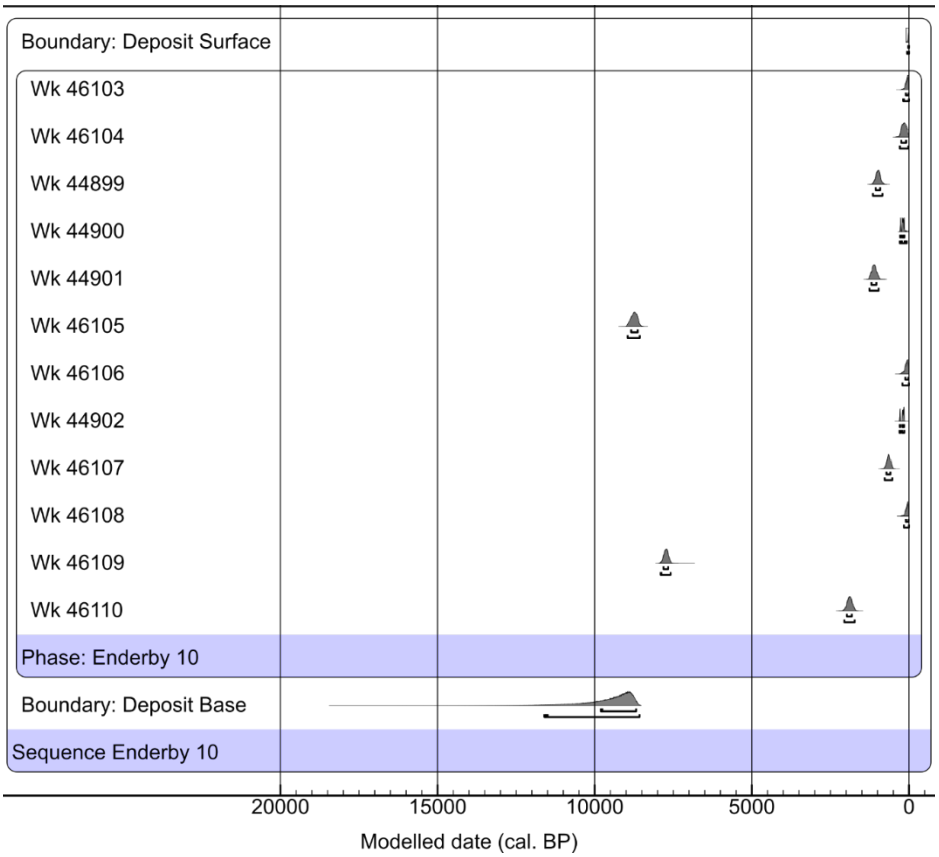

Figure 6.50. Bayesian analysis results for Enderby 10 using the basic model.

While this offers less chronological resolution, it preserves the Early and Late Holocene signatures which at least demonstrates that, while the deposit is mixed, the site was occupied throughout the Holocene. It is not possible to confidently establish meaningful chronological units using the usual Bayesian approaches. The deposit should probably be treated as a single analytical unit given inter-strata mixing is evident. This constraint is noted, but based on the stratigraphy (Figure 6.48) and the distribution of stone artefacts and lithologies (particularly in Square 562910B), the assemblage is analysed according to two broad analytical units albeit with imprecise temporal boundaries:

Analytical Unit 1: Late Holocene
Square 562910
XU1–8 Square 562910B XU1–7

Analytical Unit 2: Early Holocene
Square 562910
XU9–15 Square 562910B XU8–14

Excavated assemblage

The excavated assemblage weighed over 17.3 kg and was composed predominantly of shellfish (over 14.5 kg), stone artefacts (1.8 kg) and bone (793.71 g) and other organics (122 g; Table 6.48). Shell, bone, coral (62.1 g), crustacean (20.94 g), ochre (39.4 g) and artefacts are found throughout both analytical units. Over 10.1 kg of the shell (69.9%) was identifiable to species level: the remaining 4.4 kg (30.1%) was highly fragmented and has not been sorted to species. Shell weights are highest in the top excavation unit (3.3 kg of shell; 900 g undiagnostic shell); likely a result of treadage and taphonomic factors resulting in the removal of fine sediment and smaller material away from the intact *Terebralia* matrix. There are, however, significant shell remains throughout most of the site. Stone artefacts are also found throughout the sequence, with varying (mostly high) amounts of microdebitage. Microdebitage appears to be inversely correlated with the shell deposition (i.e. the later peak in shell is matched by a decline in knapping intensity); again, this may be a taphonomic consequence of this site being in the open and subject to extreme weather events.

UNIT	AU	FLAKED ARTEFACTS	SHELL (DIAGNOSTIC)	SHELL (UNDIAG.)	BONE (DIAGNOSTIC)	BONE (UNDIAG.)	OTHER*	TOTAL CULTURAL MATERIAL
XU01	1	416.57	3,301.46	796.01	21.53	9.31	34.24	4,579.1
XU02	1	308.76	796.6	291.65	23.62	25.98	32.38	1,478.9
XU03	1	253.16	585.83	221.74	28.53	29.55	5.25	1,124.1
XU04	1	274.55	923.41	392.56	45.83	34.68	2.17	1,673.2
XU05	1	155.8	705.81	332.39	86.15	46.89	16.68	1,343.7
XU06	1	114.54	441.59	442.36	53.99	29.96	0.61	1,083.1
XU07	1	174.03	445.8	307.58	63.86	23.00	4.66	1,018.9
XU08	1/2	32.97	723.6	215.91	42.71	34.06	10.46	1,059.7
XU09	2	52.59	743.44	213.39	25.42	36.84	7.87	1,079.5
XU10	2	0.89	534.38	394.04	21.03	27.55	4.27	982.12
XU11	2	46.86	476.83	359.35	13.21	18.76	1.81	916.8
XU12	2	7.74	187.04	140.78	12.85	16.43	0.69	365.5
XU13	2	41.76	175.55	75.87	4.29	11.19	0.51	309.2
XU14	2	1.2	136.7	76.55	0.20	2.38	0.01	217.0
XU15	2	2.36	2.8	120.79	0.07	3.75	0.3	130.1
Total		1,883.78	10,180.84	4,380.97	443.29	350.43	121.91	17,361.2

Table 6.48. Square 562910 (A and B): weights of cultural materials in grams.
*Includes barnacle, coral, seeds, land snail, charcoal, organics

Economic shellfish

Over 10 kg of identifiable economic shellfish remains were recovered from the 1.0 m x 0.5 m excavation at Enderby 10, along with almost 4.5 kg of unidentifiable fragmented shell. A third of the identified species were recovered from the very top (XU1) of the site (Table 6.49). This is likely taphonomic – with many large whole shells being located on the surface with the fine deposits winnowed out, with the possibility that surface *Terebralia* are moved around the site in cyclonic conditions. The dominant shellfish weight contributions throughout are from the mangrove species (*Terebralia palustris*, *Terebralia semistriata*, *Terebralia* sp., *Telescopium*; Table 6.49). Two species of chiton (*Polyplacophora* sp. and *Acanthopleura* sp.) are the second largest shellfish contributor after *Terebralia*. Present in both AUs, they are more abundant in the later Holocene unit.

Sandy/muddy intertidal species such as Baler (*Melo* sp.) and *Syrinx* sp. contribute to the next most commonly represented habitats (by weight), although the presence of these larger shells is not necessarily dietary. These only appear as fragmentary remains throughout this excavation (i.e. no complete shells were recovered), and there is a correlation between higher *Melo* weights and microdebitage. This may be an index of occupation intensity. The *Syrinx* fragment was only found in XU1 of 562910.

XU	CHITON	MELO AMPHORA	MUREX	SACCOSTREA	TEREBRALIA SPP.	OTHER	TOTAL
XU01	317.90	187.80	0.85	45.49	2625.60	123.82	3,301.46
XU02	179.60	114.70	0	3.80	497.70	0.80	796.60
XU03	167.55	132.10	0	2.92	279.89	3.37	585.83
XU04	233.25	161.16	18.29	0.48	499.83	10.40	923.41
XU05	138.54	61.96	48.43	1.10	448.57	7.21	705.81
XU06	97.00	58.05	12.25	0.30	263.99	10.00	441.59
XU07	80.00	85.72	12.63	3.09	263.96	0.40	445.80
XU08	94.10	34.50	14.40	2.30	563.80	14.50	723.60
XU09	66.65	139.30	20.74	0.65	511.80	4.30	743.44
XU10	67.99	32.06	8.79	8.74	362.68	54.12	534.38
XU11	65.60	17.09	5.30	3.09	369.20	16.55	476.83
XU12	14.27	2.86	2.11	0	167.80	0	187.04
XU13	2.38	1.32	2	0	169.85	0	175.55
XU14	1.70	0	0	0	135.00	0	136.70
XU15	0.30	0.20	0	0	2.30	0	2.80
	1,526.83	1,028.82	145.79	71.96	7,161.97	245.47	10,180.84

Table 6.49. Square 562910: dominant economic shellfish species in each of the combined XU (weights in grams).

Rocky platform species, especially chiton (both species) and Rock Oyster (*Saccostrea* sp.) are present throughout, with most being found in XU1. Other rocky platform species are present in low numbers (*Nerita* sp. and *Patella* sp.), with highest densities – again – in the Late Holocene. Many (very light) *Dentalium* (tusk, or scaphopod) shells were also recovered from this square. These are discussed below.

Most (78%) of the shellfish is found in the Late Holocene (AU1) compared to the earlier occupation layer (22%), but the habitat proportions between these units are remarkably similar (Table 6.50, Figure 6.53).

AU	CHITON	MELO AMPHORA	MUREX	SACCOSTREA	TEREBRALIA SPP.	OTHER	TOTAL	%F
1	1,307.94	835.99	106.85	59.48	5,443.34	170.5	7,924.1	77.83346
2	218.89	192.83	38.94	12.48	1,718.63	74.97	2,256.7	22.16654

Table 6.50. Proportions of major species in the two analytical units.

Crustacean shell, predominantly fragments of crab chelae (claws), is present throughout the deposit but is most abundant in AU1 (14.89 g, 71.12%; Table 6.51). Two species of crab are most likely represented by the crustacean *Thalamita crenata* (Notched Swimmer Crab) and *Scylla* sp. *cf. Scylla serrata* (Brown Mud Crab). Both taxa are found on mangrove mudflats.

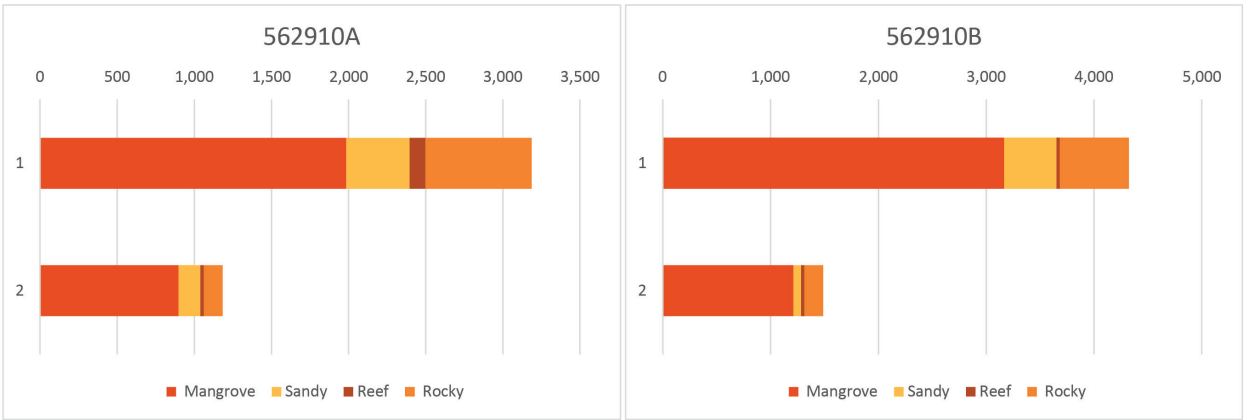

Figure 6.51. Square 562910: proportions of species, coded for habitat in the excavation units of both quadrants (weights in grams).

When the analytical units are grouped and coded for habitat, it is clear that there is only a minor dietary shift between the Early Holocene and Late Holocene (Table 6.51, Figure 6.51), despite the weight of shell deposited in the Late Holocene being almost three times the amount brought in during the earlier occupation period. Mangal species dominate throughout (AU2 79%: AU1 69%) but with >80% in AU2 (from 562910B) and a low of 62% (in AU1 in 562910).

While the inversions in the radiocarbon dates indicate that the occupation deposit has been mixed – probably through a combination of intensive occupation, bioturbation / exposure to the elements and the interment of skeletal remains – the overall pattern for occupation of this inland waterhole is of mangrove-focused shellfish collection supplemented by a mixed sandy beach and rocky platform / reef focus (initially) accounting for 20% of catch (in the Early Holocene), and up to 30% by the Late Holocene (Figure 6.52). This accords well with the dates and landscape evolution described by Semeniuk and Wurm (1987), which observes that the mangrove forest initially prospered between the western (largest) and middle portions of Enderby Island. Indeed, there are extant mangrove populations still in the centre of Enderby Island and in patches at the northern and at several eastern beaches (Figure 6.53).

HABITAT	SPECIES	AU1	AU2	TOTAL	%F
Mangrove mudflats	Terebralia palustris, Terebralia semistriata, Terebralia sp., Telescopium	5,150.1	2,111.4	7,261.5	71.3
Rocky	Saccostrea, Trochid, Turbo sp., Chiton, Barnacles, Nodulosa sp., Nerita sp.	898.6	210.8	1,109.4	10.9
Coral/reef flats	Murex, Acrosterigma sp., Cerethidae sp., Murex sp.	133.0	53.3	186.3	1.8
Sandy/muddy Intertidal	Melo amphora, Syrinx aruanus	1,328.5	294.9	1,623.4	15.9
Mangrove mudflats	Large crab (indet.)	14.9	6.0	20.9	
Total shellfish		7,510.1	2,670.4	10,180.5	100

Table 6.51. Identifiable shellfish species in the two analytical units (weight in grams).

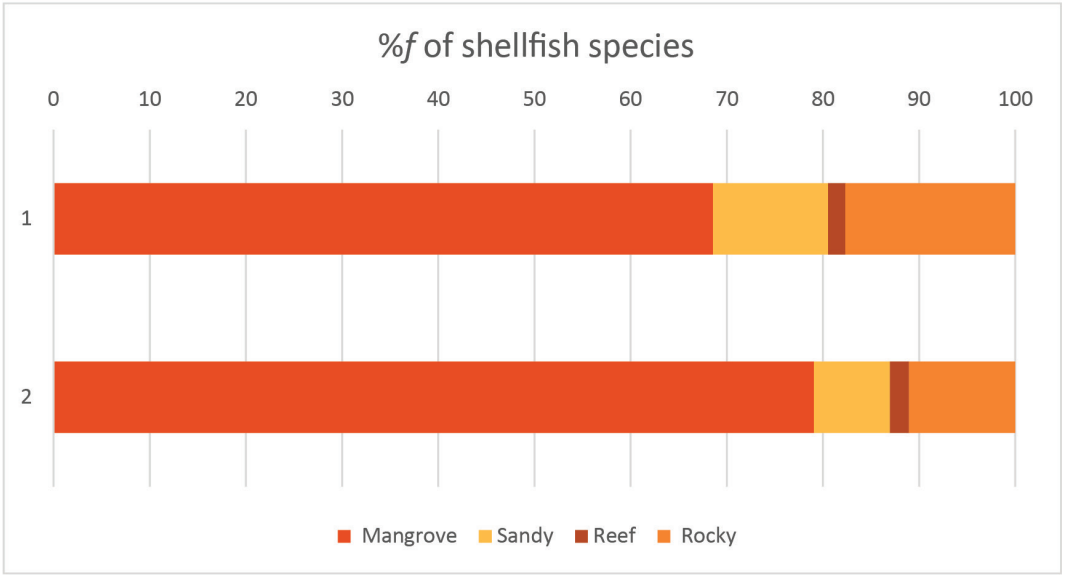

Figure 6.52. Square 562910 combined: habitat (%f) of shellfish species found in the two analytical units.

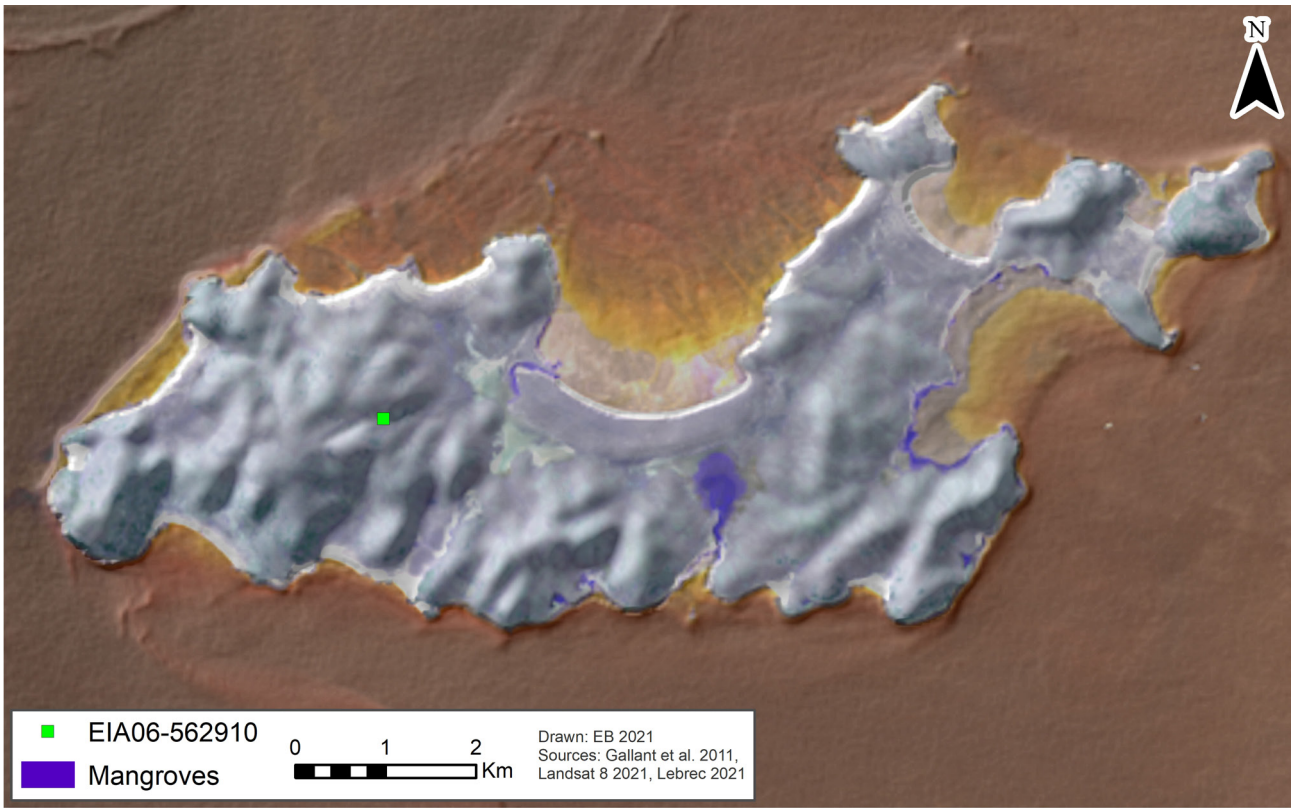

Figure 6.53. False colour image (red, near-infrared and blue) of Enderby Island showing locations of contemporary established mangrove habitats (blue) relative to EIA06-562910.

Vertebrate fauna

Vertebrate faunal remains from the Enderby 10 assemblage included bone and tooth fragments, mostly from mammals, reptiles and fish. A total of 10,179 vertebrate faunal specimens were recorded, of which 2,305 (22.6%) were identifiable to Family level or lower. Mammals make up most of the assemblage by count and weight (n = 6,802, 377.00 g), closely followed by reptiles – mostly turtle – (n = 1,940, 354.32 g) and fish (n = 1,172, 58.77 g). Figure 6.54 illustrates the distribution of the vertebrate faunal remains by excavation unit. The Late Holocene AU1 layer contains almost 70% of the bone recovered, dominated by terrestrial mammals and marine reptiles (turtle) and a small but consistent quantity of fish. Much less vertebrate fauna was recovered from the lower XUs, although mammal, turtle and fish are still well represented in AU2 (Figure 6.54). Assemblage composition varies slightly across the excavation units (Figure 6.55), with an increase in fish at the surface of the site (XU1) and a noticeable increase in the abundance of turtle in XUs 4–7 of both squares. Fish, mammal and marine reptile are consistently present across both the Early and Late Holocene units.

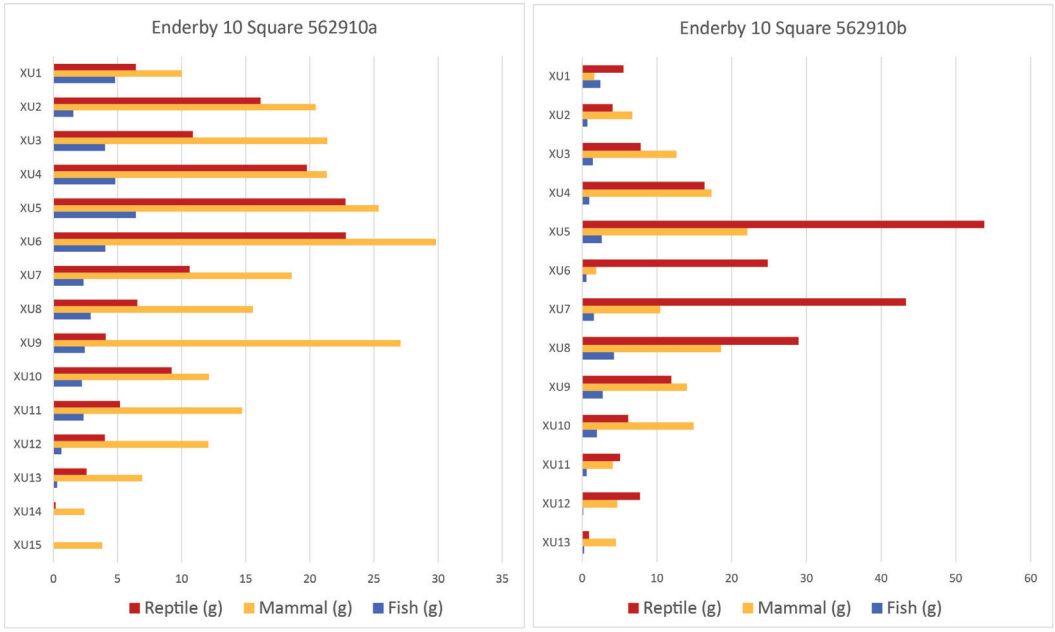

Figure 6.54. Square 562910: distribution of bone (weight in grams) in excavation units.

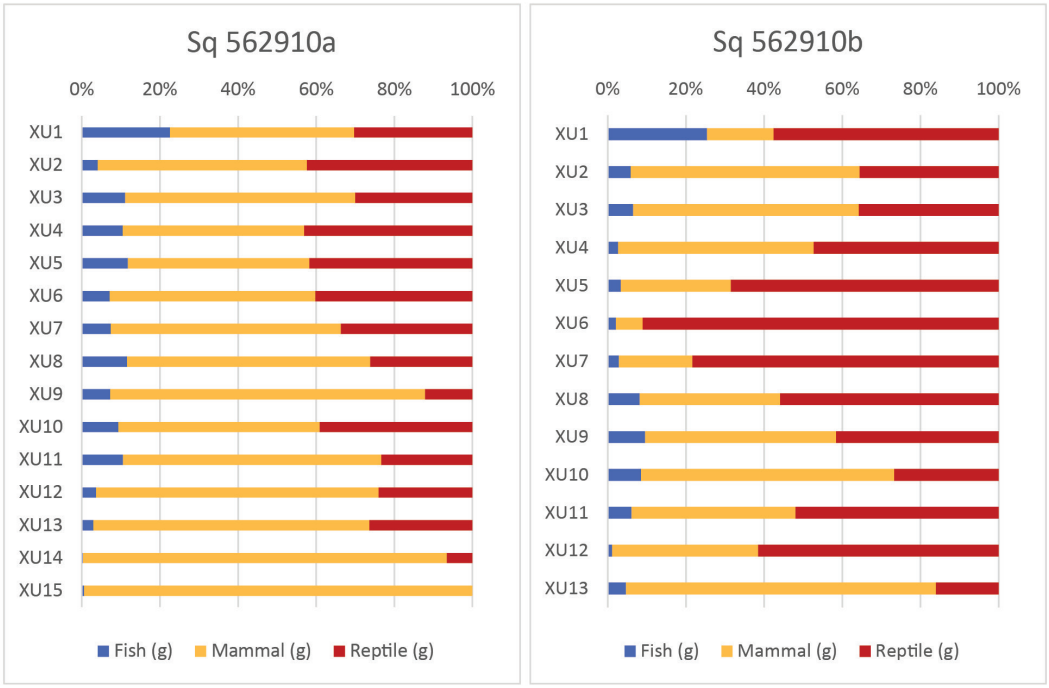

Figure 6.55. Square 562910: distribution of fish, mammal and reptile bone (% by weight) in excavation units.

Approximately 10% (by weight) of the overall bone assemblage shows evidence of burning (Table 6.52), with blackened/charred bone almost twice as abundant as calcined bone in both analytical units. Blackened and calcined bone is slightly more abundant in AU2 (Table 6.52 and Figure 6.56), which may be due to differential preservation (Aplin et al. 2016) or more intense fires during this earlier period.

	UNBURNT		BLACKENED		CALCINED	
	G	%	G	%	G	%
AU1	506.28	90.03	38.71	6.88	17.33	3.08
AU2	218.68	86.85	21.03	8.35	12.07	4.79
Total	724.96	89.05	59.74	7.34	29.40	3.61

Table 6.52. Square 562910: burnt bone (weight in grams).

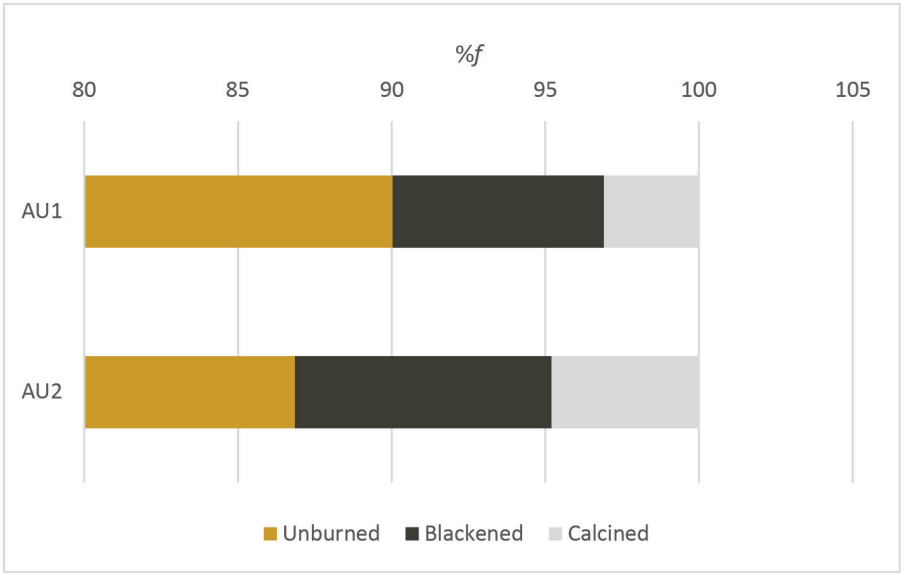

Figure 6.56. Square 562910: distribution of burnt bone (% by weight) in excavation units.

Mammal and turtle bone showed similar rates of burning, with c. 10% of turtle bone burned or charred across both units, compared to c. 10% of mammal bone in AU1 and c. 15% in AU2. Fish bone also showed evidence of burning, but overall less burnt or charred fish bones (c. 2% in AU2, c. 4% in AU1) were recovered. This likely results from the fish bone being more fragile and susceptible to a range of decay and taphonomic processes.

The vertebrate fauna identified in the Square 562910 assemblage is shown as the number of identified specimens (NISP; Table 6.53), along with a count of total number of fragments that could not be identified to a meaningful taxonomic level. While mammal bone was heavily fragmented and generally in poor to fair condition, much of the cranial and dental material was identifiable to genus and/or species. Unidentified mammal bone fragments could be discerned from fish or reptile but could not be identified beyond this category.

Marine turtle (Family *Cheloniidae*) and unidentified fish composed the bulk (by bone weight) of the identifiable taxa within both phases of the assemblage. This reinforces the presence of marine species in both the Early and Late Holocene occupation phases of the site. Fish pharyngeal grinding plates, dentaries and isolated teeth are common throughout the assemblage and are indicative of reef fishes, such as parrotfish and wrasse, although identifications have not yet been made on these specimens due to a lack of comparative reference material.

	ANALYTICAL UNIT	
	AU1	AU2
MAMMALS		
Dasyurids		
Dasyuridae indet.	1	1
Bandicoots		
Isoodon sp. cf. Isoodon auratus	–	1
Isoodon sp. indet.		2
Kangaroos and wallabies		
Petrogale sp. cf. Petrogale rothschildi	49	8
Macropus sp. cf. Macropus robustus	2	–
Unidentified medium macropod	33	2
RODENTS		
Notomys longicaudatus	–	1
Rattus tunneyi	2	–
Rattus sp. indet.	4	–
Muridae indet.	2	1
REPTILES		
Snakes		
Unidentified snake	–	1
Marine turtles		
Unidentified marine turtle	1,436	760
FISH		
Unidentified fish	842	337
Unidentified shark	1	–
TOTAL NISP	2,372	1,114
Medium mammal fragments	9	3
Large mammal fragments	1	–
Unidentified mammal fragments	3,967	2,713
Total no. of fragments	6,349	3,830

Table 6.53. Total vertebrate element count (NISP) for combined excavation squares 562910.

Otoliths were common (Figure 6.57) in the assemblage (n = 187), with the majority (n = 140, 74.87%) recovered from Late Holocene AU1. Taxonomic identifications have not been confirmed on these otoliths, but most appear to be from the same species of very small fish, and their extremely small size (less than 5 mm diameter) and abundance may indicate the use of nets or other bulk collection methods. These small otoliths are morphologically like and tentatively identified as Hardyhead (Family *Atherinidae*, also known as silversides

or whitebait), a small fish (probably less than 10 cm in length) that forms large, multi-species schools that are common in shallow coastal waters (Figure 6.58).

A single tooth of a small shark was also identified in the Late Holocene assemblage. Together, these fish and turtle specimens demonstrate hunting and fishing practices that targeted a wide range of marine animals, such as was demonstrated in the final phase of occupation at Boodie Cave when the sea was proximal at 7,000 years ago (Veth et al. 2017).

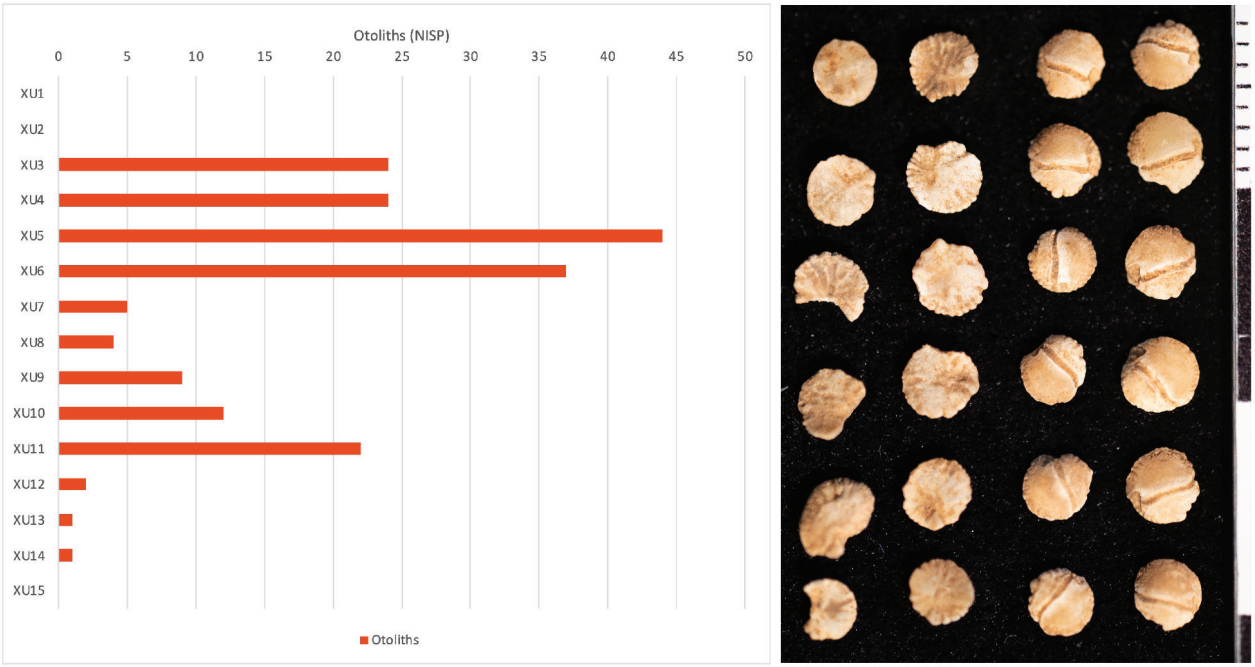

Figure 6.57. Square 562910: otoliths and their distribution throughout the sequence.

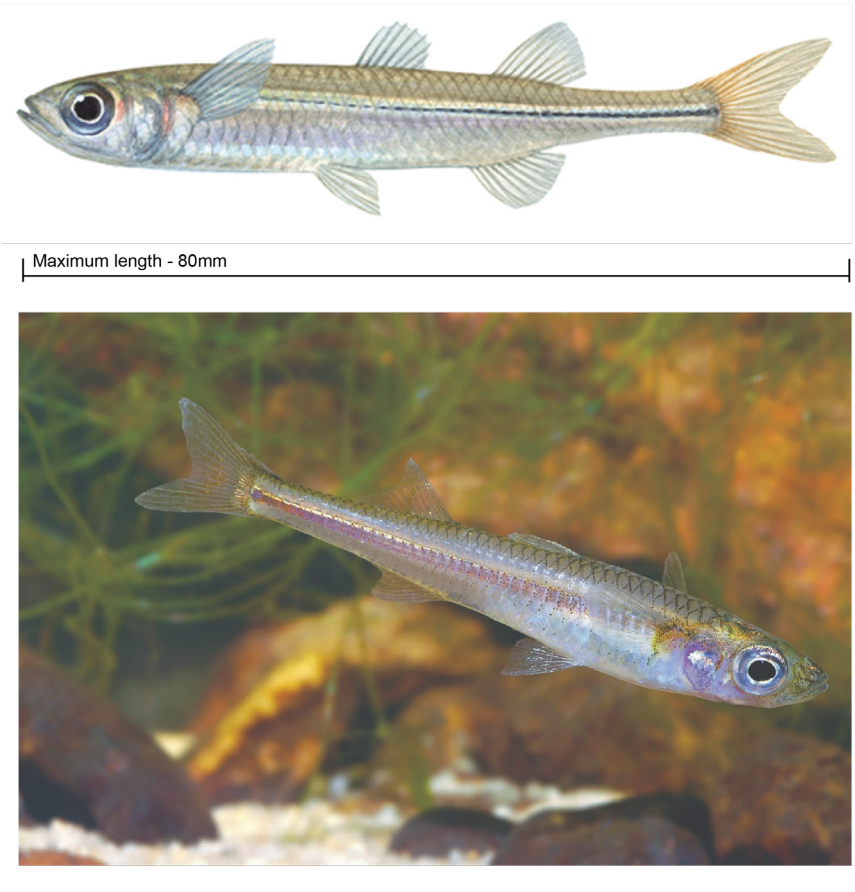

Figure 6.58. Western Hardyhead (whitebait), suspected to be the fish responsible for the otoliths at EIA-010. Image: Rickard Zerpe, 2019 (https://rivers.dwer.wa.gov.au/species/leptatherina-wallacei/).

Macropods were common in the faunal assemblage, with rock wallabies (*Petrogale* sp.) making up 50–53% of the identified mammals in both analytical units (Figure 6.59). It is possible that some specimens are *Petrogale lateralis*, which was once widespread through the Pilbara and remains extant on Barrow and Depuch islands (Pearson 2013). However, based on size, morphology and distribution, it is more likely that the specimens are the Rothschild's Rock Wallaby (*Petrogale rothschildi*), which comprises the extant Dampier Archipelago rock wallaby population and features in confirmed species previously identified from Enderby Island. The Rothschild's Rock Wallaby is a medium-sized macropod with a mean adult body weight ranging from c. 2.6–3.9 kg for individuals on the islands of the Dampier Archipelago (Pearson and Eldridge 2008; Pearson 2013). During the daytime, it seeks refuge in and around caves, rock outcrops, and rock piles with deep, shady crevices, foraging nearby at night for soft grasses, fruits and herbs (Pearson 2013).

Two specimens of a much larger macropod, tentatively identified as Euro (*Macropus robustus*), were identified in the Late Holocene assemblage. Like the rock wallaby, euros show a preference for rocky environments and shelter in the shade of rocky outcrops, but also extend into hilly and plains country. Although euros are no longer extant on Enderby Island, they persist on similarly sized islands in the archipelago, including West Lewis and West Intercourse islands (Morris 1990), so it would appear they continued to occupy Enderby Island for some time after islandisation.

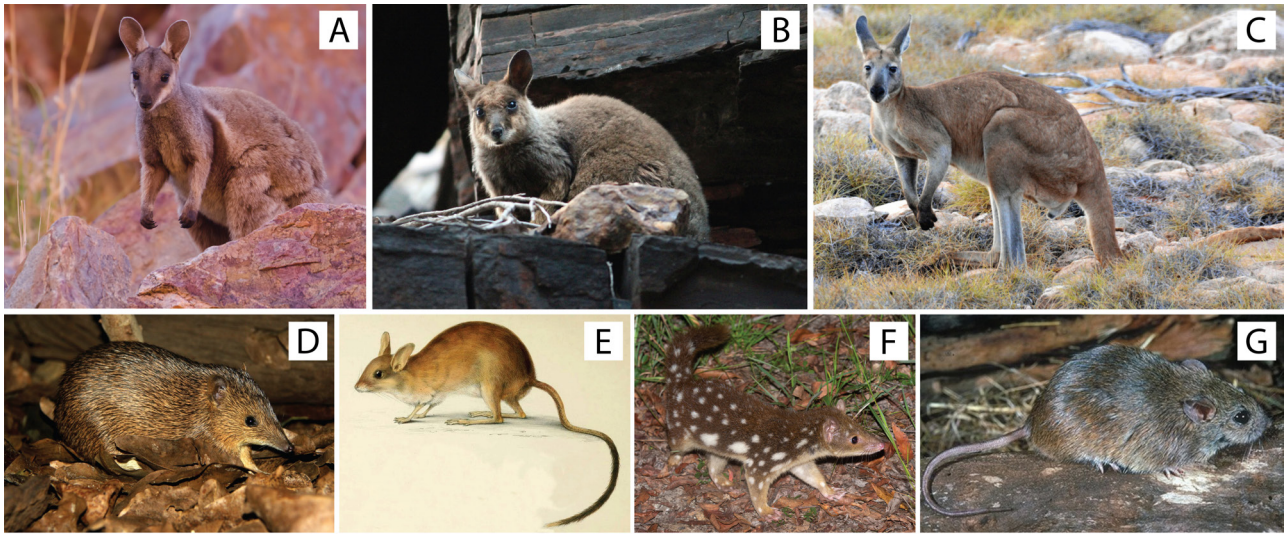

Figure 6.59. Dominant mammal species likely represented in the Enderby 10 site's midden A) *Petrogale laterali*, B) *Petrogale rothschildi*, C) *Macropus robustus*, D) *Isoodon auratus*, E) *Notomys longicaudatus*, F) *Dasyuridae*, and G) *Rattus tunneyi*.

The golden bandicoot, *Isoodon auratus*, once occurred across much of northern and central Australia but is now restricted to isolated populations on Barrow Island, parts of the coastal Kimberley and several islands off the Kimberley and Arnhem Land coasts (Palmer et al. 2003). Habitat preferences of this small bandicoot are not well described (partly due to the fragmented and vulnerable nature of the remaining populations) but are generally described as vine thickets and rocky sandstone spinifex habitats (Palmer et al. 2003). Only one specimen, from the Early Holocene, was identified in the assemblage.

A small number of rodents were identified in the faunal assemblage but only three elements could be confidently identified: a maxillary fragment of a Long-tailed Hopping Mouse, *Notomys longicaudatus*, and a dentary and isolated molar from the Pale Field Rat, *Rattus tunneyi*. Now extinct, the habitat preferences of the Long-tailed Hopping Mouse are not well understood. However, its past distribution extended throughout much of inland Australia, and showed a preference for open plains with clay soils (Dixon 1983). The Pale Field Rat was once widely distributed across Australia, including into the arid interior and mesic south-west, but is today restricted to fragmented populations amongst coastal and riparian habitats with more diverse habitat exploitation during the wet season (Braithwaite and Griffiths 1996).

As noted earlier, burning was evident on some of the identified specimens, with differences in burning across species and groups. Between 22% and 25% of the identified *Petrogale* specimens (across the two analytical units) showed evidence of charring, strongly supporting cultural origins for these animals in the midden assemblage. No other identified mammal specimens showed evidence of burning. For the smaller mammals (dasyurids, rodents and bandicoots), this may reflect

their incorporation into the assemblage by non-human predation or reflect different cooking techniques. The origin of the euro specimens is less clear, as these large animals are frequently consumed by people and their dense, robust teeth are known to have been used as tools and ornaments (Balme and O'Connor 2019).

The small assemblage size precludes meaningful environmental analysis, but identification of at least five mammal species in the faunal record does suggest that the terrestrial mammal diversity was higher during the time in which the midden formed than it is today.

Stone artefacts

The excavated Enderby 10 assemblage consists of 11,652 flaked stone artefacts. A total of 2,487 artefacts are >10 mm, while the remainder (n = 9,165) is comprised of knapping debris (artefacts <10 mm). The substantial microdebitage component of this assemblage indicates significant and repeated *in situ* stone reduction at this site. This very high artefact density, combined with other economic remains, is unique amongst most Murujuga excavated sites. The lithic assemblage from Square 562910/562910B is described within the two analytical units (AUs) described earlier.

Assemblage composition

A representative sample of nine artefacts from Enderby 10 were subjected to pXRF analysis to confirm their lithologies and aid in material classification for the site (see pXRF, Chapter 2). Most artefacts are made on local andesitic basalt (97.1%, Table 6.54). This category includes a very small proportion of dacite (Figure 6.60), which is difficult to macroscopically differentiate from andesitic basalt. This is particularly the case with artefacts <1 cm in size: hence all <1 cm fragments of dark-coloured, fine-grained igneous rock were classified as andesitic basalt. It is therefore possible that the microdebitage assemblage may contain a small number of fine-grained dacite or rhyodacite artefacts. Artefacts confidently identified as dacite comprise a very small proportion of the assemblage (n = 26, 0.2%). Dacite and rhyodacite (n = 14, 0.1%) both occur locally on Enderby Island (Figure 6.1). Andesitic basalt, however, is the basal geology within and around the Enderby 10 site. *In situ* artefacts and flake scars on boulders located several metres away from the excavation square demonstrate localised quarrying activities took place here. It is highly probable that the excavated stone assemblage primarily represents local quarrying.

Quartz artefacts (n = 221, 1.9%) are also likely to have been sourced from small quartz seams on Enderby Island. However, the small number of chert and chalcedony artefacts also recovered from the squares (Table 6.54) were not sourced on the island but were transported by Aboriginal people to Enderby Island from elsewhere, most likely from the Abydos Plain where sites like Cadjeput Well at the back of Karratha are known to have outcrops of chalcedony nodules which have been quarried (Veth 1983).

	MATERIAL												
AU	ANDESITIC BASALT	%F	CHAL.	%F	CHERT	%F	DACITE	%F	QUARTZ	%F	RHYODACITE	%F	TOTAL
1	7,897	97.7	14	0.2	8	0.1	19	0.2	130	1.6	12	0.1	8,080
2	3,409	95.4	34	1.0	20	0.6	7	0.2	100	2.8	2	0.1	3,572
Total	11,306	100.0	48	100.0	28	100.0	26	100.0	230	100.0	14	100.0	11,652

Table 6.54. Enderby 10 stone artefact assemblage showing materials by analytical unit.

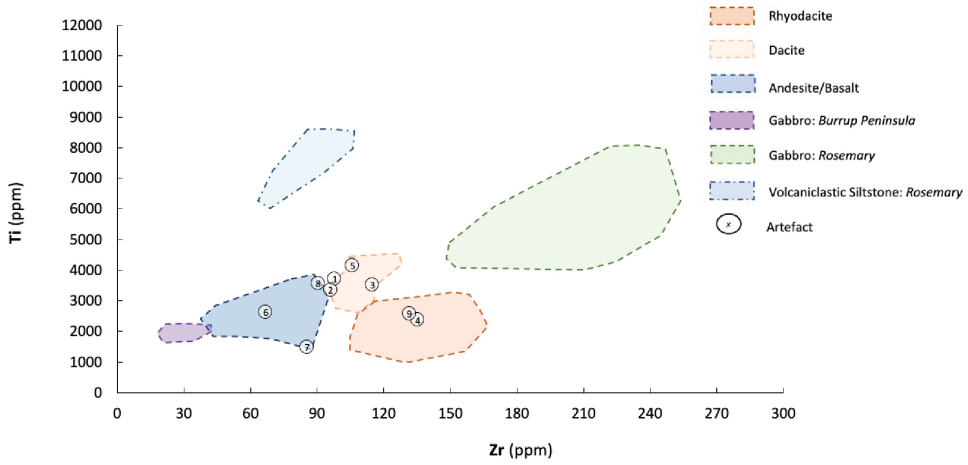

Figure 6.60. Enderby 10 artefacts overlaid on the regional distribution of raw materials sampled from across the Dampier Archipelago (see Chapter 2).

More artefacts were discarded at the site during the Late Holocene (AU1) compared with the Early Holocene (AU2, Figure 6.61). This is corroborated through a calculation of artefact discard per cubic metre when corrected for volume (Figure 6.62). This clear difference in discard between the AUs is not apparent through artefact discard per kg sediment, most likely due to an increase in natural rock component in the AU2 deposit, decreasing the sediment in the lower parts of the square.

Artefacts made on andesitic basalt predominate during both occupation phases, although a higher proportion of non-andesitic basalt artefacts (i.e. the non-local chert and chalcedony) were discarded at the site during the Early Holocene (AU1: 2.3%, AU2: 4.6%, Figure 6.61 and Table 6.54).

The Enderby 10 stone artefact assemblage is highly fragmented (Table 6.55). The andesitic basalt component (96.2% of the >1 cm assemblage) predominantly comprises broken flakes (62.5%). Transversely and longitudinally broken flakes are equally common (both n = 550, 36.7%). Artefacts made on other materials are also highly fragmented (see NAS to MNF ratio, Table 6.55). This is most likely related to high volume stone reduction and treadage from high levels of human activity at this place through time.

Only four complete and two broken andesitic basalt cores were recorded. The flake (MNF) to core ratio for the andesitic basalt assemblage is extremely high (AU1: 1,021:1, AU2: 129:1), demonstrating that cores are likely to have been removed for continued use elsewhere. A marked difference in ratio values between the Early and Late Holocene reflects the fragmented core assemblage in AU1 (1 x complete core, 2 x core fragments). Tools (n = 18) comprise only <1% of the assemblage in the >1 cm class but include a chert tool fragment. There is almost no difference in the proportions of artefact types discarded between the Early and Late Holocene. Such a low occurrence of tools is consistent with most artefacts being a product of reduction of the andesitic basalt quarry sources immediately adjacent (see Veth 1982).

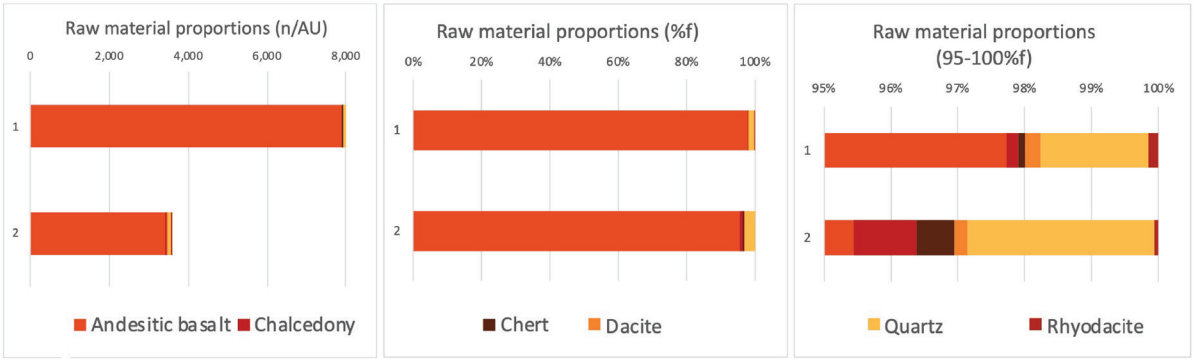

Figure 6.61. Enderby 10: proportions of raw materials in AU1 and AU2 (left and middle), and the 95–100% component in more detail (right).

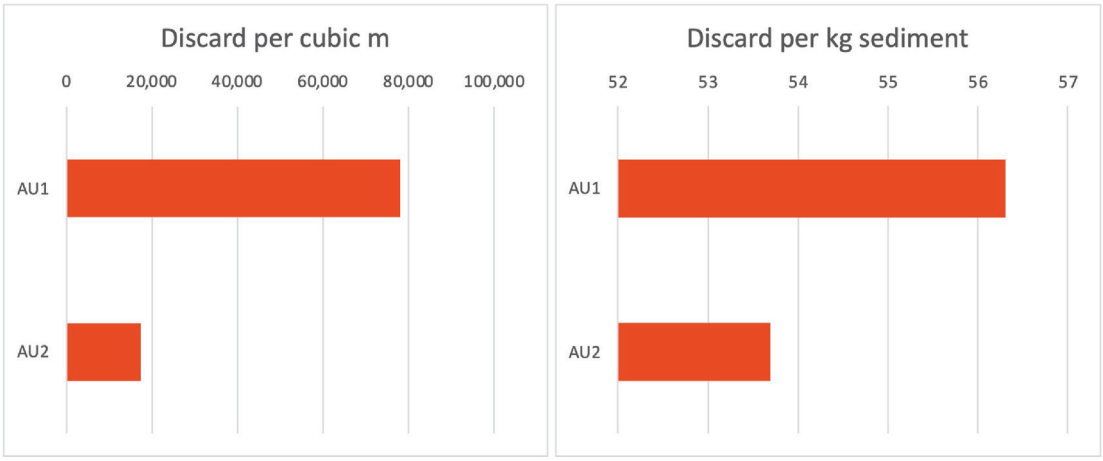

Figure 6.62. Enderby 10: artefact density per kilogram sediment and per cubic metre for each AU.

Figure 6.63. Enderby 10, showing outcropping and quarried andesitic basalt within the site.

ARTEFACT TYPE/ MATERIAL	BROKEN FLAKE		COMPLETE FLAKE		CORE/CORE FRAGMENT		TOOL		TOTAL		NAS TO MNF RATIO
	N	%	N	%	N	%	N	%	N	%	
Andesitic basalt	1,495	62.5	878	36.7	6	0.3	13	0.5	2,392	96.2	1.7
Chalcedony	12	70.6	5	29.4		0.0		0.0	17	0.7	2.0
Chert	3	33.3	3	33.3		0.0	3	33.3	9	0.4	1.4
Dacite	10	38.5	15	57.7		0.0	1	3.8	26	1.0	1.4
Quartz	25	86.2	4	13.8		0.0		0.0	29	1.2	2.9
Rhyodacite	7	50.0	7	50.0		0.0		0.0	14	0.6	1.6
Total	1,552	62.4	912	36.7	6	0.2	17	0.7	2,487	100	

Table 6.55. Enderby 10: stone assemblage composition by frequency and proportion. The microdebitage assemblage (<10 mm), including a broken backed tool (562910-XU06-LA2491), is not included here.

Assemblage reduction

The complete flake component of the Enderby 10 assemblage reveals some interesting patterns and variation in the reduction of different materials. Flakes made on non-local materials (chert and chalcedony) have higher average SDI values than those made on the locally available andesitic basalt (Table 6.56). This indicates that these chert and chalcedony flakes were typically removed from cores in a later stage of reduction, and most likely reflects distance to source. Dorsal flake scar directionality also indicates that chert and chalcedony flakes were more often removed from rotated and/or more intensively reduced cores (n = 2, 25%) than andesitic basalt flakes (n = 33, 3.8%).

Overall, however, few flakes exhibit dorsal flake scars removed from multiple directions. No chert or chalcedony flakes have remnant cortex, and only one chalcedony flake exhibits a flaked platform. However, these attributes (very little cortex and few flaked platforms) are typical across all materials and do not appear to correlate to patterns in reduction intensity. For example, despite a low average SDI value (0.9), most andesitic basalt flakes also lack cortex (n = 783, 89.1%). Given the predominantly non-cortical state of andesitic boulders sitting on the ground surface of Enderby 10

today (Figure 6.63), the low proportion of cortex in the andesitic assemblage is most likely a reflection of the source – and the fact that people have removed cortical material from available boulders to test these before moving cores to the square location for further reduction. The four quartz flakes all have two or more flake scars on their dorsal surfaces, indicating that the source nodule/s for these flakes had previous flake scars and were also comparatively intensively reduced.

A comparison of SDI values through time suggests that andesitic basalt knapped during the Late Holocene (μ 0.88 ± 0.39) was somewhat less intensively reduced than Early Holocene reduction of this material (μ 0.94 ± 0.43). However, this is not a marked difference in reduction intensity as the values are low overall and have overlapping standard deviations. Temporal assessment of other lithic materials was not undertaken as sample sizes are too small for meaningful comparison.

Non-local chert and chalcedony flakes, as well as quartz flakes, are clearly smaller than local andesitic basalt, dacite and rhyodacite flakes (Table 6.57). Again, this probably reflects distance to source: chert and chalcedony flakes were transported to Enderby Island from more distant source locations than other materials. The high standard deviation for andesitic basalt flakes (Table 6.57) indicates marked variation in flake size. Overall, however, andesitic basalt flakes are relatively small: only 24 flakes (2.7%) have a maximum length above 5 cm. Indeed, the substantial debitage assemblage attests to the overall small size of the Enderby 10 lithic assemblage.

MATERIAL	N	μ	SD
Andesitic basalt	879	0.90	0.40
Chalcedony	5	1.16	0.29
Chert	3	2.40	0.80
Dacite	15	0.59	0.19
Quartz	4	1.18	0.41
Rhyodacite	7	0.70	0.42

Table 6.56. Enderby 10: Scar Density Index (SDI) for complete flakes (excluding flakes <10 mm).

Andesitic basalt flakes discarded during the Late Holocene are, on average, slightly smaller (weight: μ 2.1 g ± 5.1, SA: 344.4 mm^2 ± 380.8) than those discarded during Early Holocene site visits (weight: μ 2.8 g ± 8.6, SA: 381.3 mm^2 ± 592.5). Again, however, the observed difference in flake size between the AUs is not especially marked and does not correlate to slight differences in SDI values.

MATERIAL	WEIGHT (G)			SURFACE AREA (MM2)	
	N	M	SD	M	SD
Andesitic basalt	879	2.4	6.2	354.5	448.2
Chalcedony	5	0.3	0.1	121.6	34.0
Chert	3	1.6	2.1	238.2	181.6
Dacite	15	6.8	14.2	628.7	828.0
Quartz	4	1.4	1.9	197.8	155.4
Rhyodacite	7	2.1	2.2	370.8	300.5

Table 6.57. Enderby 10: weight and surface area for complete flakes (i.e. >1 cm).

Although 67 blades (elongated flakes with ratio values ≥2) were recorded at the site, most flakes are squat in shape (Table 6.58).

MATERIAL	N	μ	SD
Andesitic basalt	879	1.1	0.6
Chalcedony	5	1.4	0.5
Chert	3	1.2	0.3
Dacite	15	1.0	0.4
Quartz	4	1.4	0.3
Rhyodacite	7	0.9	0.2

Table 6.58. Enderby 10: elongation ratio for complete flakes (not including flakes <1 cm).

Although sample size is small, the core assemblage demonstrates variation in the reduction of locally available andesitic basalt. Complete cores (n = 5) range in size between 66 mm and 100.5 mm (max. dimension) at the point of discard (mean max. dimension: 86.4 mm, mean weight: 252.7 g). Rotated (multi-platform) cores have higher SDI values (ranging between 2.2 and 3) than the two single-platform cores (values 0.23, 0.92). Some nodules were 'tested' for flake removal and then discarded, whereas other nodules were clearly preferred – and were used for multiple flake removals. The most intensively reduced core in comparative terms (562910B-XU08-LA2021) has four platforms, from which at least 13 flakes were removed. Of interest is a small blade core fragment (562910-XU04-LA476, Figure 6.64), which has snapped via heat fracture but has multiple elongated flake scars. The presence of this core at Enderby 10 demonstrates a preference, by the knapper, for producing standardised blades. Elongated (blade) flake scars do not occur on any other cores or core fragments (Table 6.58).

With the exception of one core, all complete cores were discarded during the Early Holocene.

Figure 6.64. Enderby 10: broken blade core (562910-XU04-LA476 *in situ*), showing blade scars and heat fractured break on the right. Scale is 10 mm.

Tool selection and use

Eighteen tools were discarded at Enderby 10. Most of these were made on the local andesitic basalt (n = 12, 66.7%), although four chert tools and a single dacite tool were also recorded. Ten tools have retouch scars and/or usewear, while eight tools have macroscopic and/or microscopic evidence for use (see next section).

Retouch intensity varied between tools. Some tools were discarded with over 80% retouch along their edges, while others had only been minimally shaped (15% of edge retouched). Most retouched artefacts exhibit informal scalar retouch. However, two chert tools (562910-XU01-LA033, 562910-XU06-LA2491) and an andesitic basalt flake (562910-XU05-LA621) exhibit very steep-edged retouch consistent with backing retouch (Figure 6.65). Backed artefacts are distinct tool types found across Australia mostly in the Mid to Late Holocene (Hamm et al. 2016; Hiscock 2008; Hiscock and Attenbrow 1998, 2004; McDonald et al. 2018a; Slack et al. 2004) but are relatively sparse in the Pilbara. The steep-edged tools found at Enderby 10 do not exhibit classic microlithic or backed blade morphology.

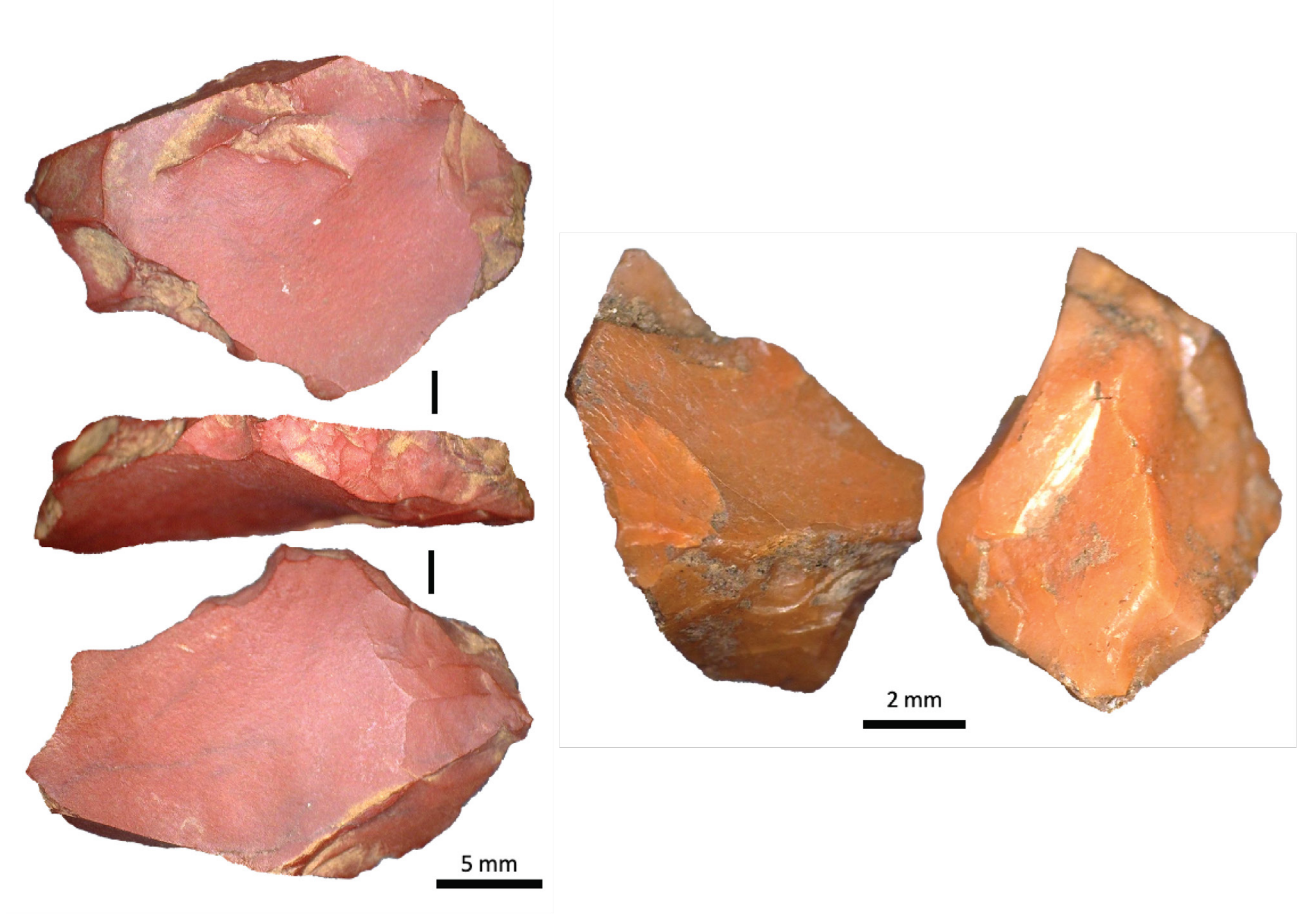

Figure 6.65. Enderby 10: chert artefacts with steep-edged retouch (left to right: 562910-XU01-LA033 and 562910-XU06-LA2491).

The nine tools made on complete flakes provide some indication of flake selection. A wide variety of flake sizes and shapes were selected for tool use. However, tools are, on average, much larger (weight: μ = 12.3 ± 16.7, surface area: μ = 846 mm² ± 712.4 mm²) than the assemblage's available flakes (Table 6.57).

Usewear and residue analysis

Twenty artefacts from the Enderby 10 assemblage were inspected for microscopic usewear based on macroscopic assessment (i.e. retouch scars, macroscopic evidence for use and/or the likelihood of having microscopic use). These included seventeen of the tools recorded (Table 6.59). Eight artefacts were sampled for residues based on microscopic inspection.

Microscopic usewear was identified on 15 (75%) of the inspected artefacts (Table 6.59 and Table 6.60). Of interest are two retouched flakes (562910B-XU06-LA1824 and 562910-XU11-LA1032) which do not have any subsequent microscopic usewear or residues. This indicates that these tools were shaped and/or sharpened (i.e. retouched) but were discarded without having been utilised. It is also possible that the retouching of these artefacts removed previous usewear along a worked edge, but this is less likely.

	USEWEAR		NO USEWEAR	
	N	%	N	%
AU1	6	66.7	3	33.3
AU2	9	81.8	2	18.2
Total	15	75	5	25

Table 6.59. Enderby 10: stone artefacts with evidence of microscopic usewear.

		MACROSCOPIC EDGE WEAR		POLISH		SHALLOW EDGE SCARRING		STRIATIONS		EDGE ROUNDING	
		N	%	N	%	N	%	N	%	N	%
AU1	Y	9	100	4	44.4	6	66.7	1	11.1	1	11.1
	N	0		5	55.6	3	33.3	8	88.9	8	88.9
AU2	Y	11	100	4	36.4	9	81.8	1	9.1	2	18.2
	N	0		7	63.6	2	18.2	10	90.9	9	81.8
Total		20		20		20		20		20	

Table 6.60. Enderby 10: usewear types identified on the 20 analysed stone artefacts.

Eight of the 20 artefacts from 562910/562910B which were subject to microscopic analysis were also tested for plant fibres and blood. Three artefacts from AU1 and four of the five tools from AU2 were found to contain plant fibres (Table 6.61). None of these artefacts tested positive for blood.

The plant residues recorded are predominantly non-diagnostic, comprising small, elongated fibres and amorphous cellulose (Figure 6.66). Large amounts of silica were also recovered from two Early Holocene artefacts (562910B-XU12-LA2460, 562910B-XU08-LA2043) and one from within the Later Holocene period (AU1, 562910-XU06-LA2491) which are heavily polished and with evidence of being used intensively (Figure 6.67). Although silica is present in soils, the high concentration and distinct morphology of the silica recovered from the artefacts suggests that it is related to use, rather than soil contamination. It is likely these related to the processing of plant material.

	NOT TESTED		TESTED		PLANT FIBRES	POSITIVE BLOOD TESTS
	N	%	N	%	N	N
AU1	8	73	3	27	89	0
AU2	4	45	5	55	55	0
Total	12	60	8	40	144	0

Table 6.61. Enderby 10: proportion of artefacts with microscopic usewear tested for residues and the results.

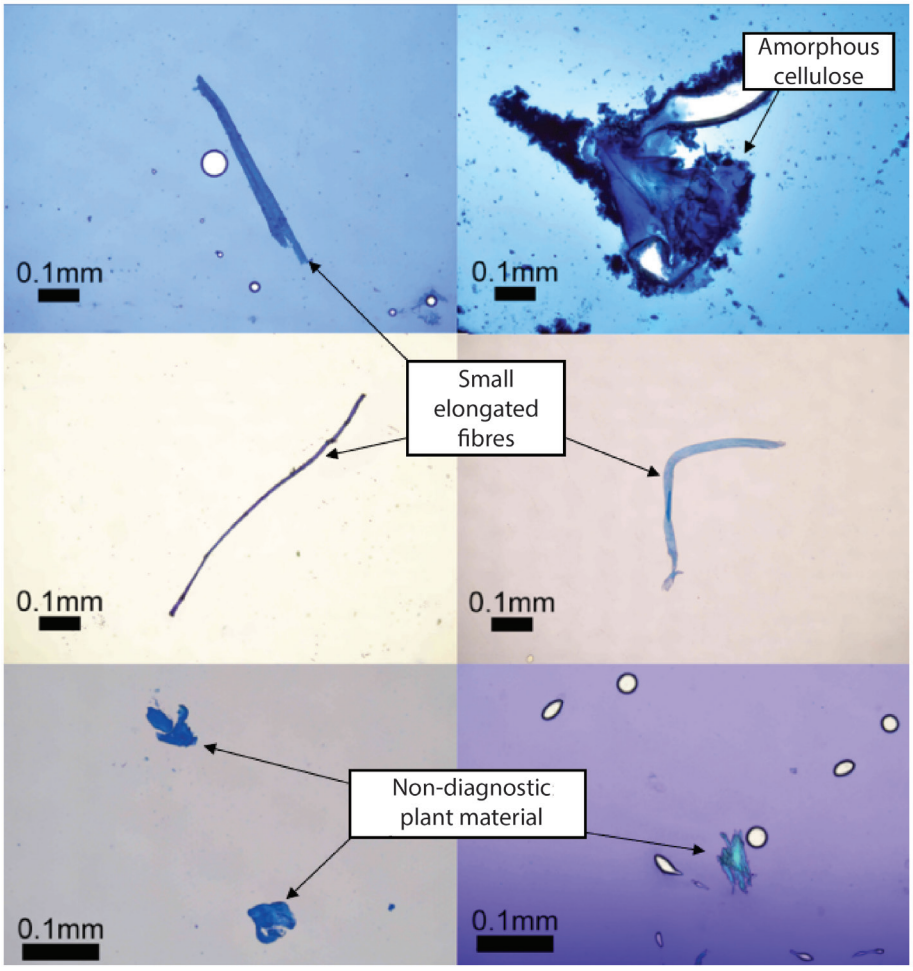

Figure 6.66. Enderby 10: typical plant residues recovered from tested artefacts.

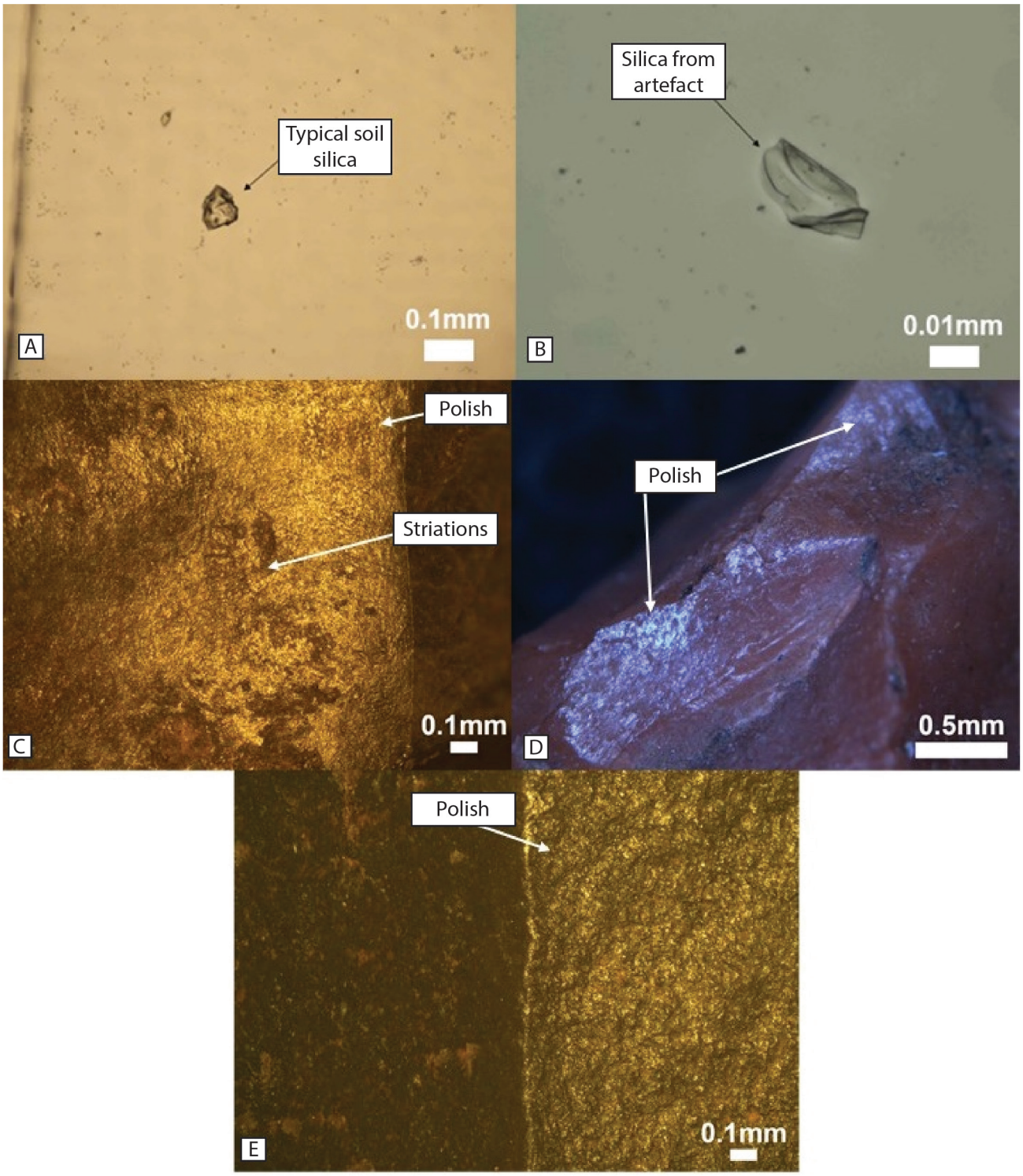

Figure 6.67. Enderby 10: morphological differences seen in silica recovered from a soil sample (A) and silica recovered from artefact 562910B-XU12-LA2460 (B); artefacts 562910B-XU12-LA2460 (C), 562910-XU06-LA2491 (D) and 562910B-XU08-LA2043 (E) had high concentrations of silica and are heavily polished.

Of this site's artefacts identified as tools, three have particular significance.

Artefact 562910-XU01-LA034 is a Late Holocene dark grey andesitic flake (Figure 6.68). Noteworthy residues recovered from the artefact are consistent with starch, yeast, bone, silica and plant material. Starch grains occur in seeds, roots and tubers, and plant leaves, and their presence on artefacts is therefore closely associated with the processing of food material (Ridge 1991). While a yeast cell with a hyphal outgrowth was recovered from the artefact, yeast also occurs in shallow soils and cannot therefore be definitively linked to artefact use (Yurkov 2017). A fragment with a matrix consistent with cancellous bone was also recovered; however, this artefact tested negative for blood.

The shallow edge-scarring terminations on this artefact are consistent with it being used on materials ranging from soft to medium hardness (Claud et al. 2019).

The wide variety of residues present on the artefact support this range of material use, and it is likely that the artefact was part of a multipurpose toolkit that was used to process different types of plants and animals.

Artefact 562910-XU09-LA893 is a large andesitic basalt chopping tool recovered from AU2. The artefact has focalised shallow edge scarring on both sides of one margin and a bevelled section and desert varnish on one side (Figure 6.69). The artefact tested negative for blood and no residues were recovered.

The shallow edge scarring is consistent with use on a hard substance (Claud et al. 2019). Given the size and weight of the artefact, it would have made a suitable woodworking tool. While plant fibres and/or woody tissue would be expected to be recovered from a woodworking tool, taphonomic factors in cyclonic open deposits might dissolve wood, possibly accounting for the absence of residues on the artefact. Bevelling is typically associated with grinding; however, the artefact surface is uneven and impractically small for such a purpose, and the bevelling is likely related to some other unknown prior activity. This focalised usewear, and absence of other evidence of use, suggests that this tool underwent limited use on a hard substance before being discarded.

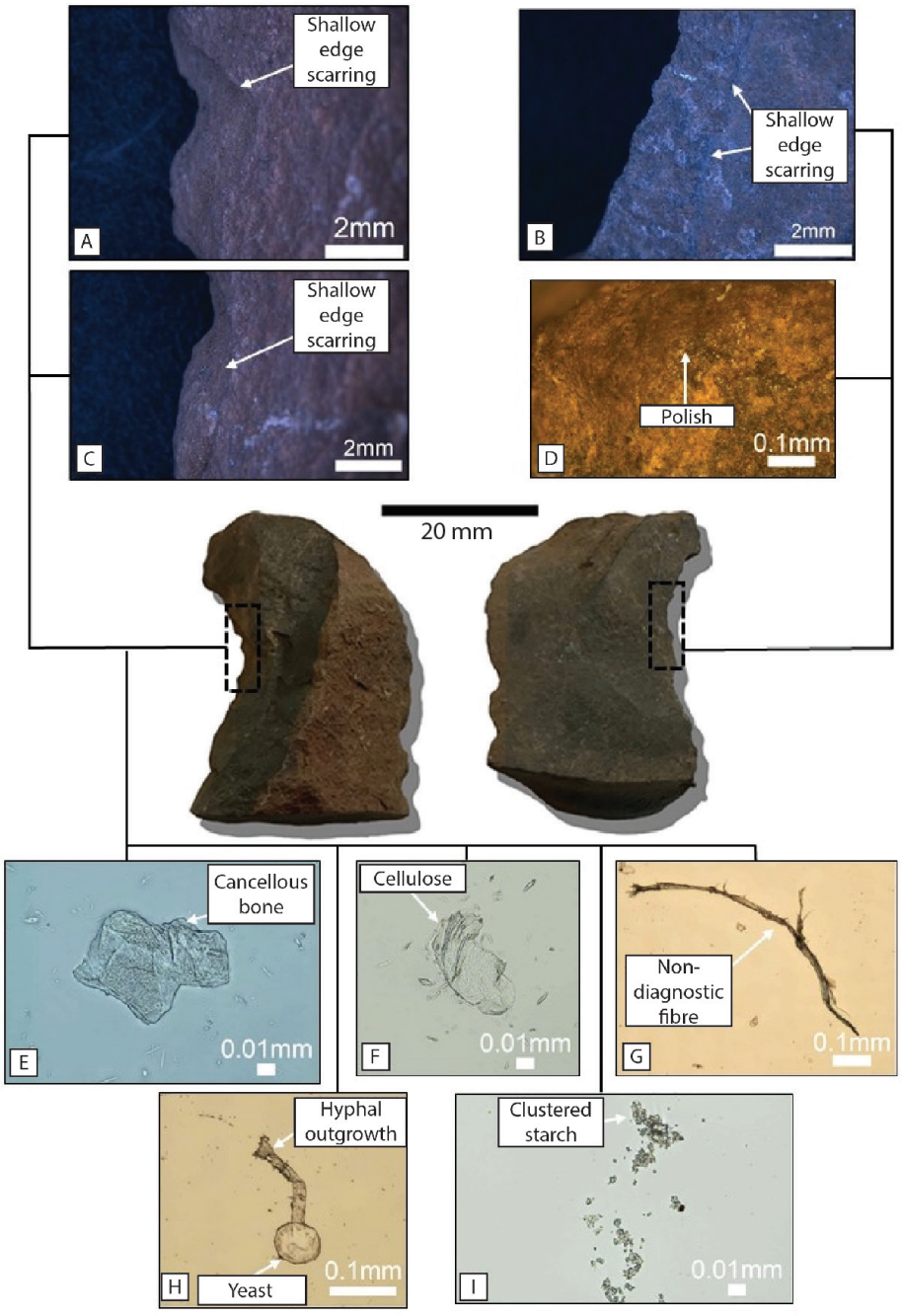

Figure 6.68. Enderby 10: artefact 562910-XU01-LA034. Usewear on the artefact showing shallow edge scarring and polish (A–D). Residues recovered include bone (E), cellulose and non-diagnostic plant fibres (F–G), yeast (H) and clustered starch (I).

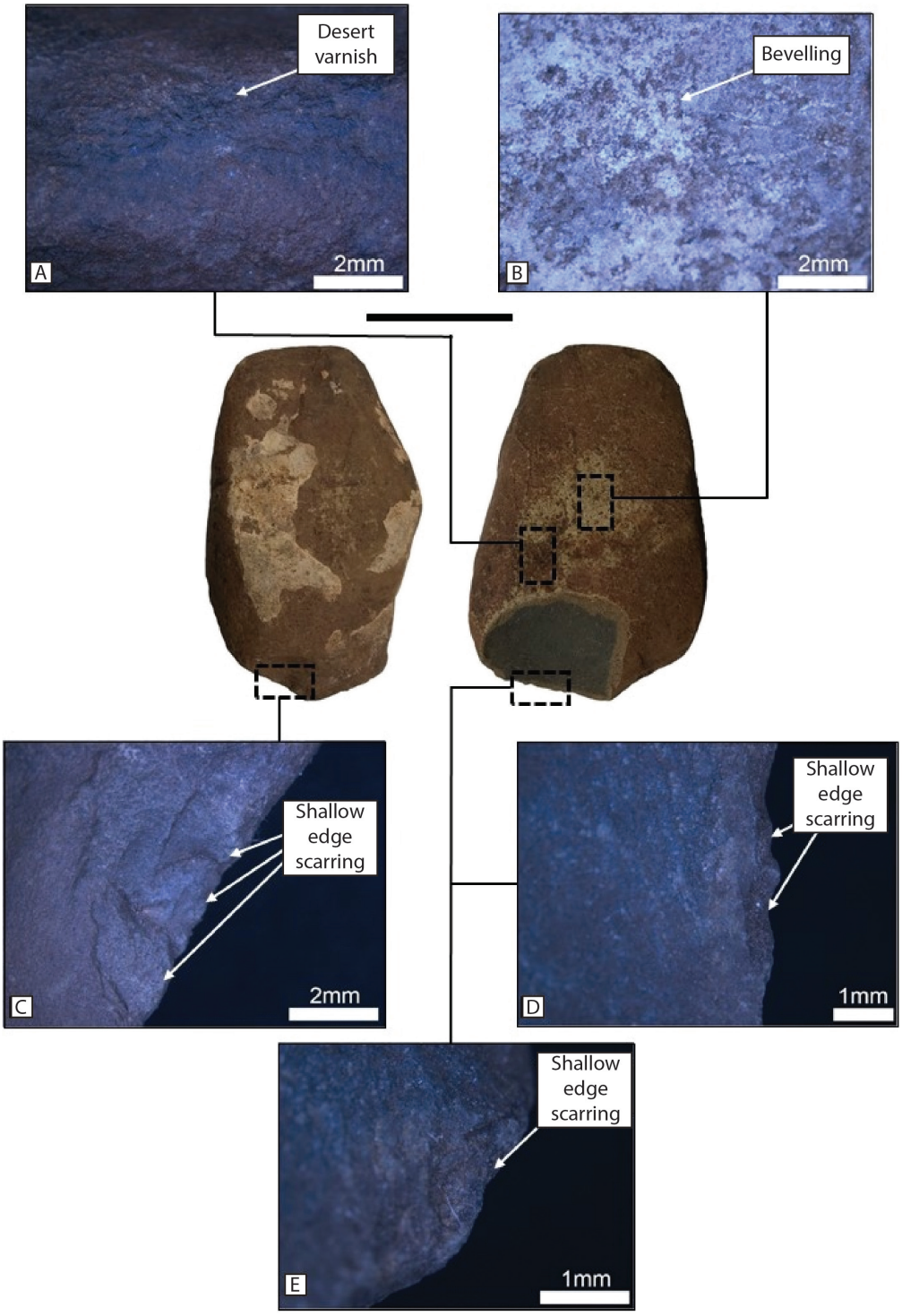

Figure 6.69. Enderby 10: artefact 562910-XU09-LA893. Desert varnish (A), bevelling (B) and shallow edge scarring (C–E).

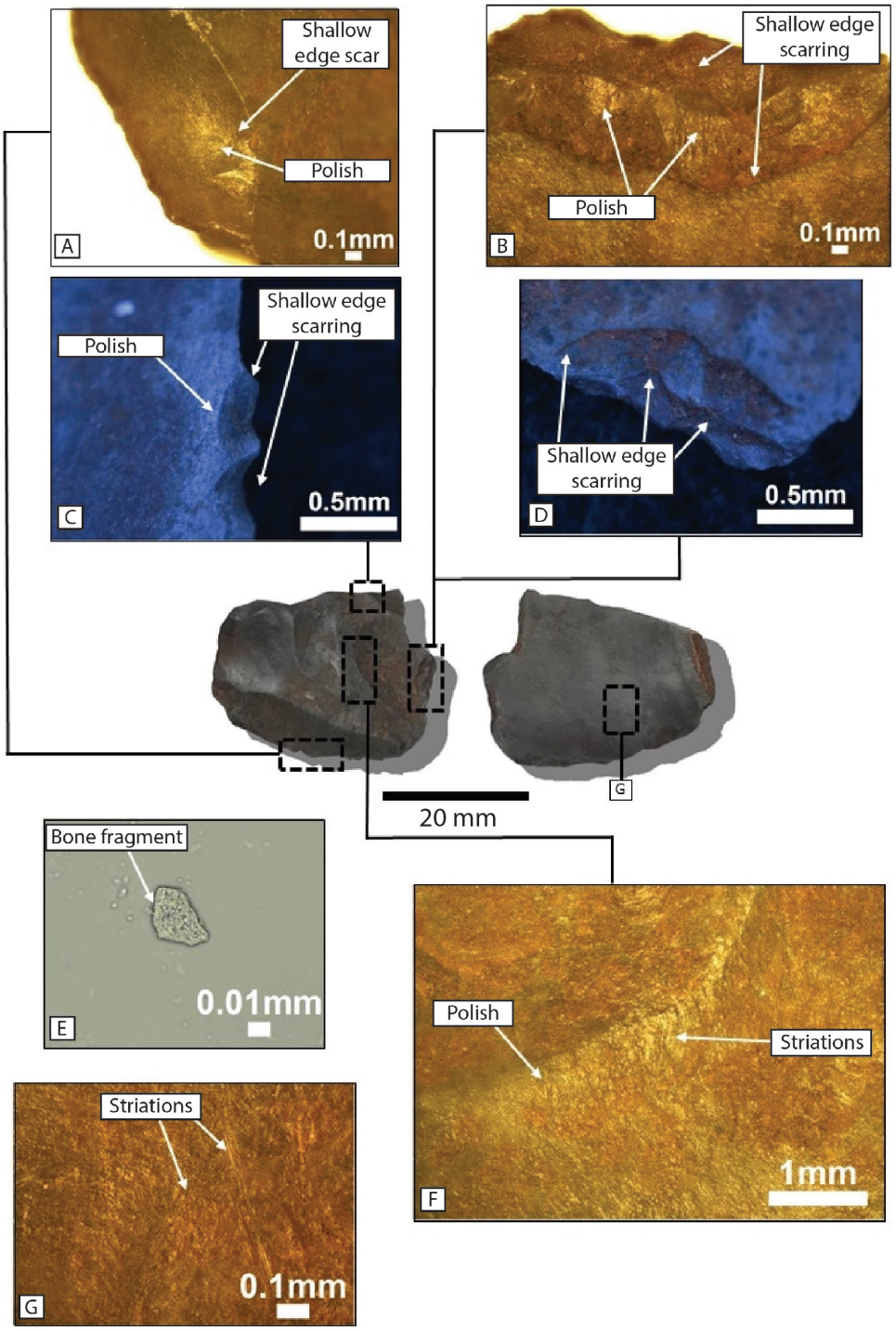

Figure 6.70. Enderby 10: artefact 562910B-XU12-LA2460. Intensive usewear covers much of the artefact (A–D, F and G). Residue is consistent with bone (E).

Artefact 562910B-XU12-LA2460 is a small, dark grey chert flake with evidence of intensive use (Figure 6.70). More than 40 shallow edge scars extend along the margins of the artefact, with polish and multidirectional striations spreading across both ventral and dorsal surfaces and into the scarring. A bone fragment was identified during residue analysis; however, no other residues were recovered, and the artefact tested negative for blood.

The range of scar terminations suggest that artefact 562910B-XU12-LA2460 was used on a wide variety of materials of varying hardness (Claud et al. 2019). The polish and striations cover much of the artefact and indicate that it was used intensively enough for material to be removed along the edges to form scarring, and polish to develop inside the negative scars. As usewear analysis indicates intensive use, it would be reasonable to expect residues would have been preserved on this Early Holocene artefact. However, given the site's open location and exposure to frequent cyclones, residues have not been preserved.

Dentalium beads

An extraordinary total of 963 pieces of *Dentalium* (tusk shells, also known as scaphopods) were found in squares 562910 and 562910B. Most of those in Square 562910 were analysed and measured by Wade Goldwyer, who undertook an analysis of the bead manufacturing at this site (Goldwyer 2018). His analysis identified that the dominant scaphopod species made into beads here was *Laevidentalium lubricatum*. All the *Dentalium* pieces at Enderby 10 have been photographed and all were re-analysed for this chapter. Additional beads were encountered during the sorting of 2 mm residues (after Goldwyer's analysis), taking the total for Square 562910 to 476. These, as well as the 487 *Dentalium* pieces found in 562910B, were counted to ensure internal consistency of this data set.

Goldwyer's research focused on distinguishing between bead discard and bead manufacture. He concluded that the most important distinction to be made about beads/fragments was portion frequency (Figure 6.72), breakage pattern and edge-wear. He concluded that Enderby 10 is a scaphopod bead-manufacturing site because the 562910 sample consisted mainly of posterior ends of *Dentalium* shells. This portion is usually discarded because it is too narrow to be threaded on string/hair.

The 963 pieces of *Dentalium* were found throughout squares 562910A and B, of which 963 had identifiable characteristics (Table 6.62). These were evenly distributed between the two squares and through the profile. They were found from the surface through to XU15 in Square 562910, and from XU1–XU13 in Square 562910B (Figure 6.71). Very few anterior ends were recovered. Most pieces (61%) found were posterior ends, followed (at 38%) by medial fragments (Figure 6.71).

	562910							562910B			
XU	ANTERIOR	MEDIAL	POSTERIOR	W	N/A	TOTAL	XU	ANTERIOR	MEDIAL	POSTERIOR	TOTAL
Surface		2	2	1		5	1		22	8	30
01		19	12		8	39	2		18	22	40
02		12	8			20	3		7	15	22
03		16	26			42	4		23	15	38
04		14	26			40	5		9	19	28
05	1	12	37			50	6		9	27	36
06		8	45			53	7		15	25	40
07	1	3	22			26	8	1	30	38	69
08		11	24			35	9		18	39	57
09	2	7	26			35	10		20	27	47
10	1	15	25			41	11		24	28	52
11		15	23		6	44	12		11	11	22
12		6	11	1		18	13		2	4	6
13		11	9			20					
14		3				3					
15		2	3			5					
Total	5	156	299	2	14	476		1	208	276	487
Site total	6	364	575			963					

Table 6.62. Squares 562910 and 562910B: *Dentalium* counts.

There is a slight trend for more of these fragments to be found in the upper portion of Square 562910, and the inverse pattern is found in Square 562910B. There is also a minor trend towards more posterior ends in AU2 but, given the potentially mixed strata, it is probably unwise to make too much of this. It is assumed that the interment of human remains in Square 562910B XU12 has resulted in a greater distribution of this material throughout the sequence in that square.

Given the Late Holocene age determinations for the two *Dentalium* pieces (Wk-44899, Wk-44901), it is assumed that these very small items have been dispersed downwards through the deposit through taphonomic processes. The presence of a hearth dated to 155 calibrated years ago in XU2 (with *Dentalium* beads above and below this) is part of the mystery created by the site's major dated inversions. It is likely that this late hearth and associated occupation intersected with / disturbed the earlier bead-manufacturing location. Short of dating further beads in all XUs, it is concluded that this bead manufacturing took place between 1,200 and 1,600 years ago, in a focused and limited period. It would be worth testing this by dating additional beads from the lower levels of the site given the two received age determinations are from within AU1 (XU2 and XU4). The other interpretation is that bead manufacture was a persistent site activity through time.

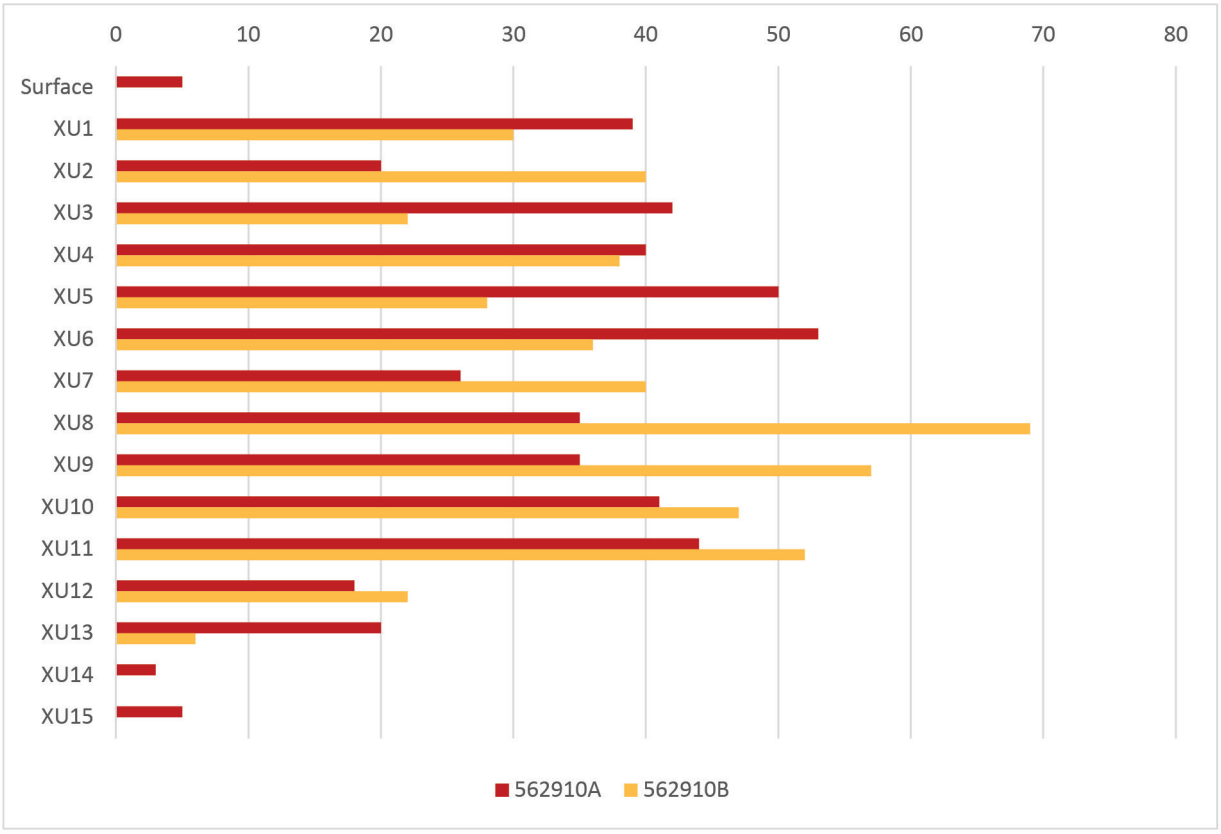

Figure 6.71. Distribution of Dentalium pieces in each XU in squares 562910 and 562910B.

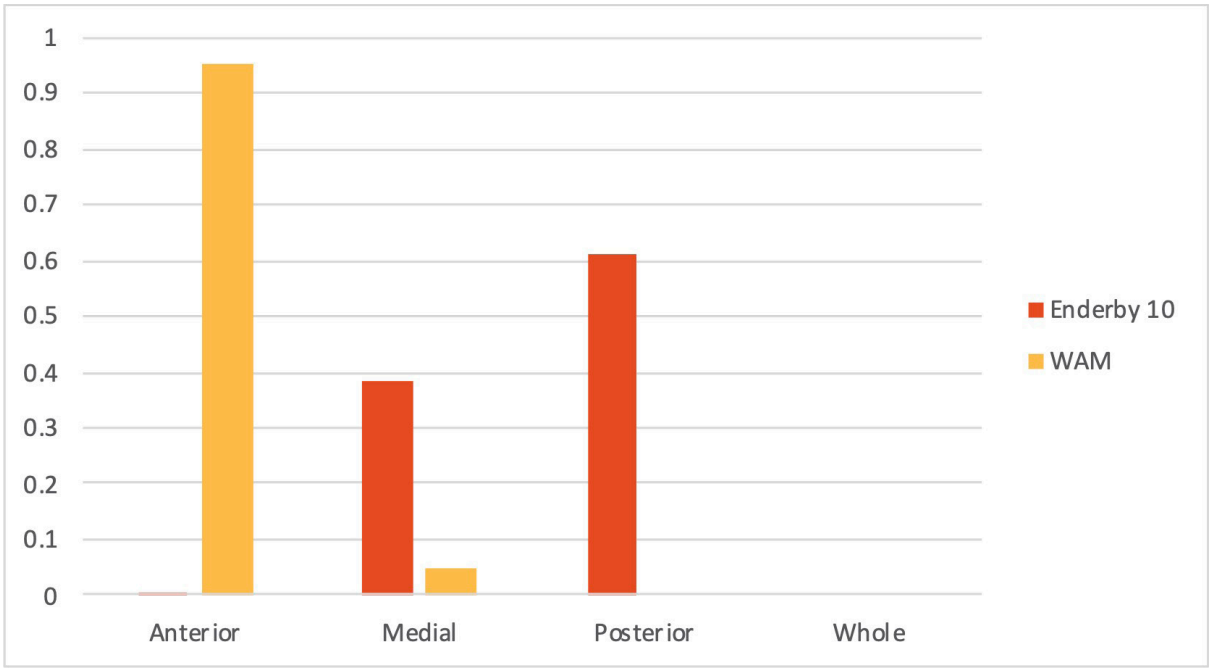

Figure 6.72. Enderby 10: Dentalium portions (top) compared to the WA Museum counts (bottom – from Goldwyer 2018: Figure 23).

Goldwyer concluded (based on the WA Museum collections) that Aboriginal people used only anterior portions for the beads. The archaeological evidence would suggest that medial portions are also used.

Another feature analysed by Goldwyer (2018) was the breakage pattern (edge-state), which he argued was an indication of intentionality, i.e. whether these fragments had resulted from focused manufacture. Goldwyer's (2018) definitions are illustrated in Table 6.63.

In our analysis of Square 562910B, we also identified bead fragments that had combinations of two breakage patterns – i.e. different on either end.

The *Dentalium* assemblage at Enderby 10 has mostly (27%) straight breaks; however, a lot of variability is noted (Table 6.65). Longitudinal (17.5%) and concave (16.5%) breaks were present on roughly the same proportion of

Dentalium pieces. Around 10% of the fragments had at least one jagged edge.

Edge rounding was measured by Wade Goldwyer using microscopic examination, as he was interested in manufacturing processes, i.e. as an indication of whether the beads had been worn before being discarded in this site. He used the following edge-rounding definitions (see Table 6.64).

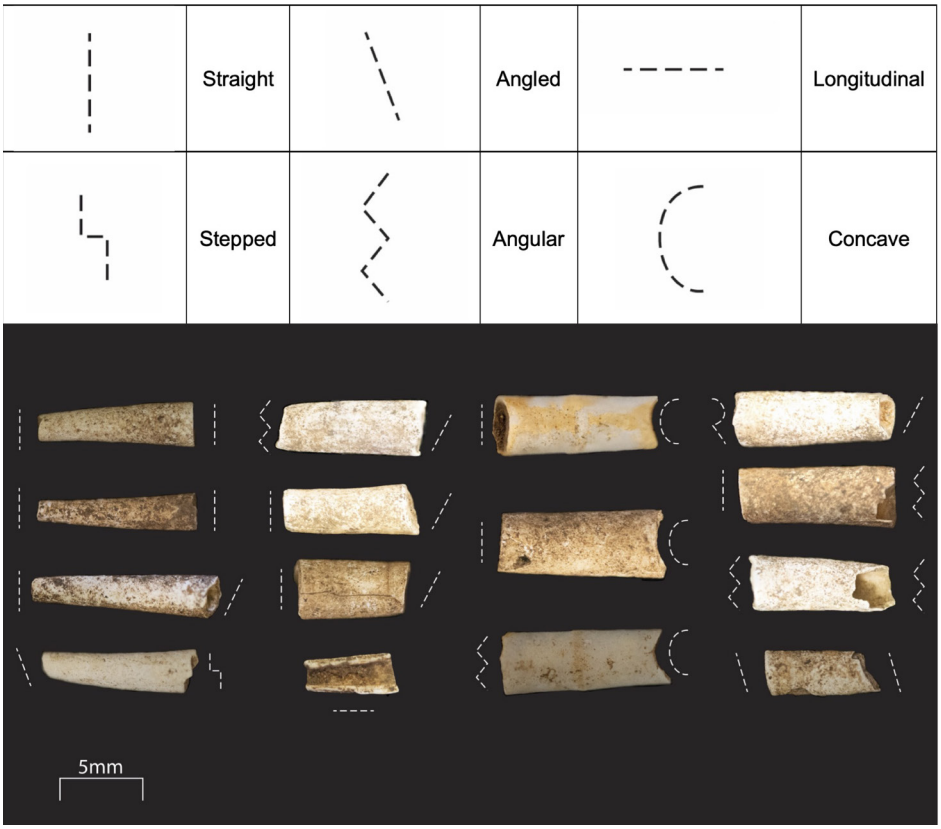

Table 6.63. Breakage patterns examples from the assemblage (medial and posterior fragments).

Goldwyer found that 85% of the Enderby 10 Square 562910 *Dentalium* pieces had no edge-rounding (Goldwyer 2018: Figure 25) and interpreted this as demonstrating that this was predominantly manufacturing debris (not loss during usewear). This feature was not measured during the current analysis of the second test square as it required microscopic analysis. This proportion is relatively consistent throughout the entire assemblage for 562910 (Table 6.66). The weathered condition of many fragments made this characteristic difficult to assess.

The size range of the *Dentalium* fragments in the two squares is shown in Figure 6.73. The notable tail of larger fragments at Enderby 10 reflects the number of posterior fragments discarded during manufacture. The WA Museum collection, which is generally larger in size (albeit from a smaller sample of beads), was interpreted by Goldwyer as having been made for trade: there was very little wear on the museum collections, and these were strung on manufactured string (Goldwyer 2018: Conclusions).

Wear	Shell Example
0	
1	
2	

Table 6.64. Dentalium edge-rounding.

BREAKAGE PATTERN	A	%F	M	%F	P	%F	TOTAL	%F
Angular			15	4.1	80	13.8	95	10.0
Concave	2	*33*	54	14.8	101	17.4	157	16.5
Jagged	1	*17*	16	4.4	73	12.6	90	9.5
Longitudinal			128	35.2	38	6.6	166	17.5
Stepped			9	2.5	74	12.8	83	8.7
Straight	3	*50*	43	11.8	213	36.8	259	27.3
Angular – stepped			8	2.2			8	0.8
Angular – straight			14	3.8			14	1.5
Concave – angular			1	0.3			1	0.1
Concave – jagged			4	1.1			4	0.4
Concave – stepped			2	0.5			2	0.2
Concave – straight			6	1.6			6	0.6
Jagged – angular			3	0.8			3	0.3
Jagged – stepped			12	3.3			12	1.3
Jagged – straight			22	6.0			22	2.3
Stepped – straight			27	7.4			27	2.8
Total	6		364		579		949	

Table 6.65. Square 562910: Dentalium breakage patterns shown according to portions.

XU	0	1	2	TOTAL
0	1	4		5
1	16	15		31
2	11	8	1	20
3	37	5		42
4	35	5		40
5	45	5		50
6	53			53
7	22	3	1	26
8	31	4		35
9	33	2		35
10	37	4		41
11	32	6		38
12	16	2		18
13	19	1		20
14	5	3		8
Total	393 (85.1%)	67 (14.5%)	2 (0.4)	462

Table 6.66. Square 562910: Dentalium pieces – edge-rounding (using Goldwyer's 2018 data).

All the fragments found at Enderby 10 are between 0.61 mm and 31.4 mm in maximum dimension, with most of them (64%) falling in the 4–10 mm size increments. There is only a very slight difference in the proportions (not the size ranges) found in the two adjacent test squares. The median *Dentalium* fragment size for the assemblage is 6 mm long. The sizes of these archaeological fragments are very different to those found in the historical collection of scaphopod necklaces at the WAM (see Figure 6.73), where the highest frequency size categories are between 20 and 24 mm.

SQUARE 562910		SQUARE 562910B	
Median	6.335	Median	6.07
Range	29.06	Range	30.23
Minimum	0.61	Minimum	1.18
Maximum	29.67	Maximum	31.41
Count	462	Count	487

Table 6.67. Enderby 10 Square 562910: total length ranges (mm) of individual fragments in the two squares.

The average weights of the beads in the two squares are also very similar (but not identical) to each other (Table 6.68). The minimum weight is 0.06 g, while the maximum is 1.18 g.

SQUARE 562910		SQUARE 562910B	
Range	1.12	Range	0.38
Minimum	0.06	Minimum	0.01
Maximum	1.18	Maximum	0.39
Median	0.79	Median	0.03
Count	474	Count	487

Table 6.68. Enderby 10 Square 562910: weight ranges (g) of individual beads in the two squares.

SQUARE 562910		SQUARE 562910B	
Median	2.58	Median	2.59
Range	4.27	Range	4.21
Minimum	0.16	Minimum	0.91
Maximum	4.43	Maximum	5.12
Count	461	Count	487

Table 6.69. Enderby 10 Square 562910: maximum shell width (break point, mm) ranges for individual beads in the two squares.

The size of a whole adult *Dentalium* shell is c. 4 cm (40 mm). The posterior end of the shell is very narrow and

cannot be strung because the aperture is too narrow, even for human hair. The anterior end is the widest; given the median length of the fragments found at Enderby 10 is 6 mm, you could presume that the bead manufacture would result in a posterior end (removing the most narrow/unsuitable part for inserting string) and that two or three beads might be manufactured per shell.

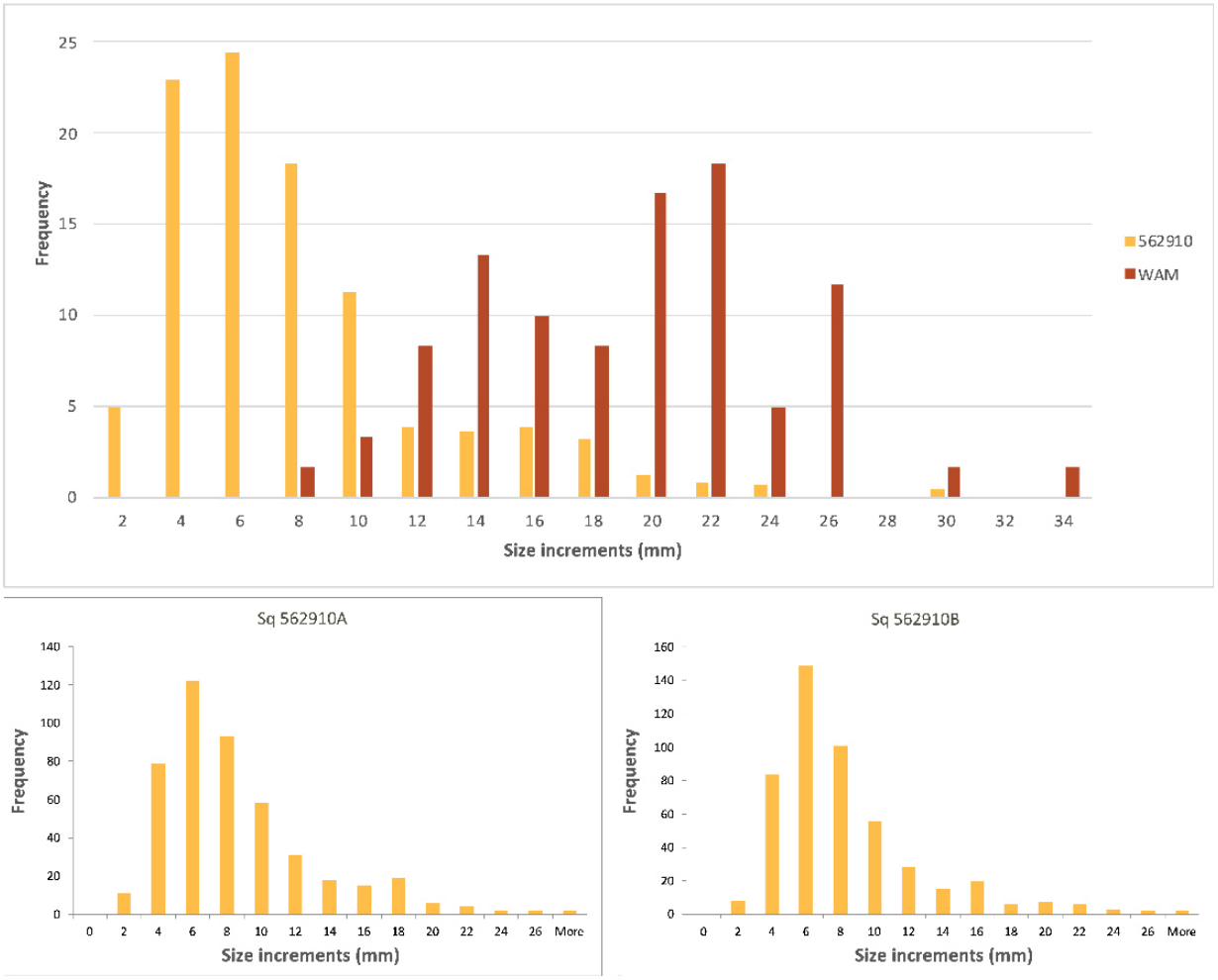

Figure 6.73. Square 562910: size ranges (mm) for (top) Dentalium fragments excavated compared to the WA Museum collections (from Goldwyer 2018: Figure 25); (bottom) size ranges found in the two analysed squares.

The 32 longest *Dentalium* fragments (longer than 19mm) are all posterior ends. In these cases, it can be assumed that the removal of the posterior ends reduced the potential beads to roughly 20 mm: hence you would expect to have one anterior and one or two medial sections from each successful manufacturing effort from one single whole *Dentalium* shell.

Given we have recorded an MNI of 575 posterior ends, we can conclude that at least this number of *Dentalium* were brought to the centre of Enderby Island to manufacture beads. It is possible that this is a significant under-estimate given the small size of our sample square.

Discussion

The shellfish and vertebrate faunal records from Enderby 10 indicate a persistent mixed marine and terrestrial focus from the Early Holocene with greater incorporation of diverse coastal resources as they became more accessible following sea level rise. Early Holocene records demonstrate use of terrestrial mammals (predominantly rock wallabies), marine turtles and small quantities of fish and shellfish, with coastal resource exploitation probably focused on mangroves. During the Late Holocene occupation phase, smaller macropods became more abundant in the faunal assemblage, which could reflect exploitation of an island-bound rock wallaby population. Two macropod specimens (tentatively identified as Euro, *Macropus robustus*) identified in the Late Holocene faunal assemblage are based on isolated tooth fragments (a lower molar and a lower incisor), with a few long un-speciated long-bone fragments. These fragmentary remains show no evidence of burning

and there is no other evidence for the contemporary presence of euros on the island after its separation from the mainland (Morris 1990). This may indicate an island extinction. Conversely the transport of these teeth to this location in the Late Holocene may have occurred as part of a toolkit and/or symbolic paraphernalia rather than for consumption (Akerman 1995). In the absence of larger skeletal *Macropus* sp. elements which would usually survive even in poor taphonomic conditions, this is a very real interpretive possibility.

The presence of turtles throughout the occupation sequence from the Early Holocene faunal record is in line with rock art records throughout the Dampier Archipelago that indicate close connection with coastal resources – including marine turtles – from the earliest phases of rock art production through islandisation (de Koning 2014; Mulvaney 2015; Veth et al. 2017). Overall, the faunal assemblage demonstrates a relatively stable and consistent pattern of vertebrate exploitation across the transition from peninsula to island.

Turtles are also the most depicted zoomorphs in the rock art (n = 26; Figure 6.74), especially in CS3 and CS4 (Figure 6.75). Two of these are shown in hunting scenes with small anthropomorphs surrounding the turtle – and three with long lines depicted to the head of the turtle. Most of the motifs are pecked or abraded or combinations of pecking and abrasion.

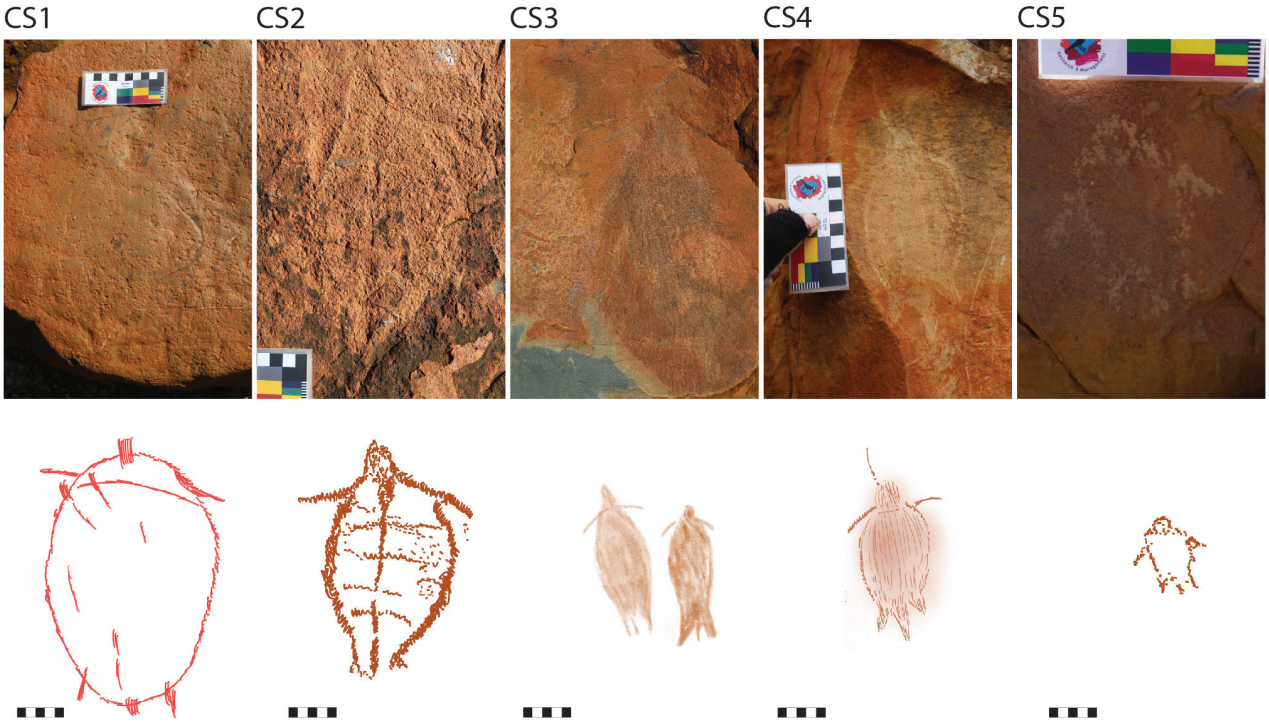

Figure 6.74. Enderby 10: rock pool showing turtles in different contrast states – of increasing contrast from left to right. There is an interesting diminution of size through time.

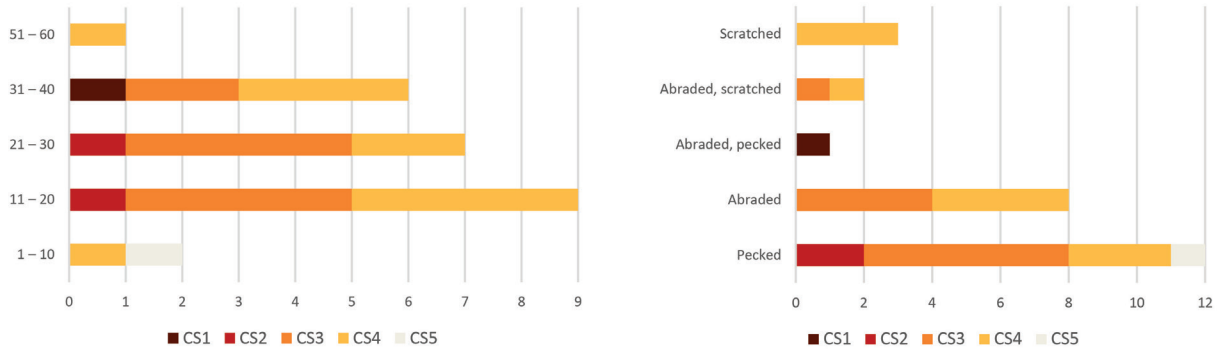

Figure 6.75. Enderby 10: turtles – comparing (left) contrast state and size; and (right) technique and contrast state.

The fact that this Enderby midden does not show the usual transition from *Terebralia* to *Anadara* at 3.8 ka (Clune and Harrison 2009) is likely because this outer island is not subject to the same level of progradation as seen with the inner embayments and Nickol Bay (Semeniuk and Wurm 1987). This is an important economic observation that goes a long way towards the cultural selection of economic species versus the

ecological productivity driving dietary assemblages. It is also an important distinction between the midden assemblages recorded on the Abydos Plain surrounding the archipelago – and the characteristics of middens on the outer versus inner islands.

The high-density stone assemblage recovered from squares 562910 and 562910B at Enderby 10 is unique to the Dampier Archipelago. This substantial assemblage primarily reflects repeated and extensive on-site quarrying and reduction of andesitic basalt by Aboriginal people who repeatedly visited the site throughout the Holocene to undertake a range of activities. Indeed, the highly fragmented nature of the assemblage most likely reflects intensive knapping, as well as trampling damage from repeated human activities at this place throughout this time. Stone knapping activities at the site were most intensive during the Late Holocene, and there is a possible correlation between *Melo* shells (water containers) in the deposit and phases of the most intensive knapping activity.

Although a high volume of andesitic basalt was knapped in this small test excavation, nodules were typically non-intensively reduced in a similar manner through time. Given this low-intensity reduction, small artefact sizes are most likely to reflect small original nodule size rather than reduction intensity. The low proportion of andesitic basalt cores, coupled with low SDI values and extremely high flake to core ratios, may reflect the removal of quarried and partially reduced nodules away from this test square. This is an artefact transport behaviour typical of quarries and associated reduction areas. Given the small size of the square that was excavated, it is possible that this result is an artefact of sampling. The presence of a blade core (Late Holocene) and elongated flakes (Early and Late Holocene) in the Enderby 10 deposit indicates some targeted blade production. However, blades occur only in small quantities in the assemblage, indicating that knappers visiting Enderby 10 were not predominantly focused on blade manufacturing (or that these items were transported away from this place). Indeed, the discard of so few tools at this place (<1% of the total assemblage) correlates to overall assemblage characteristics which indicate relatively expedient knapping behaviours typical of quarry (material extraction) locations where high-quality material is abundantly available.

The presence of other local and non-local materials at Enderby 10 shows that the people who visited this place had transported flakes and/or nodules to this location from elsewhere in the landscape. Attributes on chert and chalcedony flakes indicate that the nodules from which these flakes were removed had been also relatively intensively reduced. This is not surprising as these rarer lithologies were sourced from distances of at least 30 km from Enderby Island. Significantly, three tools with steep-edged retouch consistent with backing were all discarded during the Late Holocene. Backed artefacts in Australia are mostly identified as Mid to Late Holocene tools (Hamm et al. 2016; Hiscock 2008; Hiscock and Attenbrow 1998, 2004; McDonald et al. 2018a; Slack et al. 2004), but this artefact type is rarely documented across Murujuga. These tools – two of which are made on non-local chert – may represent discarded components of a mobile toolkit.

Although quartz occurs in only small quantities at this site, nodule/s of this material also appear to have been favoured for flake production, particularly during the Early Holocene. Lithologies, other than andesitic basalt, were more commonly discarded during the Early rather than Late Holocene phase of occupation. This could reflect several behaviours relating to occupation duration, tool-stone preferences or mobility distance and/or frequency. For example, a higher proportion of non-local materials could indicate comparatively longer occupation *durations* during the Early Holocene, as non-local materials have a higher chance of being discarded as occupation durations increase. Alternatively, highly mobile groups carrying toolkits made on different materials may have visited the site more *frequently* during the Early Holocene, leading to a cumulatively higher frequency discard of materials other than local basalt when compared to the Late Holocene. Given the higher volume of andesitic basalt at Enderby 10 during the Late Holocene, it appears that later phase occupations were more intensive (duration and/or frequency) than site visits during the Early Holocene. This is supported by the other cultural remains at the site in more recent times.

Recent research in north-west Australia (Fullagar et al. 2017; Hayes et al. 2018; Reynen and Morse 2016) on use/residue has proposed that many grinding patches in the north-west may have been used not only to process seed, but also to process fibres etc. which could then be used to make nets/baskets. Plant tissue and wooden objects are rare in the Australian archaeological record but distinctive stone tools, such as grinding stones and ground-edge hatchets, are relatively common and they provide strong indirect evidence for plant food processing and woodworking respectively. Ethnohistorical references to the Aboriginal use of stone tools for technologies related to fibrecraft, basketry, hafting adhesives and fixative sealants (with gum, wax and resin) are also rare but all these tasks were probably more common than records indicate (Reynen and Morse 2016). Reynen and Morse further observed that it may be difficult for usewear and residue analysis to determine if

grinding stones were used to target *Triodia* (spinifex) for fibre, food or other plant products. Further experimental research is needed to refine criteria for identifying archaeological fibre-processing tools.

Given that grinding patches are extensive across the Enderby 10 site (Figure 6.40), in proximity to a water source, and that the very small otoliths recovered here indicate that fish were very likely caught with fibre technology, it's very likely that these grinding patches are the result of plant processing to produce fibrecrafts. This will be worth testing with detailed residue analysis in the future.

Significant finds from this excavation

Fragmentary human skeletal remains (a secondary – or even tertiary – burial) were uncovered in the Early Holocene levels in 562910B.

- The first evidence for *Dentalium* bead manufacturing was recovered from both squares. At least 571 (MNI) *Dentalium* shells were transported to this location c. 1,200 cal. BP.
- 187 very small otoliths from a whitebait-sized species indicate that people were likely using either nets or baskets to catch very small fish, which they then transported to the centre of the island to consume.
- Plant processing (seed grinding, fibrecraft production) was undertaken extensively across the site, with over 190 grinding patches recorded in the areas around the main pool.
- Only two of the eight artefacts tested microscopically did *not* contain evidence for plant processing. Plant fibres were found on tools in both analytical units.
- Turtles were being consumed at this site from the earliest time of occupation until the recent past, and a mixed terrestrial and maritime diet is a characteristic of both phases of site use. These are some of the earliest turtle remains recovered in Australia.
- There is evidence for terrestrial species being present in the earlier phases which did not survive into the Late Holocene with islandisation: these species are currently unknown across the islands.
- Stone tools were used for a range of different purposes, and the substantial debris component of this assemblage – as well as the presence of quarries *in situ* blocks at the site – indicates that stone material at the site was the source of intensive localised repeated *in situ* stone reduction / tool production.
- The earlier phase of occupation suggests that people were more mobile than during later site visits, as there are exotic raw materials (chert, chalcedony) in these earlier layers, whereas the later use of the location indicates a preference for the local bedrock material.
- Artists at this site have always produced mostly geometric motifs (including incised line sets, which are located away from the main occupation area). Human figures were depicted mostly in the mid–late art production period.
- Dietary preferences at the site match motif subject choice. Both macropods and fish are important subject choices throughout the entire art production phases as well as being consumed at the site through time. There is a clear increase in the site's main production phases (CS3 and 4) of turtles, fish and birds.
- The early and continuing presence of *Terebralia* procured from mangrove stands as the key dietary molluscan species is very different to the mainland and inshore island sequences where changing coastal geomorphology sees them replaced by sand-affiliated species such as *Anadara granosa* after 4,000 years ago. This illustrates different coastal processes in the nearshore and distant island systems.

Enderby Island Sample Area 8

In this sample area, stone structures and rock art were recorded on a rocky storm beach just above the high tide mark (Figure 6.78). This most north-westerly part of the island faces out to sea and north towards Goodwyn and (further) Rosemary islands. This location was initially recorded in 2004 to provide advice about historical archaeological sites in the National Heritage Listed Dampier Archipelago National Park (Paterson 2006; Paterson and Souter 2004; Souter et al. 2006). The site was known to early surveys (WA Museum, 1970s and 1980s) but had not been located despite searches. It was reported to CALM (now DBCA) by local resident Warren Richards, who also took the survey team to the remains of the shipwreck *Japatra* site located on the beach c. 200 m due west.

In 2004 the site was observed to include a series

of coral and stone structures, and one rectangular structure was interpreted as a grave – with a whale bone as a grave marker at its western end. The other stone structures were located on the rocky surface and there was no evidence that these involved excavations into the rocky ground. These were assumed in 2004 to have either been shelters or burials now eroded by an aggressive coastal environment over time. Ten engraved stones were recorded at this time: Aboriginal rock engravings on portable pieces of rock near the stone structures.

Historical accounts support this interpretation. In 1851 the captain of the *Saucy Jack* reported seeing on Enderby Island three burials, whale bones, a recent well and Aboriginal tracks.

> *Island. 13th., landed on Enderby Island, observed numerous fresh native foot-marks on the beach, and inside the sand ridge a recently dug well in a small gully, but the water in it was salt. Numerous whale bones strewed the beach, and I observed three graves lying side by side; I should not think they were native, probably those of some unfortunate whalers. (Perth Gazette and Independent Journal of Politics and News 1851)*

In 1879 Pemberton Walcott from the *Prescott* described seeing five stone graves around 18 inches high that he considered were about two decades old (i.e. from the 1850s: cited in Paterson 2006: 102).

The MLP project's focus on this site hoped to better understand the presence of historical whalers in the archipelago, particularly given the discovery of whalers' inscriptions from the 1840s on Rosemary and West Lewis islands (Paterson et al. 2019).

Stone structures

The 14 structures recorded on the rocky coastal terrace are made of weathering stones, beach rock and coral (Table 6.70, Figure 6.77), arranged roughly equidistant from the shore.

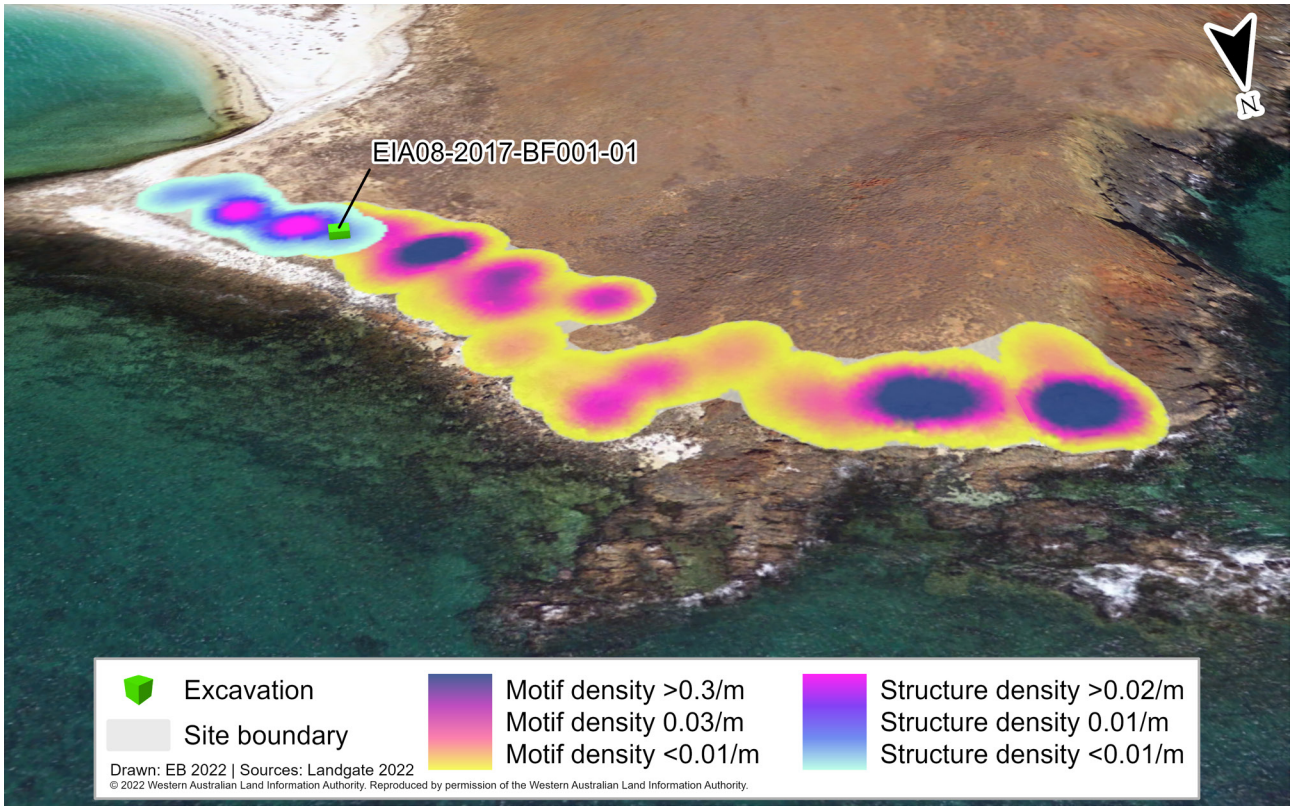

Figure 6.76. Enderby Island Area 8, showing location of the excavation square amongst the background of engraving and stone feature density.

All structures are made of the local stone being removed from the centre of the feature to form a low walled structure (Figure 6.77). Most of these are curvilinear forms with only two (EIA08-2017-BF001-01 and -16) being rectilinear. A plot of the dimensions reveals a range of diameters largely confined to 1–2 m across (Figure 6.78). There were no surface artefacts associated with these features other than flotsam.

A rectangular stone features was excavated, having been observed to contain sediment in 2003 and again in 2017. Prior to excavation, suggestions of function included a grave or shelter. The assumed historical nature of these structures was not confirmed by the archaeological evidence.

Figure 6.77. Enderby Island Area 8: stone feature variability.

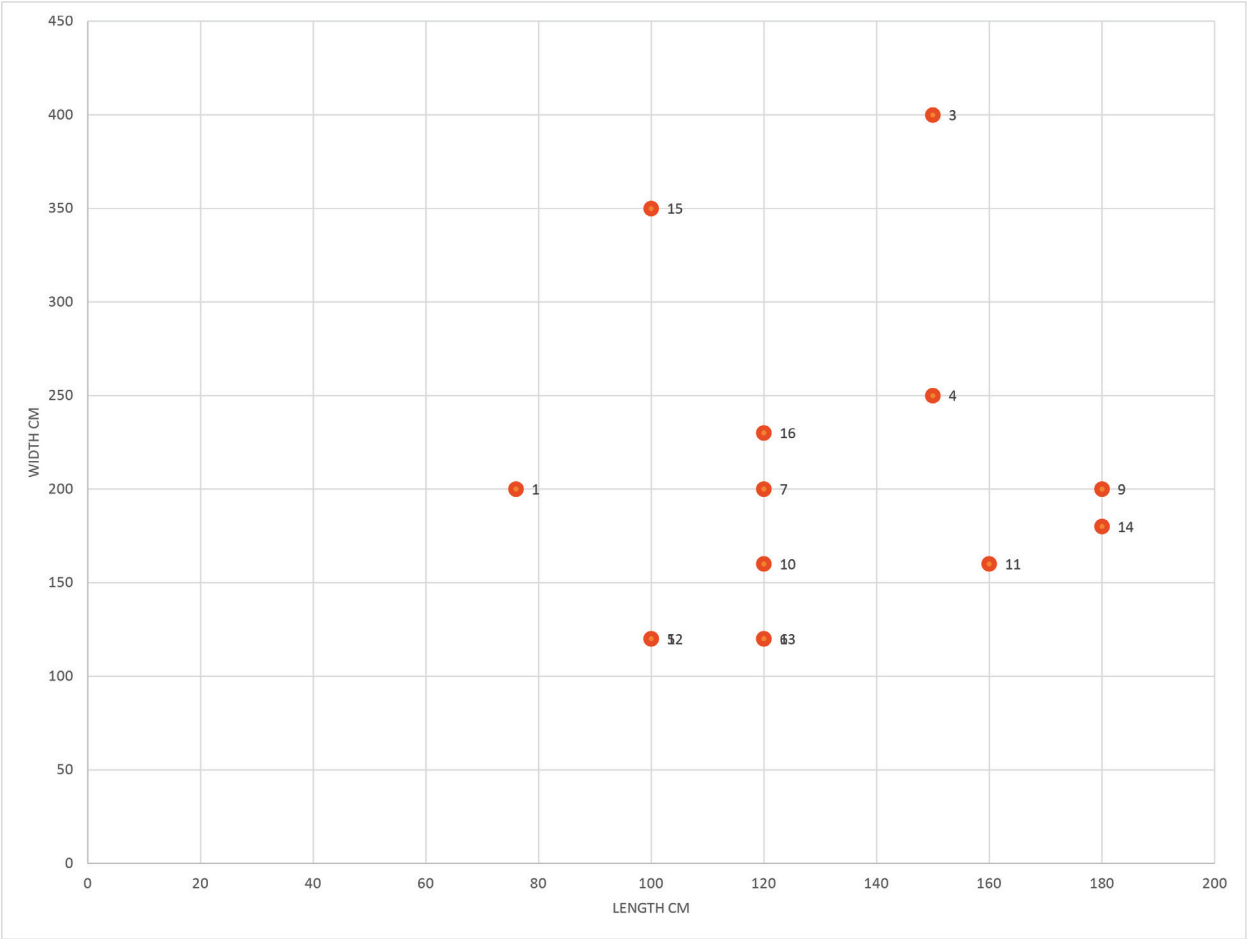

Figure 6.78. Distribution of stone structures by maximum length and width.

Excavation of EIA08-2017-BF001-01

The only structure assessed to have potential for archaeological excavation was EIA08-2017-BF001-01. Since being recorded in 2003 a large amount of material had been deposited at the eastern end of the structure, presumably overlaying *in* situ material from 2003. This appeared to be a sea eagle or osprey nest (Figure 6.80). Given the potential that the structure has been used as a bird's nest for a longer period of time, with cycles of accumulation and erosion, we decided to excavate the eastern end of the stone structure and leave the nest mound intact.

The excavation was conducted in two 50 cm-wide trenches within the structure (c. 66 cm wide), denoted as 'D' and 'E' (see Figure 6.79). The stone walls were left intact; these were around 30–40 cm thick and made of loosely stacked stones and coral. Towards the base the stones were larger, and the maximum height of the walls was c. 50 cm. The stones were placed as to provide a flat vertical 'wall' for the interior of the structure, while the exterior walls were less sheer, and mounded.

On the surface were undiagnostic large fragments of bone assumed to be whale bone: in 2003 these were located at the western end of the structure, and by 2017 were more fragmented and found on the surface extending from the structure towards the west (samples a, b and c: collected for absolute dating).

The excavation of trenches D and E involved three arbitrary XUs of c. 5–10 cm. There was no significant difference between the two trenches (Table 6.71) and are summarised here as an amalgamated D+E trench (Figure 6.79).

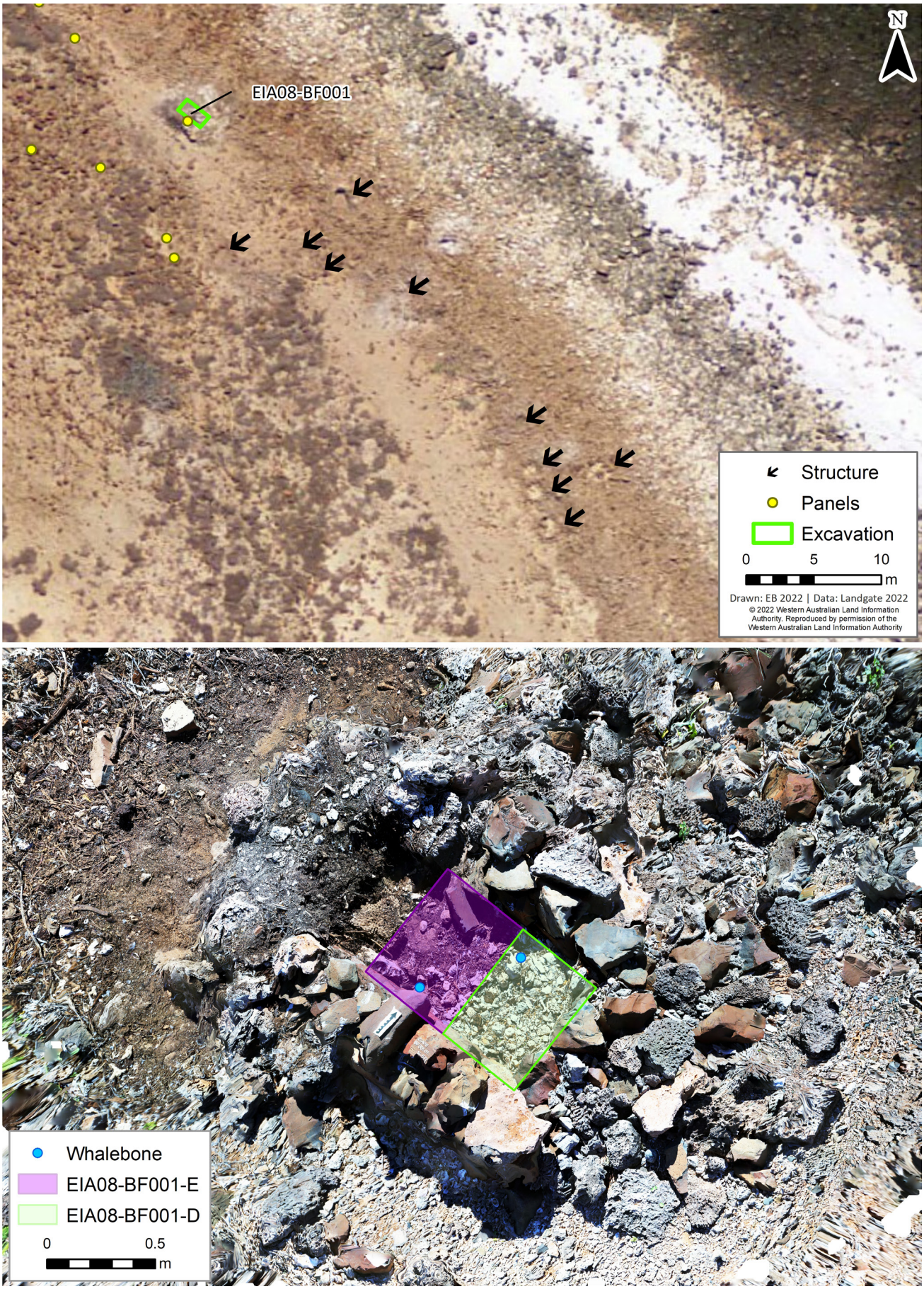

Figure 6.79. Site plan showing locations of stone structures (top) and EIA08-2017-BF001-01 trenches D and E.

Figure 6.80. Structure EIA08-2017-BF001-01: (left) in 2003; (right) in 2017.

Figure 6.81. Structure EIA08-2017-BF001-01 during excavation, facing towards the western end of the structure before excavation (top); start of excavation (middle) and at ends of XU1–3.

XU	PH	SEDIMENT	FINDS
1	8.5	Coral and stone mixed with brown, dry, silty soil	Coral and stone rubble. Fragments of larger bone (including whale)
2	8.5	Coral and stone mixed with brown, dry, silty soil. Transition to inclusion of charcoal and ash in sediment	Bone, burnt oyster shell and lens of burnt ash at base. Some stone appeared burnt. Fauna included: macropod, fish, larger mammal (whale? turtle?). Sparse stone artefacts
3	9	Dry, silty soil with ash content	Reached platform of coral, shell and stone

Table 6.70. Summary of excavations at EIA08-2017-BF001-01 Trench D+E.

XU	OTHER SHELL (G)	ECONOMIC SHELL (G)	WHALE? (G)	OTHER BONE (G)	LITHICS	IRON
1	50	–	447	1,358	2 basalt flakes 50 x 40 x 20 mm (W/L, P platform); 50 x 42 x 18 mm LBF, P platform	–
2	62.5	819	1,116	57	1 basalt MP core 65 x 59 x 45 mm	Metal box fragment
2		73.3		58	2 microdebitage pieces	

Table 6.71. Summary of finds at EIA08-2017-BF001-01.

Discussion

The nature of the finds at EIA08-2017-BF001-01 suggest several possible cultural uses, including burning. The stone artefacts included flakes and a core of locally available basalt, but it is not clear whether: (1) these were present on the coastal platform prior to the structure being built; (2) they relate to the use of the structure; or (3) they postdate the construction of the structure and may represent their use by Aboriginal people. The rock art along this coast (see Chapter 5) may be either contemporary or earlier/later than the stone structures. The presence of historical materials is restricted to ferric fragments of a square-edged container, such as a matchbox, and a small number of fragments from a wire nail. Given the amount of flotsam in the area, this material is not conclusive as to these structures being historical in age.

A preliminary analysis of faunal remains suggests that most of the excavated material was the result of a nesting bird (possibly eagle) returning to the nest with small terrestrial and marine animals. The high pH is consistent with bird guano (but also shell midden, although economic shell densities were relatively low). The presence of the whale bone fragments suggests human agency, while the other bones could have been transported by birds or humans.

Interpretation

The excavations of structure EIA08-2017-BF001-01 revealed evidence for faunal transport as well as burning. The distinctly rectangular structure has vertical inner walls and buttressed outer walls. It is worth noting that the rectangular structure EIA08-2017-BF001-01 differed from the 13 other stone structures on the coastal platform, which tended to be circular. These are either isolated or grouped.

Several possible explanations can now be considered:

1. Burial(s). The hypothesis that EIA08-2017-BF001-01 is a grave cannot be rejected or confirmed. However, no skeletal remains were encountered in the excavated portion of the structure. If it was a grave, it is assumed that the body would have been placed on the rocky platform and covered in sediment. Other historical burials on the islands (e.g. Dolphin Island) were interred in sandy sediments. The historical accounts reference more than one grave. There is no evidence to indicate the other structures here were graves, either from their morphology with a central cavity or arrangement relative to each other.
2. Shelter(s). It is plausible these were rudimentary shelters, deliberately located at a point where they could be seen by ships nearing the island. If this was the case it may well be that EIA08-2017-BF001-01 – being of a different design – served a different function. The presence of charcoal and evidence for burning suggests a possible fireplace or a signal fire. The presence of terrestrial and marine fauna is not inconsistent with the fireplace explanation.
3. A whaling site. Given the presence of whalers in the Dampier Archipelago from the early 19th century onwards, some form of relationship with whaling activities could be considered. Based on inscriptions found on Rosemary and West Lewis islands, we

have argued that whalers would have made landfall for water, fuel and hunting (Paterson et al. 2018) – resources they would have also found on Enderby Island. The American whalers were ship based but may have established temporary shore stations. And, in the 1870s, a more permanent shore-based whaling station with fireplaces and trypots was established on Malus Island (Paterson 2006). While there is an absence of artefacts associated with whalers and whaling, there is the whale bone to consider. Structure EIA08-2017-BF001-01 is similar in size to a trypot fireplace – both those on-shore and aboard whaling vessels (Figure 6.81) being rectangular and of similar dimensions. Similar circular structures aligned along the coast have been observed at a shore-based whaling station on Amsterdam Island (north Atlantic) (Figure 6.82). Obviously, the metal trypots have been removed subsequently (i.e. unlike at Malus Island); however, the various rocky surfaces here could be tested for lipids to test this possible interpretation.

Our excavations here have not reached a definitive conclusion, and these structures – and another similar one located on the southern side of Enderby Island in Area 2 – deserve further investigation.

Figure 6.82. Whale trypots, St Helana Island (http://sainthelenaisland.info/whaling.htm).

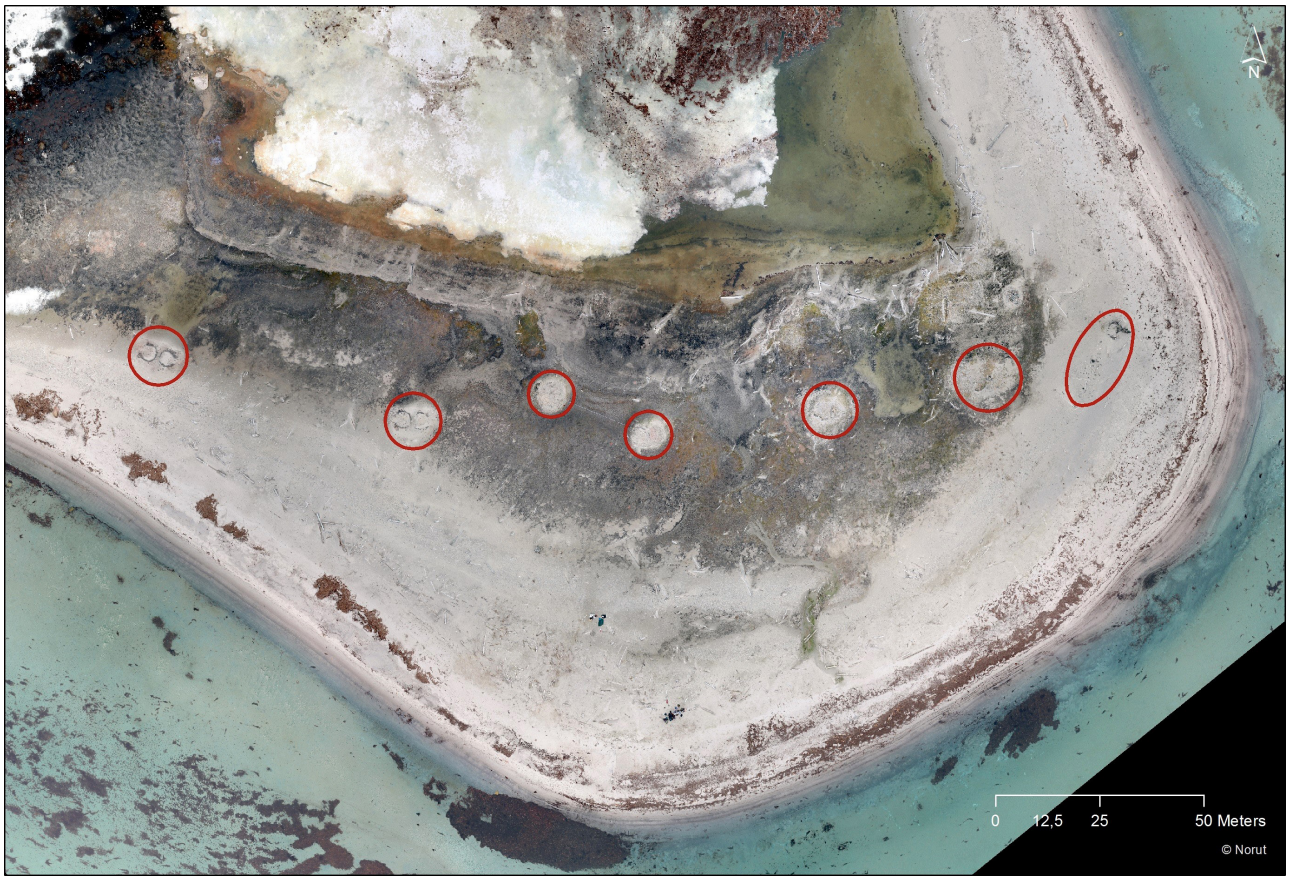

Figure 6.83. Circular bases for trypots at Svalbard (Thuestad et al. 2015).

References

Akerman, K. 1995. The use of bone, shell, and teeth by Aboriginal Australians. In *Ancient Peoples and Landscapes*, ed. E. Johnson, pp. 173–183. Lubbock: Museum of Texas Tech University.

Aplin, K., T. Manne and V. Attenbrow. 2016. Using a 3-stage burning categorization to assess post-depositional degradation of archaeofaunal assemblages: some observations based on multiple prehistoric sites in Australasia. *Journal of Archaeological Science: Reports* 7: 700–714.

Balme, J. and S. O'Connor. 2019. Bead making in Aboriginal Australia from the deep past to European arrival: materials, methods, and meanings. *Palaeoanthropology*, 2019: 177–195.

Bird, Caroline and Rhoads, Jim. 2020. *Crafting Country: Aboriginal Archaeology in the Eastern Chichester Ranges, Northwest Australia*. Tom Austen Brown Studies in Australasian Archaeology. Sydney: Sydney University Press.

Blunt, Zane. 2019. Sea Level Rise and Islandisation: How did the Reconfiguration of Murujuga's Holocene Landscape Influence Indigenous People's Occupation and Resource Exploitation on Enderby and Rosemary Islands? Unpublished BA (Hons) thesis, Archaeology and Centre for Rock Art Research + Management, University of Western Australia.

Braithwaite, R. W. and Griffiths, A. D. 1996. The paradox of Rattus tunneyi: endangerment of a native pest. *Wildlife Research* 23(1): 1–21. https://doi.org/10.1071/WR9960001

Bronk Ramsey, C. 2008. Deposition models for chronological records. *Quaternary Science Reviews* 27: 42–60. https://doi.org/10.1016/j.quascirev.2007.01.019

Bronk Ramsey, C. 2009a. Bayesian analysis of radiocarbon dates. *Radiocarbon* 51: 337–360. https://doi.org/10.1017/S0033822200033865

Bronk Ramsey C. 2009b. Dealing with outliers and offsets in radiocarbon dating. *Radiocarbon* 51: 1023–1045. https://doi.org/10.1017/S0033822200034093

Claud, E, C. Thiebaut, M. Deschamps, A. Coudenneau, C. Lemorini, V. Mourre and F. Venditti. 2019. The use-wear studies on the lithic industries. *Palethnologie* 10. https://doi.org/10.4000/palethnologie.4137

Clune, Genevieve and Harrison, Rodney. 2009. Coastal shell middens of the Abydos coastal plain, Western Australia. *Archaeology in Oceania* 44(S1): 70–80. https://doi.org/10.1002/j.1834-4453.2009.tb00069.x

De Koning, S. 2014. Thatharruga: A Stylistic Analysis of Turtle Engravings on the Dampier Archipelago. Unpublished BA (Hons) thesis, Centre for Rock Art Research + Management, University of Western Australia.

Dixon. J. 1983. Long-tailed hopping mouse. In *The Complete Book of Australian Mammals*, ed. R. Strahan. Sydney: Angus & Robertson.

Esri. 2022. *Esri World Imagery*. Accessed via Web Mapping Service. World Imagery provides one meter or better satellite and aerial imagery in many parts of the world and lower resolution satellite imagery worldwide. The map includes 15m TerraColor imagery and 2.5m SPOT Imagery, USGS 15m Landsat imagery, Digital Globe. Recent 1m USDA NAIP imagery, 1 meter resolution imagery from GeoEye IKONOS, AeroGRID, and IGN and by the GIS User Community. Map image is the intellectual property of Esri and is used herein under license. Copyright © 2022 Esri and its licensors. All rights reserved. For more information visit https://services.arcgisonline.com/ArcGIS/rest/services/World_Imagery/MapServer Florabase. 2021. *Trachymene eleracea (Domin) B.L.Burtt*. https://florabase.dpaw.wa.gov.au/browse/profile/6278

Esri. 2022. *Esri World Imagery*. Accessed via Web Mapping Service. World Imagery provides one metre or better satellite and aerial imagery in many parts of the world and lower resolution satellite imagery worldwide. The map includes 15m TerraColor imagery and 2.5m SPOT

Imagery, USGS 15m Landsat imagery, Digital Globe. Recent 1m USDA NAIP imagery, 1 metre resolution imagery from GeoEye IKONOS, AeroGRID, and IGN and by the GIS User Community. Map image is the intellectual property of Esri and is used herein under license. Copyright © 2022 Esri and its licensors. All rights reserved. For more information visit <https://services.arcgisonline.com/ArcGIS/rest/services/World_Imagery/MapServer>.

Florabase. 2021. *Trachymene eleracea (Domin) B.L.Burtt*. Perth: Department of Biodiversity, Conservation and Attractions. https://florabase.dpaw.wa.gov.au/browse/profile/6278

Fullagar, R., B. Stephenson and E. Hayes 2017. Grinding grounds: function and distribution of grinding stones from an open site in the Pilbara, Western Australia. *Quaternary International* 427: 175–183. https://doi.org/10.1016/j.quaint.2015.11.141

Gallant, J.C., T.I. Dowling, A.M. Read, N. Wilson, P. Tickle and C. Inskeep. 2011. *SRTM-derived 1 Second Digital Elevation Models* Version 1.0. Canberra: Geoscience Australia.

Goldwyer, W. 2018. An Archaeological Investigation of Late Holocene Shell Bead Manufacture, Dampier Archipelago, Northwestern Australia. Unpublished BA (Hons) thesis, Centre for Rock Art Research + Management, University of Western Australia.

Hacker, J. 2017. *Lidar Data from Deep History of Sea Country*. Adelaide: Flinders University.

Hamm, G., P. Mitchell, L. Arnold, G. Prideaux, D. Questiaux, N. Spooner, V. A. Levchenko, E. C. Foley, T. H. Worthy, B. Stephenson, V. Coulthard, C. Coulthard, S. Wilton and D. Johnston. 2016. Cultural innovation and megafauna interaction in the early settlement of arid Australia. *Nature* 539: 280–283. https://doi.org/10.1038/nature20125

Hayes, E., R. Fullagar, K. Mulvaney and K. Connell. 2018. Food or fibercraft? Grinding stones and Aboriginal use of Triodia grass (spinifex). *Quaternary International* 468: 271–283. https://doi.org/10.1016/j.quaint.2016.08.010

Hickman, A. H. and Strong, C. A. 2003. *Dampier – Barrow Island, W.A. 1:250 000 Geological Series Explanatory Notes*, 2nd edn. Perth: Department of Industry and Resources, Western Australian Government.

Hiscock, P. 2008. *Archaeology of Ancient Australia*. London: Routledge.

Hiscock, P. and V. Attenbrow. 1998. Early Holocene backed artefacts from Australia. *Archaeology of Oceania* 33(2): 49–62. https://doi.org/10.1002/j.1834-4453.1998.tb00404.x

Hiscock, P. and V. Attenbrow. 2004. A revised sequence of backed artefact production at Capertee 3, New South Wales. *Archaeology in Oceania* 39(2): 94–99. https://doi.org/10.1002/j.1834-4453.2004.tb00566.x

King, Phillip Parker. 1818. *Remark Book. King Family Papers*. MLMSS 5277 microfilm reel CY2565, items 1–3. Mitchell Library, Sydney.

Landgate. 2017–2022. *WA Now Mosaic (LGATE-320)* [data set]. Accessed via Web Mapping Service <https://catalogue.data.wa.gov.au/dataset/wa-now-aerial-photography-mosaic>. All aerial images reproduced by permission of the Western Australian Land Information Authority, Perth.

Landsat. 2021. *Sentinel-1B Interferometric Wide Swath Level* 1. Images courtesy of the US Geological Survey.

Lebrec, U., V. Paumard, M. J. O'Leary and S. C. Lang. 2021a. Towards a regional high-resolution bathymetry of the North West Shelf of Australia based on Sentinel-2 satellite images, 3D seismic surveys, and historical datasets. *Earth System Science Data* 13: 5191–5212. *https://doi.org/10.5194/essd-13-5191-2021*

Lebrec, U., V. Paumard, M. J. O'Leary and S. C. Lang. 2021. Towards a regional high-resolution bathymetry of the North West Shelf of Australia based on Sentinel-2 satellite images, 3D seismic surveys, and historical datasets. *Earth System Science Data*: Open Access 13: 5191–5212. https://doi.org/10.5194/essd-13-5191-2021

Landgate. 2021. LGATE320 Imagery. Accessed via Web Mapping Service https://catalogue.data.wa.gov.au/dataset/wa-now-aerial-photography-mosaic. All aerial images reproduced by permission of the Western Australian Land Information Authority, Perth.

Landsat. 2021. *Sentinel-1B Interferometric Wide Swath* Level 1. Images courtesy of the US Geological Survey.

McDonald, J.J. and M. Berry. 2016. Murujuga, Northwestern Australia: when arid hunter-gatherers became coastal foragers. *Journal of Island and Coastal Archaeology* 12: 24–43. https://doi.org/10.1080/15564894.2015.1125971

McDonald, Jo and Peter Veth. 2006. A Study of the Distribution of Rock Art and Stone Structures on the Dampier Archipelago. Jo McDonald Cultural Heritage Management Pty Ltd. Unpublished report to Heritage Division, Department of Environment and Heritage, Australian Government, Canberra.

McDonald, J., W. Reynen and R. Fullagar. 2018a. Testing predictions for symmetry, variability and chronology of backed artefact production in Australia's Western Desert. *Archaeology in Oceania* 53(3): 179–190. https://doi.org/10.1002/arco.5162

Matheson, C. and M. Veall. 2014. Presumptive blood test using Hemastix with EDTA in archaeology. *Journal of Archaeological Science* 41: 230–241. https://doi.org/10.1016/j.jas.2013.08.018

Meehan, B. 1982. *Shell Bed to Shell Midden*. Canberra: Australian Institute of Aboriginal Studies.

Morris, K. D. 1990. Dampier Archipelago Nature Reserves Management Plan. Management Plan No. 18. Perth: Department of Conservation and Land Management, Western Australian Government.

Mulvaney, K. 2015. *Murujuga Marni: Rock Art of the Macropod Hunters and Mollusc Harvesters*. Perth: UWA Publishing.

Murray, A. S., K. J. Thomsen, N. Masuda, J. P. Buylaert and M. Jain. 2012. Identifying well-bleached quartz using the different bleaching rates of quartz and feldspar luminescence signals. *Radiation Measurements* 47(9): 688–695. https://doi.org/10.1016/j.radmeas.2012.05.006

Palmer, C., R. Taylor and A. A. Burbidge. 2003. Recovery Plan for the Golden Bandicoot (Isoodon auratus) and Golden-backed Tree-rat (Mesembriomys macrurus) 2004–2009. Darwin: Northern Territory Department of Infrastructure, Planning and Environment.

Paterson, A. 2006. Towards a historical archaeology of Western Australia's northwest. *Australasian Historical Archaeology* 24: 99–111. https://www.asha.org.au/pdf/australasian_historical_archaeology/24_04_Paterson.pdf

Paterson, A. G. and C. Souter 2004. Cultural Heritage Assessment & Management Proposal for Historical Archaeological Sites – Dampier Archipelago, Western Australia. Karratha: Conservation and Land Management (Karratha).

Pearson, D. 2013. Recovery Plan for Five Species of Rock Wallabies: Black-footed Rock Wallaby (Petrogale lateralis), Short-eared Rock Wallaby (Petrogale brachyotis), Monjon (Petrogale burbidgei), Nabarlek (Petrogale concinna), Rothschild Rock Wallaby (Petrogale rothschildi). Western Australian Wildlife Management Program no. 55. Perth: Department of Parks and Wildlife, Western Australian Government.

Pearson. D. J. and M. D. B. Eldridge 2008. Rothschild's rock wallaby Petrogale rothschildi. In *The Mammals of Australia*, 3rd edn, eds S. van Dyck and R. Strahan, pp. 389–390. Sydney: Reed New Holland.

Perth Gazette and Independent Journal of Politics and News. 1851. The 'Saucy Jack' from Shark Bay. 17 October.

Petchey, F. and S. Ulm. 2012. Marine reservoir variation in the Bismarck region: an evaluation of spatial and temporal change in ΔR and R over the last 3000 years. *Radiocarbon* 54(1): 45–58. https://doi.org/10.2458/azu_js_rc.v54i1.13050

Reynen, W. and K. Morse. 2016. Don't forget the fish – towards an archaeology of the Abydos Plain, Pilbara, Western Australia. *Australian Archaeology* 82(2): 94–105. https://doi.org/10.1080/03122417.2016.1203138

Ridge, I. 1991. *Plant Physiology*. Kent: Hodder and Stoughton.

Schiffer, M. B. 1987. *Formation Processes of the Archaeological*

Record. Albuquerque: University of New Mexico Press.

Semeniuk, V. and P. A. S. Wurm. 1987. Mangroves of the Dampier Archipelago, Western Australia. *Journal of the Royal Society of Western Australia* 69(2): 29–87.

Slack, M. J., R. L. K. Fullagar, J. H. Field and A. Border. 2004. New Pleistocene ages for backed artefact technology in Australia. *Archaeology in Oceania* 39(3): 131–137. https://doi.org/10.1002/j.1834-4453.2004.tb00569.x

Thuestad, A. E., H. Tømmervik, S. A. Solbø, S. Barlindhaug, A. C. Flyen, E. R. Myrvoll and B. Johansen. 2015. Monitoring cultural heritage environments in Svalbard: Smeerenburg, a whaling station on Amsterdam Island. *EARSeL Proceedings* 14(1): 37–50. https://doi.org/10.12760/01-2015-1-04

Veth, P. et al. 2017. Early human occupation of a maritime desert, Barrow Island, North-West Australia. *Quaternary Science Reviews* 168: 19–29.

Wells, F. E. and C.M. Lalli. 2003. Aspects of the ecology of the mudwhelks Terebralia palustris and T. semistriata in north-western Australia. In *Proceedings of the Eleventh International Marine Biological Workshop: The Marine Flora and Fauna of Dampier*, eds F. E. Wells, D. I. Walker and D. S. Jones, pp. 193–208. Perth: Western Australian Museum.

Woods, T. 2018. Tool-Stone Activity in Murujuga: An Archaeological Analysis of Holocene Raw Material Variation and Mobility in the Dampier Archipelago, Western Australia. Unpublished BA (Hons) thesis, Archaeology and Centre for Rock Art Research + Management, University of Western Australia.

Yurkov, A. 2017. Yeasts of the soil – obscure but precious. *Ecoyeast Review* 34(5): 369–378. https://doi.org/10.1002/yea.3310

First published in 2022 by
UWA Publishing
Crawley, Western Australia 6009
www.uwap.uwa.edu.au
UWAP is an imprint of UWA Publishing,
a division of The University of Western Australia.

ISBN: 978-1-76080-240-0
Design by Upside Creative.